Final Report

BED26-977-12

Evaluation of Midblock Pedestrian Signals (MPS)

Prepared by

Mohamed Abdel-Aty, Ph.D., P.E.
Md Jamil Ahsan, Ph.D., E.I.
Nafis Anwari, Ph.D.
Ahmed S. Abdelrahman, Ph.D.
Siyuan Tang
Zubayer Islam, Ph.D.

University of Central Florida
Department of Civil, Environmental & Construction Engineering
Orlando, FL 32816-2450

September 2025

TECHNICAL REPORT DOCUMENTATION PAGE

1. Report No.	2. Government Accession No.	3. Recipient's Catalog No.
4. Title and Subtitle Evaluation of Midblock Pedestrian Signals (MPS)		5. Report Date September 25, 2025 6. Performing Organization Code
7. Author(s) Mohamed A. Abdel-Aty, Ph.D, PE; Md Jamil Ahsan, E.I., Nafis Anwari, Ph.D., Ahmed S. Abdelrahman, Siyuan Tang, Zubayer Islam, Ph.D		8. Performing Organization Report No.
9. Performing Organization Name and Address Department of Civil, Environmental & Construction Engineering, University of Central Florida 12800 Pegasus Drive, Suite 211 Orlando, FL 32816-2450		10. Work Unit No. (TRAIS) 11. Contract or Grant No. BED26-977-12
12. Sponsoring Agency Name and Address Florida Department of Transportation		13. Type of Report and Period Covered Final Deliverable 14. Sponsoring Agency Code
15. Supplementary Note		

16. Abstract

This study evaluated the effectiveness of newly implemented Midblock Pedestrian Signals (MPS) in enhancing pedestrian safety, reducing vehicle delays, and minimizing rear-end conflicts, while comparing their performance with other midblock pedestrian crossing treatments such as Pedestrian Hybrid Beacons (PHBs), Rectangular Rapid Flashing Beacons (RRFBs), and Flashing Beacons. Extensive before-and-after CCTV video data were collected from 14 MPS locations and 5 reference sites across Florida. Due to the recent implementation of MPSs, crash data were unavailable; therefore, Surrogate Safety Measures (SSMs) were used. Results showed that MPSs significantly reduced both serious and moderate vehicle-pedestrian conflicts. Although MPS introduced more vehicle delays than RRFB and Flashing Beacon, they performed better than PHB. Rear-end conflict analysis further demonstrated significant safety improvements, particularly at sites upgraded from RRFBs and untreated conditions to MPSs. Driver yielding and pedestrian compliance rates at MPS locations reached approximately 97% and 95%, respectively, demonstrating strong user adaptation. Given their high safety performance, reduced delays compared to PHBs, and strong compliance rates, MPS systems can be considered as a preferred alternative when upgrading existing crossings or installing new pedestrian signal systems.

17. Key Word Mid-Block Pedestrian Crossings, Before-After Evaluation, Pedestrian Safety, Traffic Efficiency	18. Distribution Statement		
19. Security Classif. (of this report)	20. Security Classify (of this page) Unclassified	21. No. of Pages 107	22. Price

DISCLAIMER

The opinions, findings, and conclusions expressed in this publication are those of the authors and not necessarily those of the State of Florida Department of Transportation.

TABLE OF CONTENTS

LIST OF FIGURES

LIST OF TABLES

EXECUTIVE SUMMARY

This study evaluated the effectiveness of Midblock Pedestrian Signals (MPSs) in enhancing pedestrian safety, reducing vehicle delays, and minimizing rear-end conflicts, while comparing their performance with other midblock pedestrian crossing treatments such as Pedestrian Hybrid Beacons (PHBs), Rectangular Rapid Flashing Beacons (RRFBs), and Flashing Beacons. Extensive before-and-after CCTV video data were collected from 14 MPS locations and 5 reference sites across Florida. In total, approximately 600 hours of video footage were recorded, documenting interactions involving over 2900 pedestrians. Using advanced computer vision technology—specifically the RT-DETR model for object detection and the ByteTrack algorithm for tracking—vehicle-pedestrian interactions were analyzed in detail. Since MPSs have been newly implemented, there is limited post-implementation crash data available, the study used Surrogate Safety Measures (SSMs) to evaluate conflicts. Conflict Modification Factors (CoMFs) were calculated using Cross-Sectional (CS), Comparison Group (CG), and Empirical Bayes (EB) methods. Across all evaluation approaches and reference groups—including PHBs, RRFBs, and their combinations—MPSs consistently reduced both serious and moderate pedestrian-vehicle conflicts. Notably, when compared to PHBs, which operate similarly but differ in signal phasing, MPSs provided additional safety benefits, reducing serious and total conflicts by up to 33% and 35%, respectively. Vehicle delay was analyzed by evaluating Delay Modification Factors (DMFs) from each pedestrian-vehicle interaction. Results from all three methods (CS, CG and EB) indicated that MPSs introduce 8% to 14% more delays than RRFBs and Flashing Beacons due to the requirement for vehicles to stop during red phases. However, when compared to PHBs, MPSs demonstrated improved efficiency, reducing vehicle delays by 5% to 7%. Rear-end conflict analysis using Time to Collision (TTC) and Deceleration Rate to Avoid Collision (DRAC) also revealed substantial safety improvement, particularly at sites that transitioned from RRFBs and untreated conditions to MPSs. Regarding user behavior, the vehicle yielding rate at MPS locations was observed to be about 97%, meaning almost all drivers stopped for pedestrians, while pedestrian compliance was also above 95%, as most pedestrians followed traffic rules and crossed only after activating the signal. Given their high safety performance, reduced delays compared to PHBs, and strong compliance rates, MPS systems can be considered as a preferred alternative when upgrading existing crossings or installing new pedestrian signal systems.

1. INTRODUCTION

In 2024, Florida reported a total of 10,272 pedestrian crashes, including 651 fatalities; a decrease of approximately 18% compared to 2023 (FLHSMV, 2024). This decline can be attributed to the proactive measures implemented by the Florida Department of Transportation (FDOT) to enhance pedestrian safety (Florida Pedestrian and Bicycle Strategic Safety Plan, 2021). These include increasing the deployment of pedestrian signal systems, enhancing pedestrian and driver education programs, adding more roadway signage, and enforcing traffic laws more rigorously. While the number of pedestrian fatalities remains high, the decreasing trend shows progress in improving pedestrian safety. Notably, a majority of pedestrian crashes occur in urban areas (82%) and at non-intersection locations (75%), such as mid-blocks (NHTSA, 2020). To mitigate these risks, FDOT has introduced three types of mid-block pedestrian signals: Rectangular Rapid Flashing Beacons (RRFBs), Pedestrian Hybrid Beacons (PHBs), and Flashing Beacons.

RRFBs are designed as pedestrian-activated systems that use bright LED lights to warn drivers when a pedestrian cross (refer to **Figure 1**) (Ahsan, Abdel-Aty, Anik, et al., 2025). Researches have shown that RRFBs are most effective on roads with lower speeds and fewer pedestrian activity (Goswamy et al., 2023; Ugan et al., 2022). However, their visibility during daylight, particularly on sunny days, can be limited. This visibility challenge contributes to a continued risk of pedestrian crashes and vehicle rear-end crashes (Ahsan et al., 2024; Anwari et al., 2023). Flashing Beacons, though used less frequently, serve a similar purpose as RRFBs. While RRFBs feature a rectangular design, Flashing Beacons consist of a yellow light that flashes rapidly when activated. PHBs are traffic control systems designed to improve pedestrian safety with a unique signal pattern. These beacons remain off when inactive and are activated by a pedestrian pressing a button. The sequence begins with a flashing yellow light to alert drivers, transitions to a steady yellow light as a warning to slow down, and then displays a solid red light, requiring vehicles to stop completely. Finally, the beacon switches to a flashing red, signaling drivers to stop and proceed only if the crosswalk is clear of pedestrians. The main drawback of PHBs is that drivers are often not familiar with their operation, as they resemble standard traffic signals but only activate when pressing the pushbutton (Ahsan et al., 2024).

FDOT has recently introduced a new mid-block signal system known as the Mid-block Pedestrian Signal (MPS), starting its implementation in late 2022. Its implementation is still in the early stages, with 14 locations currently using this system across Florida. While the MPS shares some

similarities with the PHB, it differs notably in signal phase management. Unlike the PHB, which remains dark when not activated, the MPS continuously displays a green light, operating like a standard traffic signal (Ahsan, Abdel-Aty, & Abdelrahman, 2025). Upon activation, the MPS transitions to a solid yellow light (instead of the flashing yellow seen in PHBs), followed by a solid red light, and finally a flashing red light. In this way, the MPS integrates features of both PHBs and traditional traffic signals (Ahsan, Abdel-Aty, Anwari, et al., 2025).

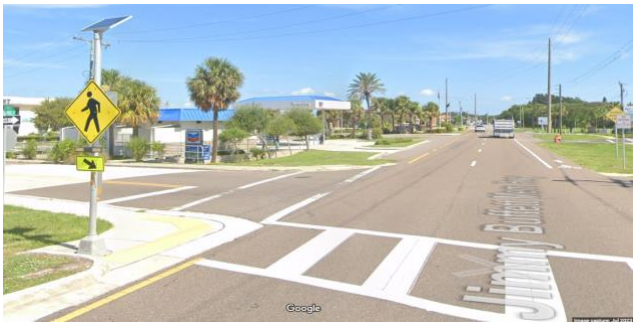

a. Rectangular Rapid Flashing Beacon (RRFB)

b. Flashing Beacon

c. Pedestrian Hybrid Beacon (PHB)

d. Mid-block Pedestrian Signal (MPS)

Figure 1 Different types of signalized mid-block pedestrian crossings (collected from Google Street View)

2. RELATED STUDIES

RRFBs are cost-effective pedestrian safety measures but have certain limitations. According to Goswamy & Abdel-Aty, (2023), RRFBs have the potential to reduce pedestrian-involved crashes by 69%. However, their impact on total vehicular crashes is minimal, and they may even increase rear-end collisions, as indicated by a Crash Modification Factor (CMF) of 1.11. This suggests that vehicles slowing or stopping for pedestrians could result in more rear-end crashes. Monsere et al., (2017) reported CMFs for pedestrian crashes as 0.64 and 0.26 using a simple before-and-after analysis, and a CMF of 0.93 for rear-end crashes using an empirical Bayes approach in Oregon. Similarly, studies by Zegeer et al., (2017) found that RRFBs reduced pedestrian crashes by 47%. However, PHBs were found to be more effective, reducing pedestrian crashes by 55%. These findings highlight the enhanced safety potential of PHBs over RRFBs, though they may come at a higher cost. Fitzpatrick et al., in two separate studies (Fitzpatrick et al., 2010, 2019), concluded that PHBs not only reduce pedestrian crashes but also decrease rear-end collisions, making them more effective than RRFBs. Additional research supports this conclusion, highlighting that PHBs outperform RRFBs in terms of overall safety benefits (Ahsan et al., 2024; Anwari et al., 2023; Ugan et al., 2022).

Regarding MPS, Fitzpatrick et al., (2024) conducted the only known study, reporting that MPS reduced pedestrian crashes by 45% and all crashes by 34% using cross-sectional method. However, this analysis encompassed both traditional MPS (which display a flashing red light during both the pedestrian walk and clearance intervals) and modified MPS (which display a steady red light during the pedestrian walk interval and a flashing red during the clearance phase). These variations complicated isolating the specific effectiveness of each type of MPS. Ahsan et al., (2025) evaluated the performance of five newly installed MPSs in Florida at locations that previously lacked signal systems. Using extensive video footage, the study employed Relative Time-to-Collision (RTTC) metrics to classify and analyze different levels of pedestrian-vehicle conflicts. The findings indicated that MPSs significantly enhance pedestrian safety by supporting safer crossings. However, the study did not compare MPSs with other mid-block signals.

To evaluate midblock signals, the referenced studies estimated CMFs using two primary methods: the Cross-Sectional (CS) approach and the Empirical Bayes (EB) Before-After technique. In these studies, Safety Performance Functions (SPFs) were developed using annual crash data to predict crash frequencies. Additional variables influencing safety, such as Annual Average Daily Traffic

(AADT), Average Daily Traffic (ADT), speed limits, median presence, pedestrian volumes, and various road geometry features, were incorporated into the analysis (refer to **Table 1**).

Table 1 Studies on the safety effectiveness of RRFB, PHB, and MPS

Study	Treatment	CMF	Methodology	Dependent Variable	Explanatory variables
(Goswamy & Abdel-Aty, 2023)	RRFB	0.31 (pedestrian crash) 1.14 (vehicular crash) 1.11 (rear-end crash)	Empirical Bayes	Crash data	AADT, median, speed limit
(Monsere et al., 2017)	RRFB	0.64 (pedestrian crash) 0.93 (rear end crash)	Simple before after and comparison group for ped crash; Empirical Bayes and Cross-sectional including above two methods for rear end crash	Crash data	AADT, bus stop
(Zegeer et al., 2017)	RRFB, PHB	0.53 (pedestrian crash at RRFB) 0.45 (ped crash at PHB)	Cross-sectional	Crash data	AADT
(Fitzpatrick et al., 2019)	PHB	0.54 (pedestrian crash) 0.71 (rear end crash)	Empirical Bayes and Cross-sectional	Crash data	No. lanes, No. pf legs, median, parking, Ped. Volume, speed limit, ADT
(Fitzpatrick et al., 2010)	PHB	0.71 (all crash) 0.85 (severe crash) 0.31 (ped crash)	Empirical Bayes	Crash data	Vehicle and ped volume, median
(Fitzpatrick et al., 2024)	MPS	0.554 (ped crash) 0.660 (all crashes)	Cross-sectional	Crash data	Various road geometry, Avg. daily traffic and pedestrian

In this study, since MPSs have been newly implemented, there is no post-implementation crash data available. Additionally, FDOT aims to expand MPS installations to more locations. Waiting several years for sufficient crash data to assess their effectiveness would not be practical for implementing a potentially promising safety strategy. A more effective alternative involves using

conflict based surrogate safety measures (SSMs), such as Post-Encroachment Time (PET), RTTC, Deceleration Rate to Avoid a Collision (DRAC). These measures offer immediate insights into potential conflicts and near-misses, enabling faster and more accurate evaluations of safety interventions. For instance, Shahdah et al., (2014) proposed a conflict-based method to estimate CMFs, addressing the limitations of traditional crash-based approaches. By integrating simulated traffic conflicts with observed crash data, their method provided reliable CMF estimates while reducing the dependence on long-term crash data. Hasanpour et al., (2025) employed SSMs to assess pedestrian-vehicle conflicts at intersections as an alternative to crash-based safety evaluations, recognizing the limitations posed by the low frequency of pedestrian crashes. Their study utilized conflict-based metrics to estimate pedestrian crash risks at signalized intersections, similar to how SPFs traditionally model crash frequency. While their work demonstrated the feasibility of using SSMs in safety performance assessments, it did not incorporate pedestrian-vehicle dynamics in the development of SPFs.

A limitation of the present studies is the heavy reliance on variables like AADT and posted speed limits in SPF development. While these variables serve as useful indicators, they fail to account for dynamic factors such as actual vehicle speeds, variability in traffic flow, and temporal changes in pedestrian-vehicle interactions. Additionally, no existing studies have conducted a comprehensive comparison among all mid-block crossing treatments, such as MPS, PHB, RRFB, Flashing Beacons, and untreated crossings. This gap in the literature makes it challenging to assess the relative safety performance of different mid-block signal systems under varying conditions. Such comparisons are critical to identifying the most effective treatments and guiding evidence-based decision-making for pedestrian safety improvements.

3. DATA COLLECTION

Data collection and processing were completed for the before study period from 15 proposed MPS sites and 4 control sites between July 2021 and December 2021. The after-period data collection began in November 2022 and was completed in January 2025. During the study, FDOT informed the research team that one location (SR A1A at Surf Side Resort) would not be implementing MPS. Consequently, we used this location as an additional control site, as the before-period data collection had already been completed. Initially, FDOT identified two control sites, and the research team added two more. Including the location at Surf Side Resort, there are now a total of five control sites. Of the 14 treatment sites, 7 were previously untreated (without any signal system), 5 had PHBs, 1 had RRFB, and 1 had a Flashing Beacon prior to the installation of MPSs. The reference groups included 3 locations with PHBs, 1 location with an RRFB, and 1 unsignalized location (refer to **Table 2** and **Figure 2**). This diverse selection of sites ensured a comprehensive evaluation of MPS effectiveness across different baseline conditions.

Table 2 Proposed MPS locations and control sites

#	District	County	On Route	At or Near Route	Treatment Type
MPS sites					
1	2	Alachua	SR 26	Stadium Entrance	New
2	2	Alachua	SR 26	NW 14th Street	New
3	2	Alachua	SR 24A/ SR 331	Gainesville-Hawthorn State Trail	Flashing Beacon to MPS
4	2	Duval	SR 212	Camden Avenue	New
5	3	Franklin	US 98	Carrabelle Beach RV Resort	New
6	4	St. Lucie	SR A1A	Ocean Harbor Villas South	PHB to MPS
7	4	St. Lucie	SR A1A	Breakers Landing	PHB to MPS
8	4	St. Lucie	SR A1A	Atlantic View Beach Club	PHB to MPS
9	4	St. Lucie	SR A1A	Angelfish Drive	PHB to MPS
10	4	St. Lucie	SR A1A	Ocean Harbor North	PHB to MPS
11	5	Marion	US 41	River Road	RRFB to MPS
12	5	Brevard	SR A1A	Surf Drive	New
13	5	Brevard	SR A1A	Antigua Drive	New
14	6	Miami-Dade	SW 1st Street	SW 19th Avenue	New
Control/reference sites					
1	2	St. Johns	SR 207	Old SR 207	PHB
2	2	St. Johns	SR A1A	San Marco Avenue	PHB
3	5	Brevard	SR A1A	N 4th St	RRFB
4	6	Miami-Dade	W Flagler St.	NW 38th Ct.	PHB
5	4	Broward	SR A1A	Surf Rider Resort	Untreated

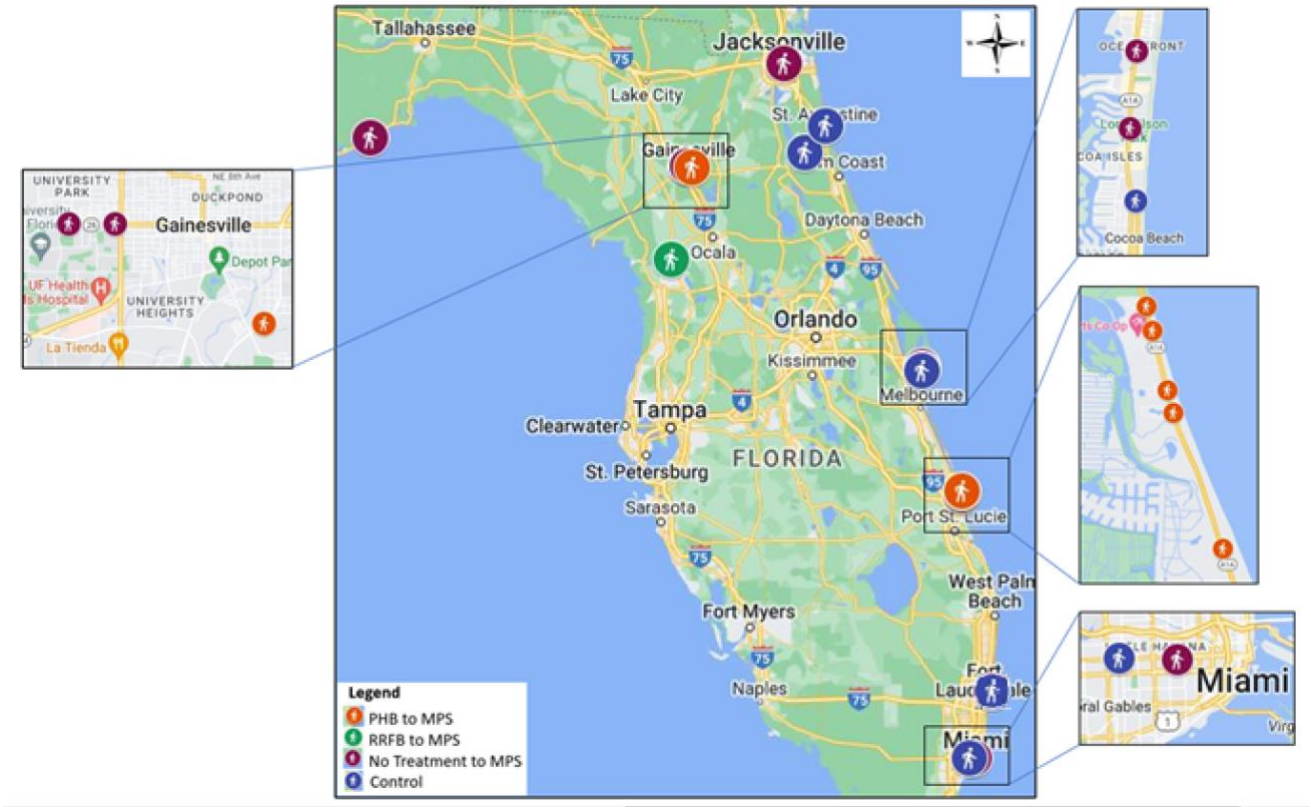

Figure 2 All study locations

Data collection was carried out using a portable CCTV camera setup, with multiple cameras strategically placed to capture activity from both directions for vehicles, pedestrians, and the signal phases. Recordings were conducted for 8 hours per day, including one weekday and one weekend, both before and after MPS installation, covering the period from morning to evening (refer to Table 3). The same data collection protocol was applied at the reference sites to ensure consistency. In total, approximately 600 hours of video footage were recorded, documenting over 2900 vehicle-pedestrian interactions. Approval was obtained from the Institutional Review Board (IRB) before the data collection began. A sample of the data collection setup and collected video screenshot are presented in **Figure 3**.

a. Camera setup

b. Captured video screenshot

Figure 3 Sample data collection from MPS site

Table 3 The before-after period data collection

#	District	County	On Route	At or Near Route	Treatment Type	Date of 'Before' Data Collection	Date of 'After' Data Collection
MPS sites							
1	2	Alachua	SR 26	Stadium Entrance	New	Dec 19, Dec 21 2021	Sept 5, Sept 7, 2024
2	2	Alachua	SR 26	NW 14th Street	New	Nov 7, Nov 9 2021	Sept 5, Sept 7, 2024
3	2	Alachua	SR 24A/ SR 331	Gainesville-Hawthorn State Trail	Flashing Beacon to MPS	Oct 13, Oct 17 2021	May 23, May 25, 2024
4	2	Duval	SR 212	Camden Avenue	New	Oct 13, Nov 7 2021	Jan 25, Jan 27, 2024
5	3	Franklin	US 98	Carrabelle Beach RV Resort	New	Oct 17, Oct 19 2021	April 13, April 15, 2024
6	4	St. Lucie	SR A1A	Ocean Harbor Villas South	PHB to MPS	Sep 15, Oct 31 2021	Jan 16, Jan 18, 2025
7	4	St. Lucie	SR A1A	Breakers Landing	PHB to MPS	Sep 12, Nov 11 2021	Dec 19, Dec 21, 2024
8	4	St. Lucie	SR A1A	Atlantic View Beach Club	PHB to MPS	Sep 12, Nov 11 2021	Dec 19, Dec 21, 2024
9	4	St. Lucie	SR A1A	Angelfish Drive	PHB to MPS	Oct 28, Oct 31 2021	Jan 16, Jan 18, 2025
10	4	St. Lucie	SR A1A	Ocean Harbor North	PHB to MPS	Sept 12, Sept 14, 2021	Jan 16, Jan 18, 2025
11	5	Marion	US 41	River Road	RRFB to MPS	July 10, July 12, 2021	Dec 7, Dec 9, 2023
12	5	Brevard	SR A1A	Surf Drive	New	Sept 21, Sept 25 2021	Dec 19, Dec 23, 2023
13	5	Brevard	SR A1A	Antigua Drive	New	Sept 18, Sept 29 2021	Dec 23, 2023 Jan 4, 2024
14	6	Miami-Dade	SW 1st Street	SW 19th Avenue	New	Nov 21, Dec 01, 2021	Nov 6, 2022, Jan 11, 2023
Control/reference Sites							
1	2	St. Johns	SR 207	Old County Rd 207	PHB	Sept 2. Sept 5, 2021	May 4, May 6, 2024
2	2	St. Johns	SR A1A	May St	PHB	Sept 2. Sept 5, 2021	Feb 8, Feb 10, 2024
3	5	Brevard	SR A1A	N 4th St	RRFB	Sept 18. Sept 21, 2021	May 11, May 13, 2023
4	6	Miami-Dade	W Flagler St.	NW 38th Ct	PHB	Oct 6, Oct 9, 2021	Sept. 19, Sept. 21, 2024
5	4	Broward	SR A1A	Surf Rider Resort	No dedicated crossing	Oct 9, Nov 22 2021	-

4. DATA PROCESSING

The collected videos were processed in three steps: object detection, object tracking, and transformation of pixel points to GPS points (refer to **Figure 4**). These steps are essential for extracting and analyzing the trajectories of different road users. The transformed GPS points were used to calculate speed, heading, and other variables required for the study. State-of-the-art computer vision technology was employed for processing the videos, using the RT-DETR model for detection and the ByteTrack algorithm for tracking, as detailed below (Ahsan, Abdel-Aty, & Abdelrahman, 2025).

Figure 4 Overall video processing stages for trajectories extraction

4.1 Object detection

Object detection is critical for identifying and localizing objects within images and videos, enabling a wide range of uses. Detection models like the YOLO series have been popular due to their balance between speed and accuracy. However, these models often rely on Non-Maximum Suppression (NMS), which can introduce delays and reduce accuracy (Bochkovskiy et al., 2020; Li et al., 2023). Recently, transformer-based models have gained attention for their ability to eliminate the need for NMS, offering a more streamlined approach to object detection. The Real-Time DEtection TRansformer (RT-DETR) stands out as an advanced solution for object detection (Zhao et al., 2024), where RT-DETR eliminates the need for NMS, enhancing both speed and accuracy. RT-DETR achieves higher performance and processing speed on object detection on the Microsoft Common

Objects in COntext (MS COCO) dataset (Lin et al., 2014), which has 80 different classes, compared to other object detection models like YOLO models such as YOLOv7 and YOLOv8 (Zhao et al., 2024). This state-of-the-art performance in both speed and accuracy underscores RT-DETR's superiority in handling real-time object detection tasks efficiently, making it an ideal choice for applications requiring precise object identification and tracking. The flowchart of the RT-DETR model is shown in **Figure 5**, presenting the process of object detection on an image identifying pedestrians and vehicles only. First, the input image is processed through ResNet50 to extract multi-scale features. These features are then fed into an attention-based model, where the encoder analyzes the image features to identify potential objects, where the objects with very low score are filtered. Following this, the decoder generates the corresponding object categories and bounding boxes for each detected object.

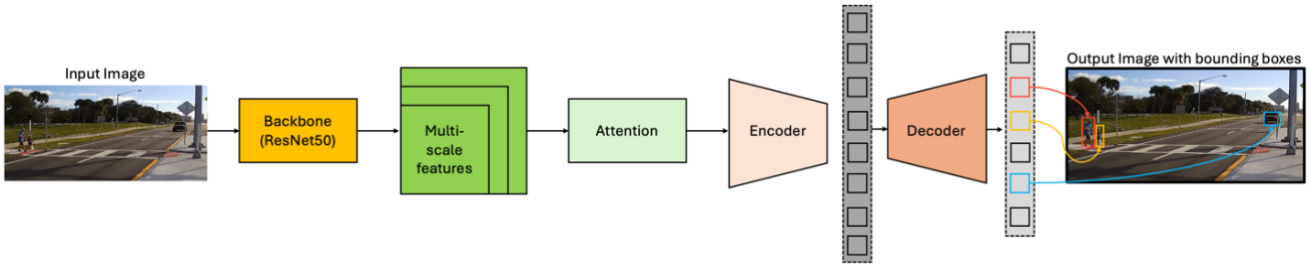

Figure 5 Flowchart of RT-DETR architecture

4.2 Object Tracking

Object tracking complements object detection by maintaining the identities of detected objects over time. ByteTrack (Y. Zhang et al., 2022) is an advanced multi-object tracking (MOT) algorithm designed to excel in tracking vehicles and pedestrians from road surveillance cameras where occlusions set as a challenge. Unlike other methods that discard low-confidence detections (Liang et al., 2022), ByteTrack uses almost every detection box, including those with low scores, to ensure accurate tracking and reduce missed objects and fragmented trajectories. By associating these detection boxes with tracklets, ByteTrack achieves superior performance. On the MOT17 dataset, ByteTrack recorded an impressive MOTA score of 80.3, IDF1 score of 77.3, and HOTA score of 63.1, running at 30 FPS on a single V100 GPU, outperforming many state-of-the-art models (Liang et al., 2022). Its effectiveness extends to other benchmarks like MOT20, HiEve, and BDD100K, demonstrating robust tracking capabilities in various challenging conditions. This makes ByteTrack particularly suitable for accurate trajectory tracking in real-world applications. **Figure 6** shows the flow chart of the ByteTrack

algorithm, where detection boxes from the RT-DETR model are input into the tracking system. For each frame, the tracking algorithm assigns new identification (ID) numbers to detected objects. In subsequent frames, it continues to track the same objects by assigning the same ID, provided they exhibit high similarity to objects in the previous frame. The similarity is determined using the Intersection over Union (IoU) score and appearance similarity score. ByteTrack employs Hungarian matching to associate objects with high similarity and filters out objects with low detection scores or those that lack a match (Kuhn, 1955). A key feature of ByteTrack is its ability to consider all detected objects, even those with low confidence, which is useful for tracking occluded objects that were previously detected but removes them if no historical detection exists.

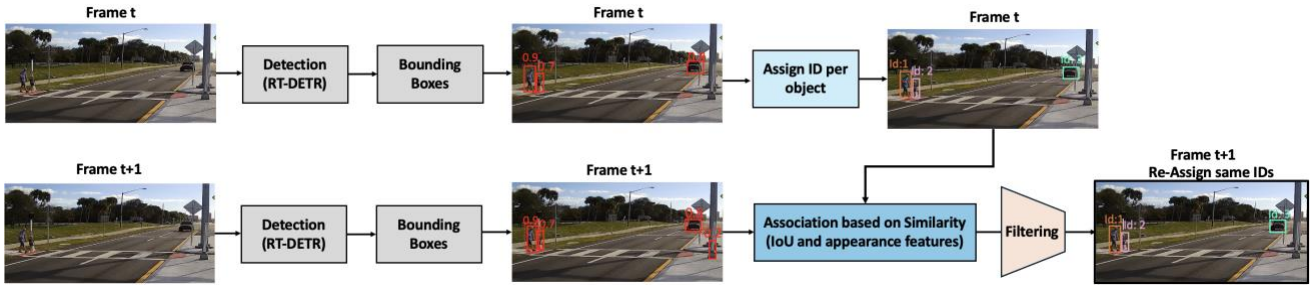

Figure 6 Flowchart of ByteTrack architecture

4.3 Perspective Transformation

After extracting trajectories of objects in the video footage, perspective transformation is applied to map the image plane in pixels to the world plane in GPS coordinates (refer to **Figure 7 (a)**). This transformation, implemented using the OpenCV library, converts pixel coordinates to GPS coordinates for each camera at its respective location (Anwari et al., 2023; S. Zhang et al., 2022). By transforming the pixel coordinates to GPS coordinates, the study could accurately extract essential variables such as distance, speed, and different SSMs of pedestrians and vehicles. This process ensures precise measurement and analysis of the interactions between vehicles and pedestrians. **Figure 7** (b) and **Figure 7** (c) provides a visual representation of the data processing technique and the resultant trajectories of the leading vehicles of each lane (blue lines) and the pedestrian (red line) of that pedestrian-vehicle interaction.

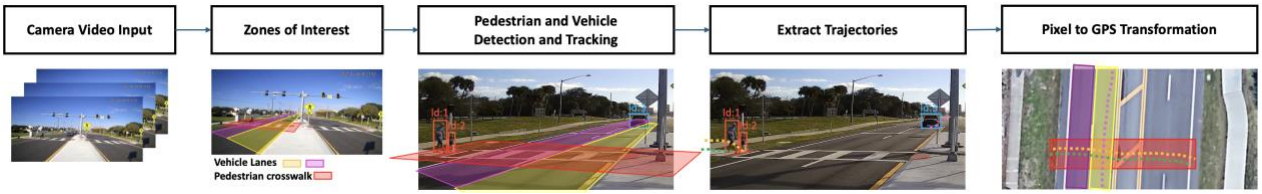

(a) Flowchart of trajectory extraction after detecting and tracking

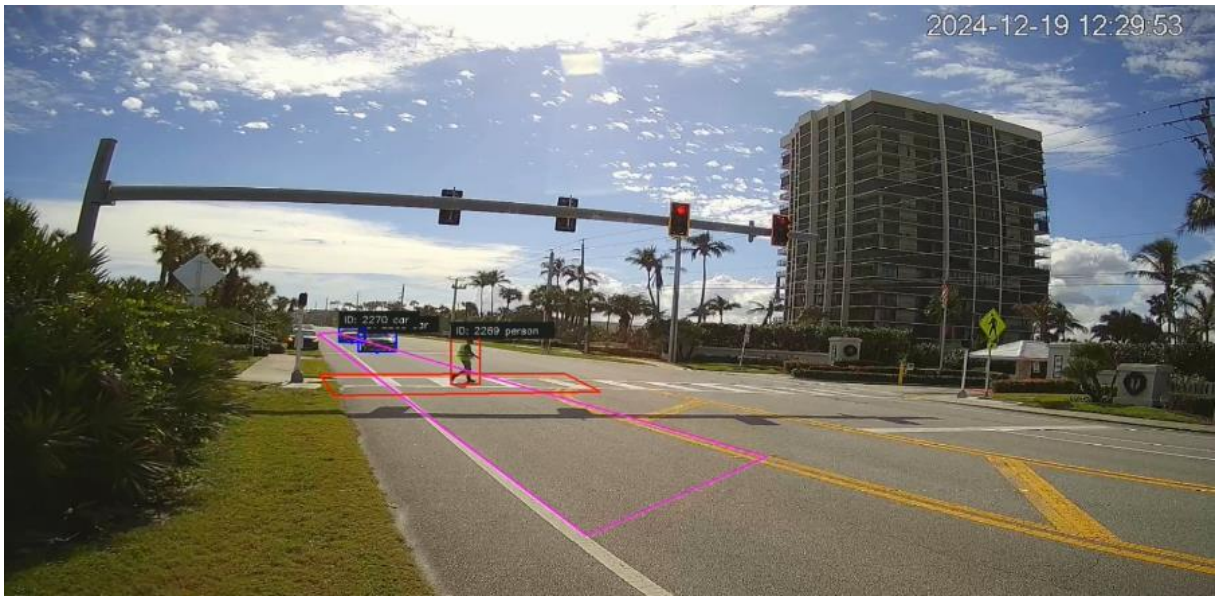

(b) Object detection and tracking in collected videos

(c) Resultant trajectories

Figure 7 Trajectory extraction after detecting and tracking

5. DESCRIPTION OF PERFORMANCE MEASURES

Different performance measures were computed based on the trajectories of vehicles and pedestrians, signal activation time, speeds of vehicles and pedestrians using computer vision and validated by manual inspection. This study has considered the following SSMs for pedestrian safety evaluation:

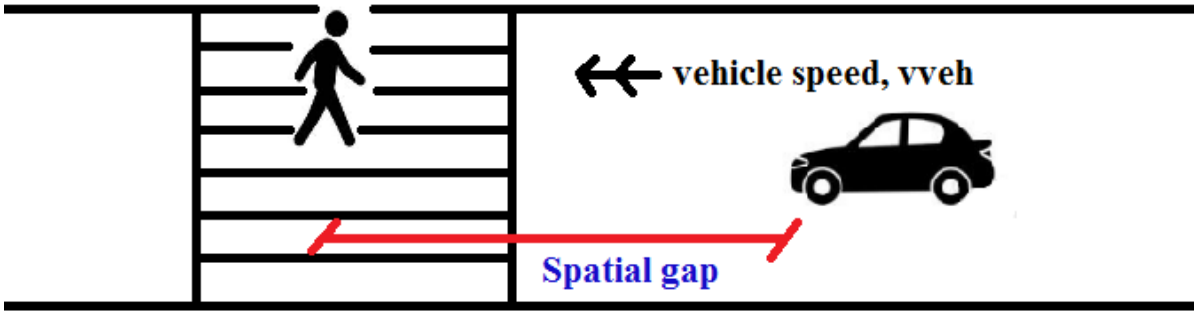

Spatial Gap

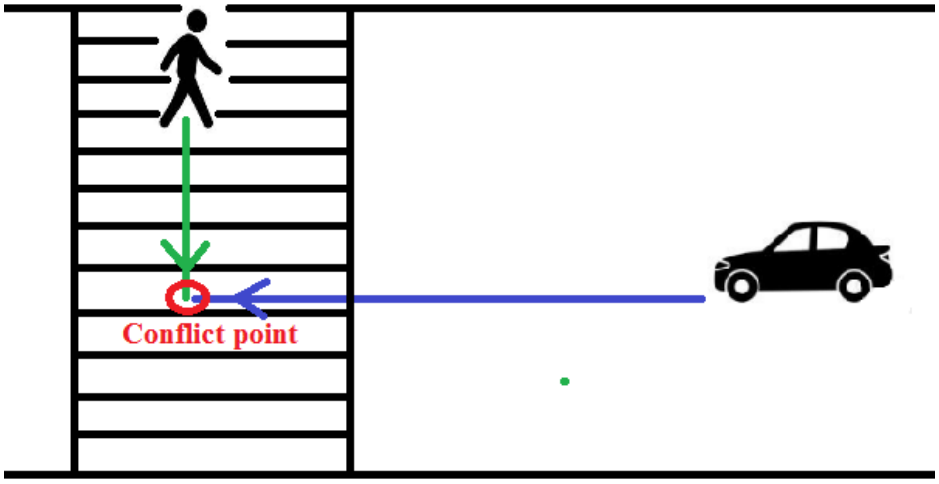

PET

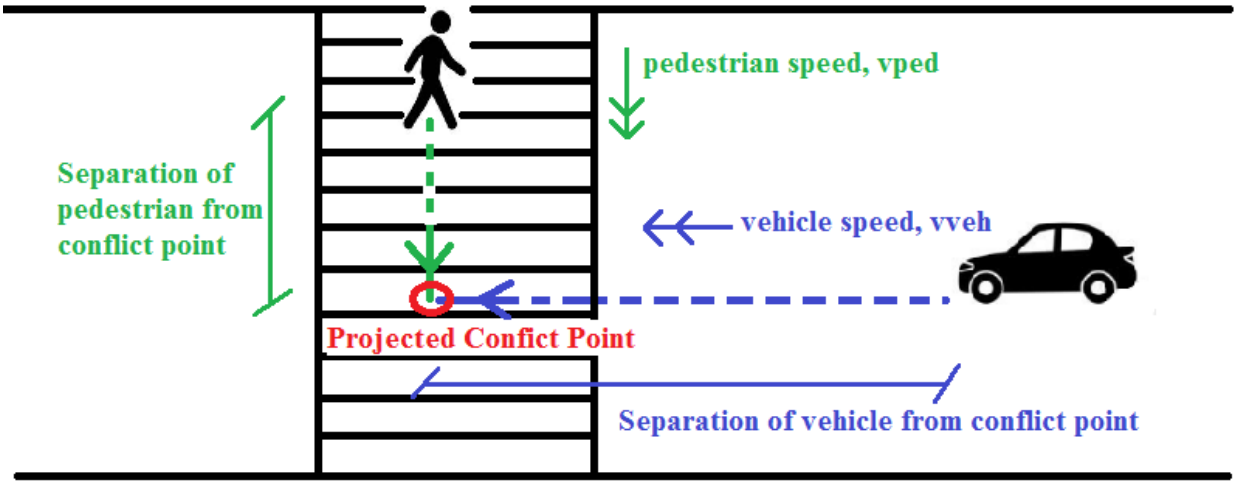

RTTC

Figure 8 Different Surrogate Safety Measures used in the Study

5.1 Post Encroachment Time (PET)

PET is the difference between the time frames in the video for a pair of pedestrian/s and vehicle when they are likely to cross each other at the conflict/intersection point in their line of path (Ahsan et al., 2024; Anwari et al., 2023). The vehicle and pedestrian trajectory are obtained from the videos, from which the coordinates of the conflict point were determined (the point where the pedestrian and the vehicle are likely to collide, which can be determined using their trajectories). The PET can be calculated by taking the difference of time when a pedestrian reaches the crossing point and the time when vehicle reaches the crossing point (refer to **Figure 8**).

PET = Time difference between when pedestrian and vehicle reach the conflict point

PET provides the ultimate outcome of a pedestrian-vehicle conflict. By definition, a PET value of zero implies the occurrence of a crash. The risk of conflict increases as the value of PET approaches zero.

5.2 Spatial gap for pedestrians

Pedestrian and vehicle GPS coordinates were used to geolocate them. The distance between the pedestrian crossing a particular lane and the nearest vehicle in that lane at a particular timeframe was defined as the spatial gap in that frame (refer to **Figure 8**) (Anwari et al., 2023). Spatial gap gives a continuous value of the conflict severity at each timeframe of the conflict. Spatial gap of zero indicates occurrence of a crash. The risk of conflict increases as the value of PET approaches zero. Spatial gap

can be used to assess the extent to which pedestrians are comfortable to be in the spatial proximity of the approaching vehicle. Thus, spatial gap is often used in gap acceptance studies. Similar to PET, spatial gap takes into account the actual trajectories of road users. However, spatial gap does not take into account the speed of the approaching vehicle.

5.3 Temporal gap for pedestrians

Temporal gap calculation used vehicle speed for the frame where a spatial gap was calculated. The spatial gap was divided by the instantaneous vehicle speed to obtain the temporal gap (in seconds) for a particular frame (Anwari et al., 2023). Thus, temporal gap is the time taken by vehicle to collide with the pedestrian if the pedestrian stopped moving and the vehicle continued its trajectory to the pedestrian at the same speed. Like the spatial gap, temporal gap gives continuous values of traffic conflict severity. In many cases, the temporal proximity is better than spatial proximity, because temporal gap integrates both space and speed simultaneously. For example, a vehicle that is coming to a rolling stop as it approaches a pedestrian may have decreasing spatial proximity. However, the decreasing speed of the vehicle will increase temporal gap and reduce the severity of the conflict. On the other hand, a vehicle moving at a high speed may be at a high spatial proximity but low temporal proximity (and thereby increasing the conflict severity). Temporal gap can indicate actions taken by the driver in response to a conflict. For example, a decrease in temporal gap followed by a rise in temporal gap can indicate that the driver is braking. A drastic increase in temporal gap can indicate an event of hard braking.

5.4 Relative Time to Collision (RTTC)

In each frame, the headway of the vehicles and crossing pedestrians were extrapolated to identify their theoretical/ projected conflict point. The separation of the pedestrian and vehicle was calculated independently from that conflict point. RTTC was then calculated by the following equation, which is also depicted in the RTTC section of **Figure 8** (Ahsan et al., 2024; Anwari et al., 2023). TTC of the pedestrian and vehicle are calculated separately in each timeframe through the following equations:

$$\text{TTCp} = \frac{separation\ between\ pedestrian\ and\ conflict\ point}{instantaneous\ pedestrian\ speed}$$

TTCv = $\frac{separation\ between\ vehicle\ and\ conflict\ point}{instantaneous\ vehicle\ speed}$

RTTC is the absolute difference between the TTCp and TTCv:

RTTC = $abs(TTCv - TTCp)$

The concept of TTC arose from vehicle-vehicle conflicts. It was originally defined as the time that remains for the paired vehicles before they collide, if both continue at their present speeds along their respective trajectories. TTC can be easily detected in the rear-end conflict events because the trajectories of the paired vehicles are assumed to be overlapped. However, it cannot be detected (or does not exist) in most of the interactions if the trajectories of the paired users intersect, for example, the pedestrian-vehicle conflict and the conflict between left-turn and opposing through vehicles. In the rear-end conflict, the following vehicle will definitely collide with the leading vehicle if the speed of the follower is higher. However, for the pedestrian-vehicle conflict, the cases that the pedestrian and the vehicle occupy the trajectory intersection point at the same moment are rare. Thus, since pedestrians and vehicles do not have continuously overlapping trajectories, the formula of TTC used in vehicle-vehicle conflicts is not suitable for pedestrian-vehicle conflicts.

6. COMPARATIVE ANALYSIS OF PHB SITES CONVERTED TO MPS

For this comparative analysis, five locations which were previously equipped with PHB and have been converted to MPS, were selected to evaluate the differences in performance and safety (refer to **Table 2**).

6.1 Leading vehicle speed

As data were collected on one weekday and one weekend day, we presented the results for both days. For calculating all variables, we focused only on the leading vehicles, as they are the first to interact with the pedestrians, because the following vehicles simply respond to the actions of the leading vehicles. From the analysis, we found that the average leading vehicle speed is higher at sites with previously PHB converted to MPS. The speed limit at these sites is 45 mph. As shown in **Figure 9** and **Table 4**, the average speed at the MPS sites is below the speed limit, whereas before for the PHB sites, it exceeds the speed limit. Therefore, it can be concluded that the MPS is more effective in maintaining vehicle speeds within the speed limits consequently enhancing pedestrian safety.

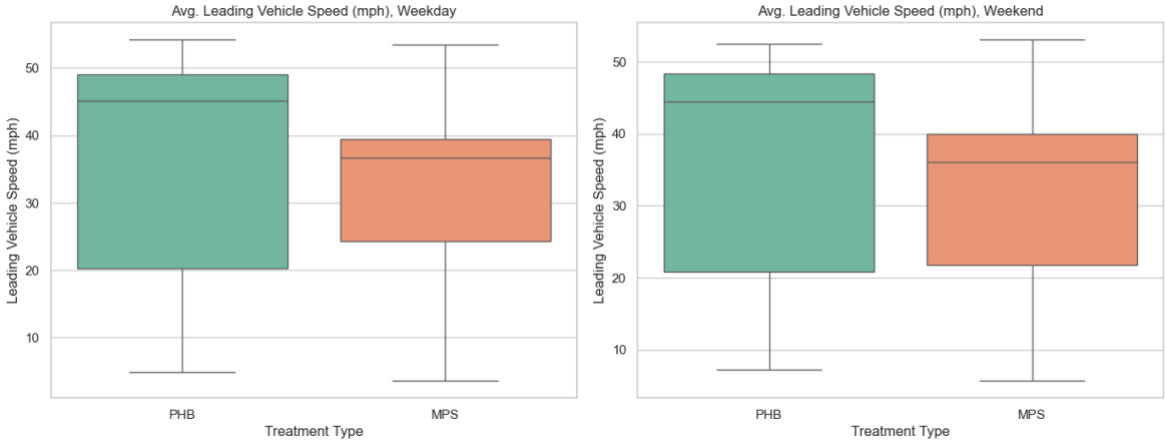

Figure 9 Average leading vehicle speed (PHB to MPS)

6.2 Surrogate Safety Measures (SSMs)

We compared four Surrogate Safety Measures (SSMs), commonly used in the literature (Anwari et al., 2023, Ahsan et al., 2024) namely Post Encroachment Time (PET), spatial gap, temporal gap, and RTTC (please refer to **Figure 10** and **Table 4**). Our analysis revealed that, for both weekdays and weekends, the MPSs, which were previously controlled by PHB, have higher values of the SSM.

This implies that MPS provides greater safety margins and enhances pedestrian safety by allowing more time and space for vehicles to respond to pedestrians.

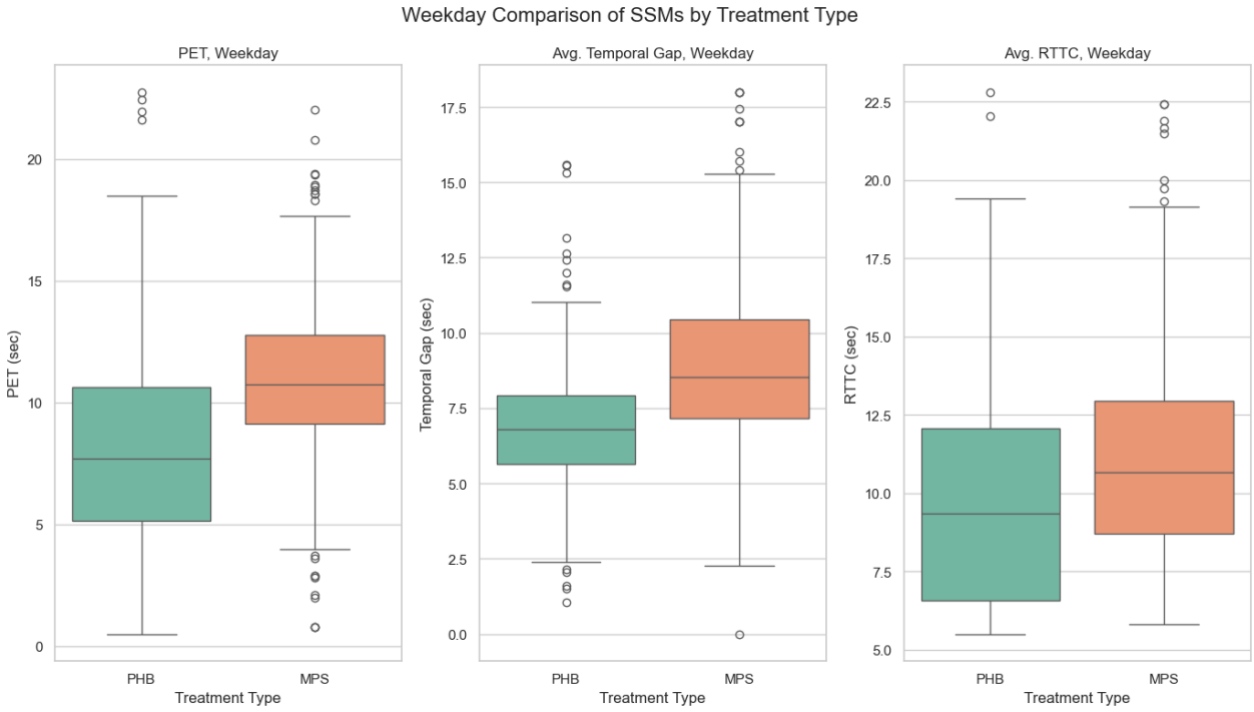

(a) Comparison of PET, Temporal Gap and RTTC on weekday

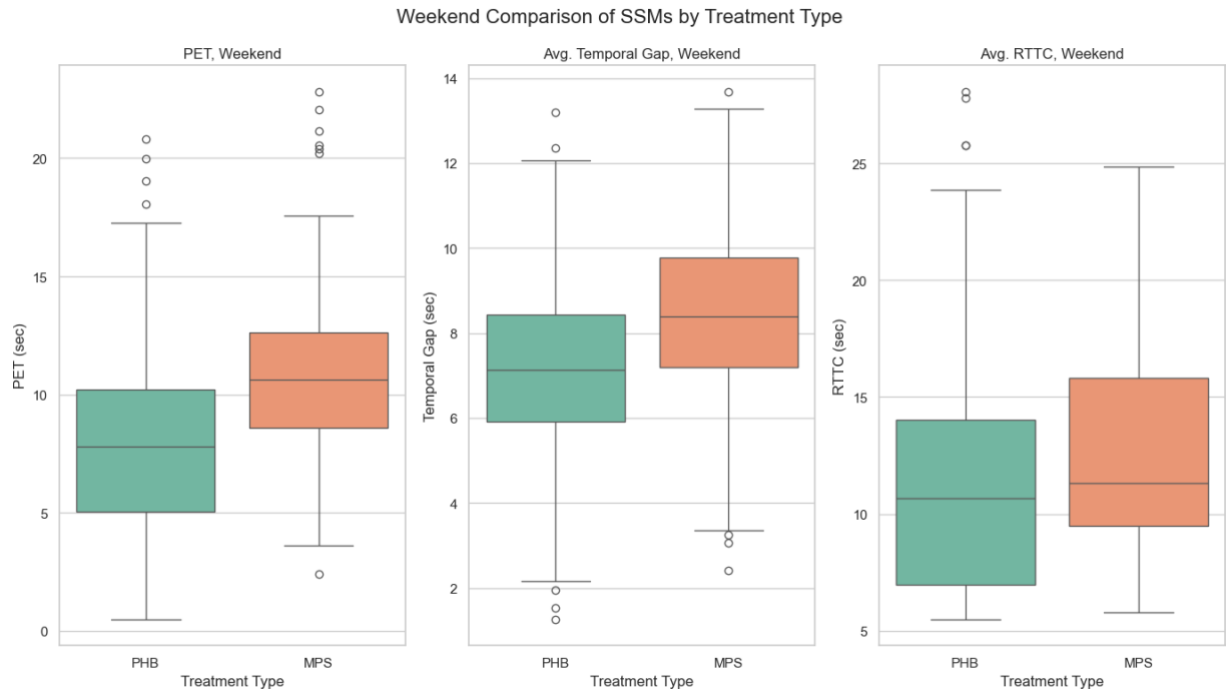

(b) Comparison of PET, Temporal Gap and RTTC on weekend

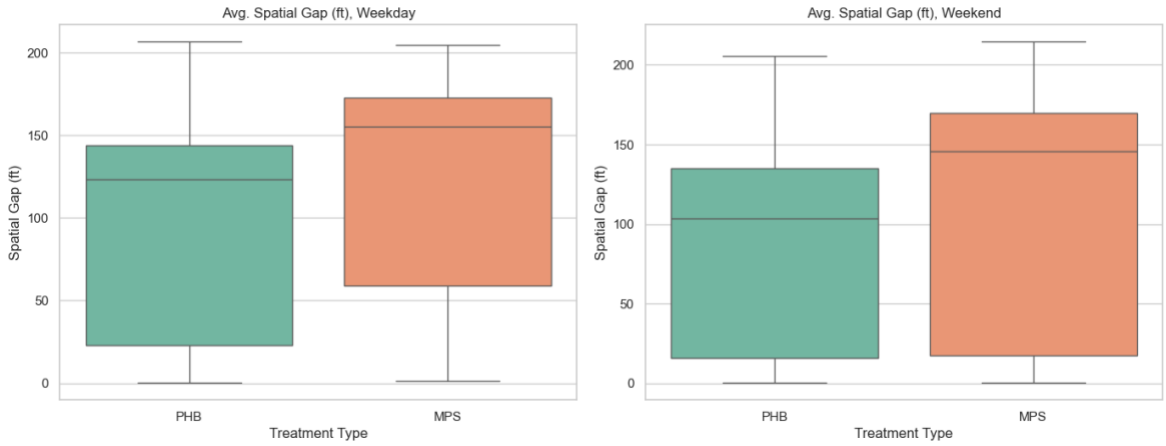

(c) Average Spatial Gap both on weekday and weekend

Figure 10 Comparison by different Surrogate Safety Measures (PHB to MPS)

6.3 Driver yielding behavior

The driver yielding rate for at MPS sites is consistently higher and more stable, with an average 0.97 and minimal variation, indicating that most drivers yield almost all the time when encountering an MPS. In contrast, the PHB shows a much wider range of yielding rates, with an average of 0.81 (please see **Table 4** and **Figure 11**). This suggests that the driver compliance is less consistent and generally lower at the PHB sites compared to the MPS sites. The MPS appears to be more effective in ensuring drivers yield to the pedestrians.

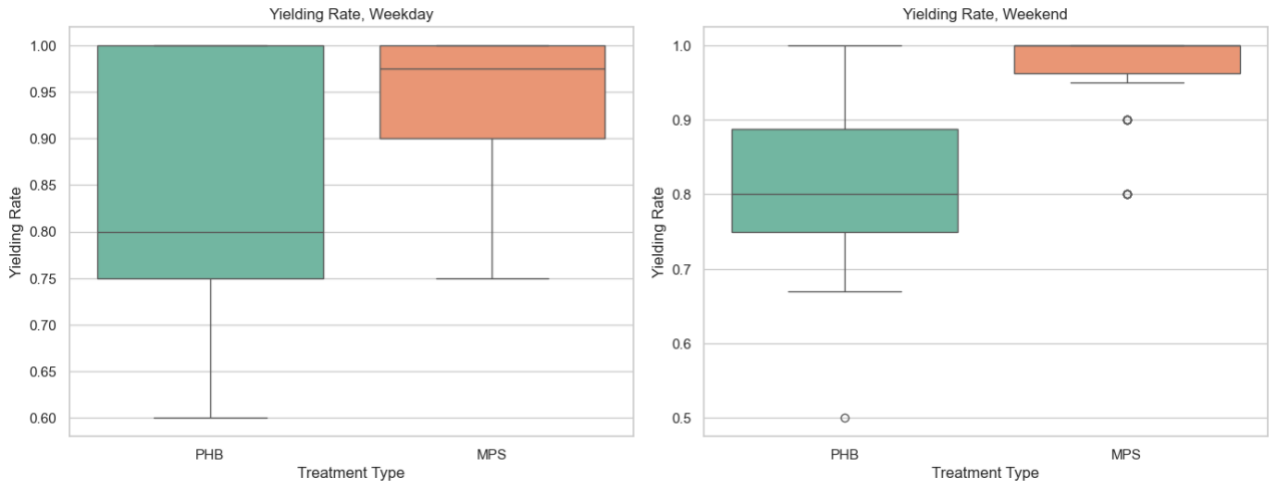

Figure 11 Driver yielding rate (PHB to MPS)

Table 4 Summary statistics for all variables (PHB to MPS)

Variable	Description	Observations (PHB/MPS)	PHB				MPS			
			Mean	Std. Dev.	Max.	Min.	Mean	Std. Dev.	Max.	Min.
Weekday										
Pedestrian count	Number of pedestrians per 15 minutes	160/160	3.2	2.3	19	1	3.5	2.6	14	1
Vehicle count	Number of vehicles per 15 minutes for both directions	160/160	74	36.45	149	21	81	39.48	137	11
Average leading vehicle speed	Average speed of leading vehicle before stopping in each lane, mph	166/190	47.49	9.47	62.6	1.97	38.10	6.93	57.32	1.56
PET	Post Encroachment Time is the time difference between when pedestrian and vehicle reach the conflict point, sec	166/190	8.30	5.10	26. 26	0.50	10.90	3.92	26.18	0.80
Spatial gap	Spatial gap is the physical distance between a pedestrian and the nearest vehicle at a given time frame, feet	166/190	103.76	60.05	241.53	0.24	126.08	67.40	226.29	1.33
Temporal gap	The spatial gap is divided by the instantaneous vehicle speed to obtain the temporal gap, sec	166/190	6.92	2.34	15.58	1.05	9.17	3.25	21.0	0.90

Table 4 Summary statistics for all variables (PHB to MPS) (cont.)

Variable	Description	Observations (PHB/MPS)	PHB				MPS			
			Max.	Min.	Max.	Min.	Max.	Min.	Max.	Min.
RTTC	Relative Time to Collision (RTTC) measures the time difference between the arrival of the first and second road users at a potential conflict point, assuming they maintain their current speeds, sec	166/190	9.04	4.07	25.30	0.5	11.21	3.79	23.04	0.56
Vehicle yielding rate	Yielding rate = Vehicles stopped or slowed / total leading vehicles	166/190	0.81	0.21	1.00	0.00	0.97	0.03	1.00	0.60
Weekend										
Pedestrian count	Number of pedestrians per 15 minutes	160/160	3.32	1.32	17	0	4.38	5.2	2.0	1
Vehicle count	Number of vehicles per 15 minutes for both directions	160/160	67.32	18.53	146	44	76.78	30.47	142	31
Average leading vehicle speed	Average speed of leading vehicle before stopping in each lane, mph	179/201	45.19	9.57	68.32	7.32	38.65	7.92	56.11	1.33
PET	Post Encroachment Time is the time difference between when pedestrian and vehicle reach the conflict point, sec	179/201	8.02	4.64	26.16	0.55	11.0	3.87	23.77	0.62

Table 4 Summary statistics for all variables (PHB to MPS) (cont.)

Variable	Description	Observations (PHB/MPS)	PHB				MPS			
			Max.	Min.	Max.	Min.	Max.	Min.	Max.	Min.
Spatial gap	Spatial gap is the physical distance between a pedestrian and the nearest vehicle at a given time frame, feet	179/201	80.76	63.77	205.58	0.23	112.22	72.49	219.19	0.53
Temporal gap	The spatial gap is divided by the instantaneous vehicle speed to obtain the temporal gap, sec	179/201	7.27	2.40	13.77	0.73	8.45	2.21	16.17	0.91
RTTC	RTTC measures the time difference between the arrival of the first and second road users at a potential conflict point, assuming they maintain their current speeds, sec	179/201	10.49	5.54	28.73	0.51	12.62	5.04	31.15	0.80
Vehicle yielding rate	Yielding rate = Vehicles stopped or slowed / total leading vehicles	179/201	0.81	0.16	1.00	0.00	0.97	0.05	1.00	0.70

6.4 Pedestrian behavior

Figure 12 illustrates pedestrian crossing behavior before and after the installation of the MPS. Initially, there was a mix of proper and improper crossings (indicating pedestrian compliance), with some pedestrians violating traffic rules by crossing without activating the signal (particularly at the PHB sites). After the MPS installation, proper crossings significantly improved. The percentage of proper crossings rose substantially, with nearly all pedestrians now following the rules and crossing only after activating the pedestrian signal phase. This demonstrates the effectiveness of the MPS in improving pedestrian compliance.

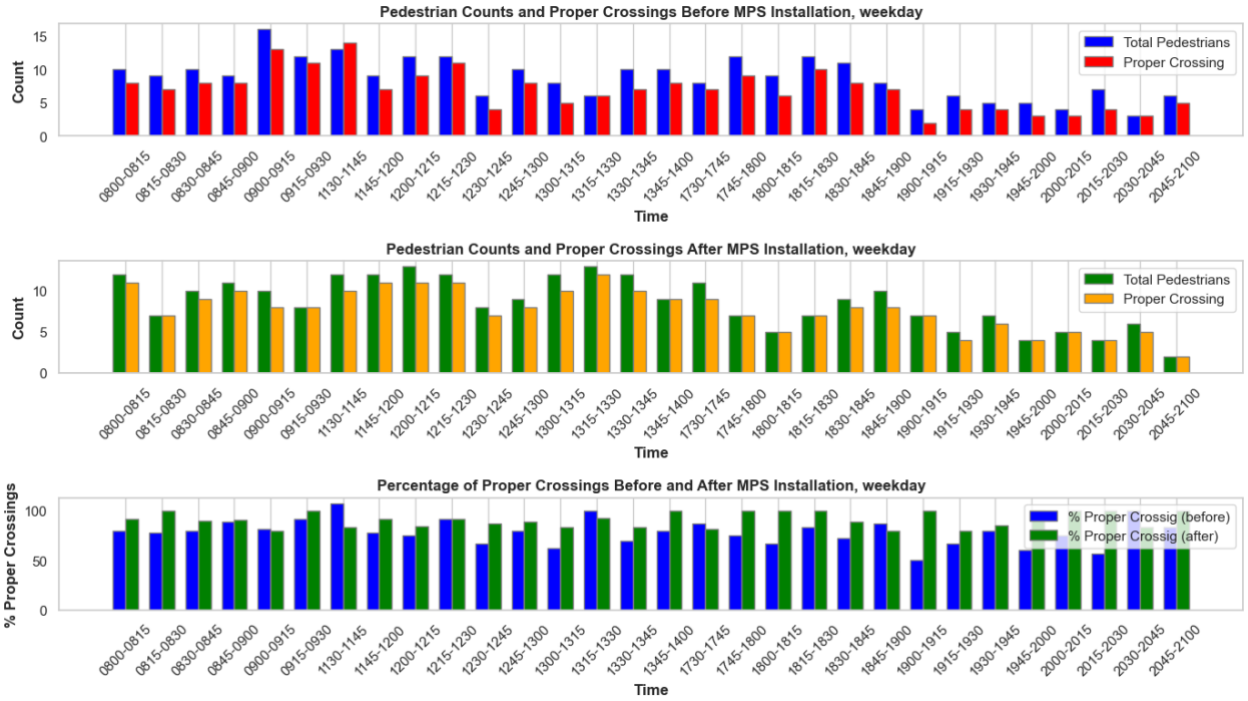

(a) Pedestrian count and proper crossing during the weekday

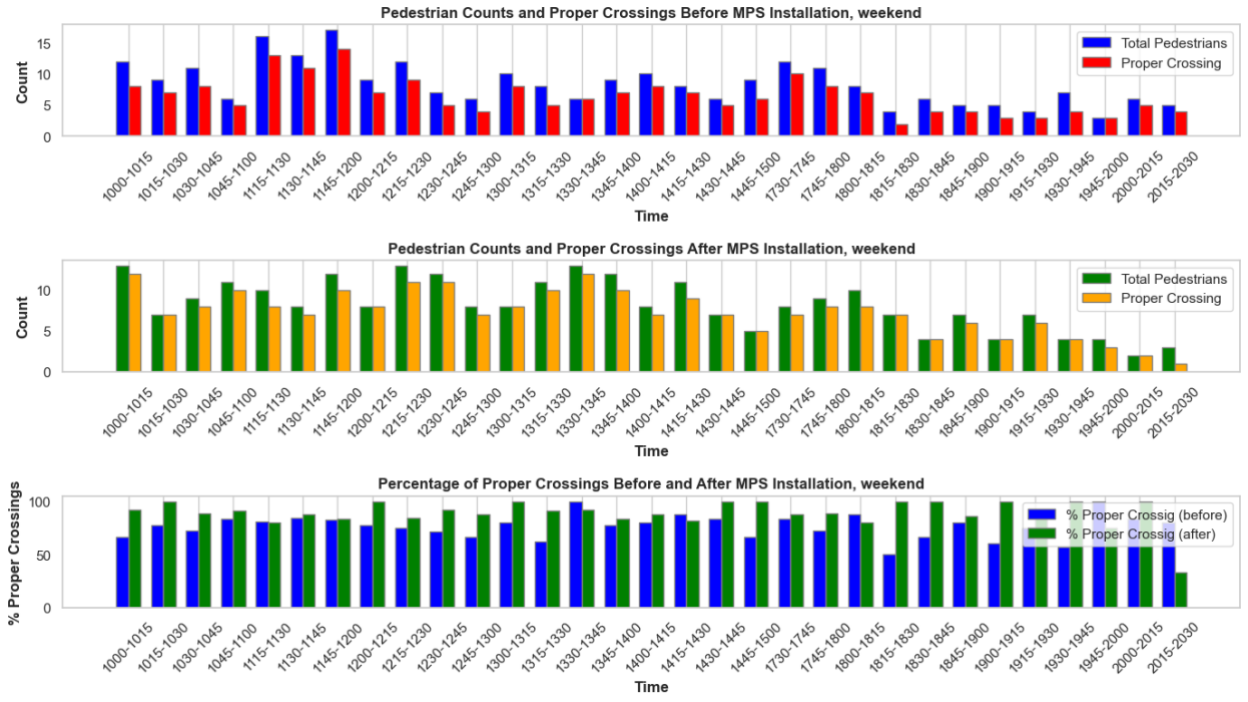

(b) Pedestrian count and proper crossing during the weekend

Figure 12 Pedestrian compliance before and after MPS installation (PHB to MPS)

7. COMPARATIVE ANALYSIS OF RRFB SITES CONVERTED TO MPS

For this comparative analysis, one location (#11), which was previously equipped with RRFB and has been converted to MPS, was selected to evaluate the differences in performance and safety.

7.1 Leading vehicle speed

From the analysis, we found that the average leading vehicle speed is higher at site previously with RRFB compared to MPS. The speed limit at this site is 35 mph. As shown in **Figure 13** and **Table 5**, the average speed at the MPS sites is below the speed limit, whereas for the RRFB sites, it exceeds the speed limit. Therefore, it can be concluded that the MPS is more effective in maintaining vehicle speeds within the speed limits consequently enhancing pedestrian safety.

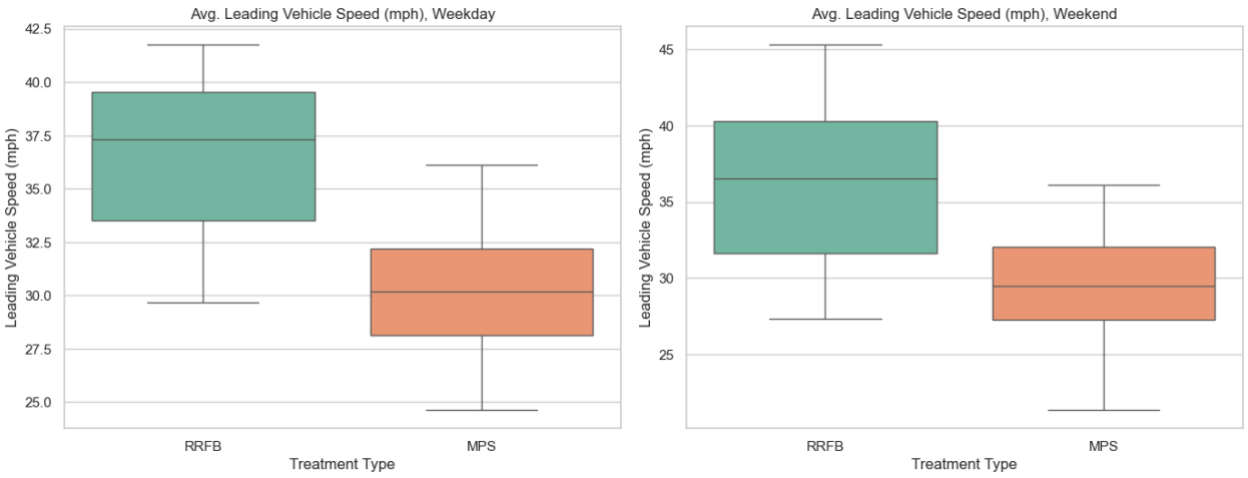

Figure 13 Average leading vehicle speed (RRFB to MPS)

7.2 Surrogate Safety Measures (SSMs)

Our analysis revealed that, for both weekdays and weekends, the MPS, which was previously an RRFB, has higher values of the SSM. This implies that MPS provides greater safety margins and enhances pedestrian safety by allowing more time and space for vehicles to respond to pedestrian crossings (please refer to **Figure 14** and **Table 5**).

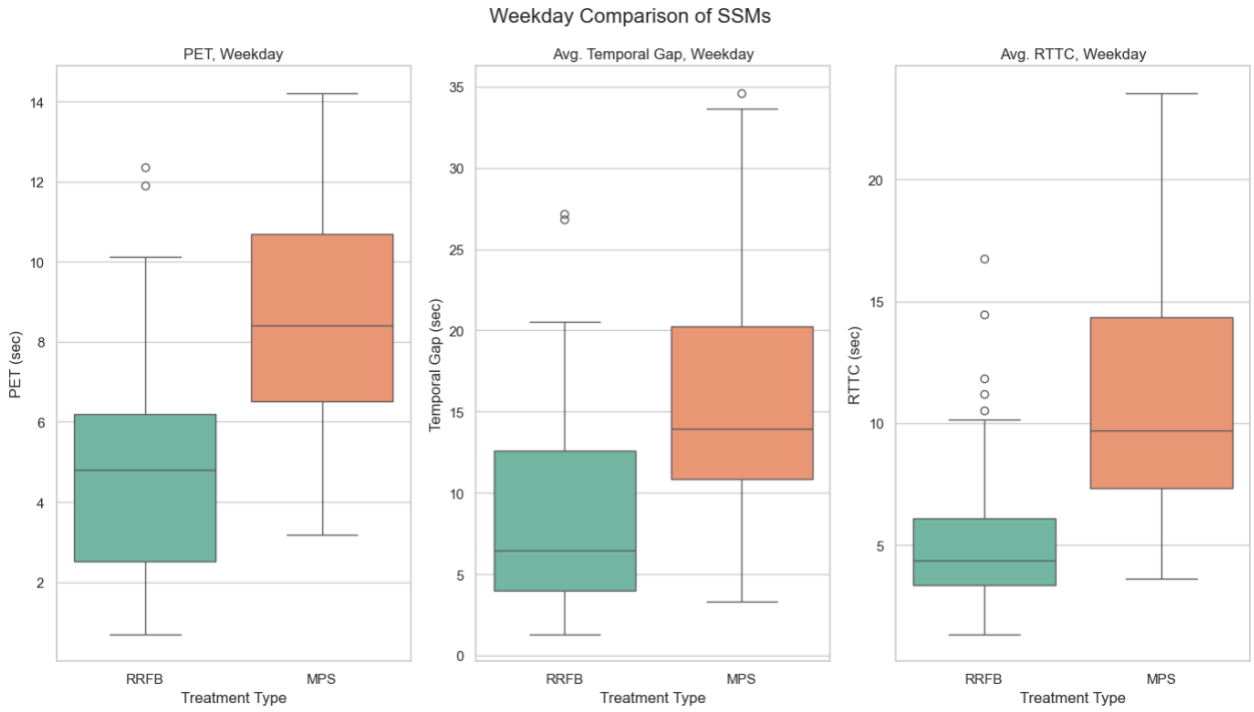

(a) Comparison of PET, Temporal Gap and RTTC on weekday

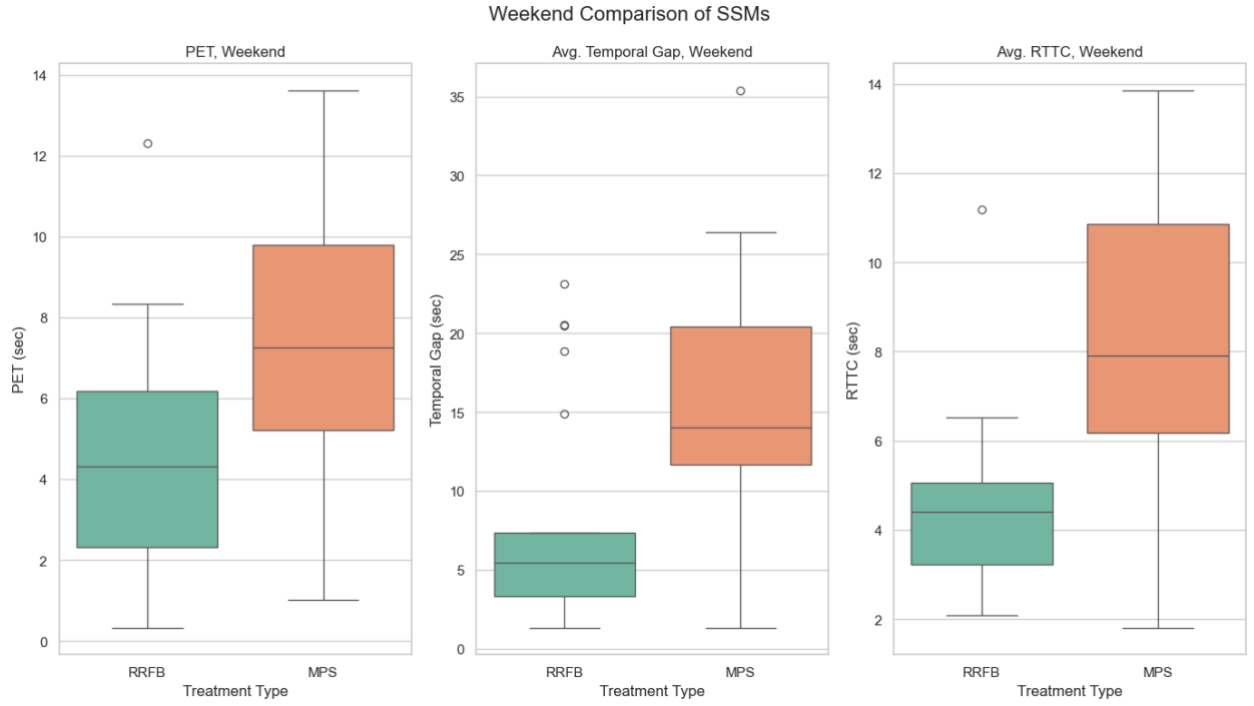

(b) Comparison of PET, Temporal Gap and RTTC on weekend

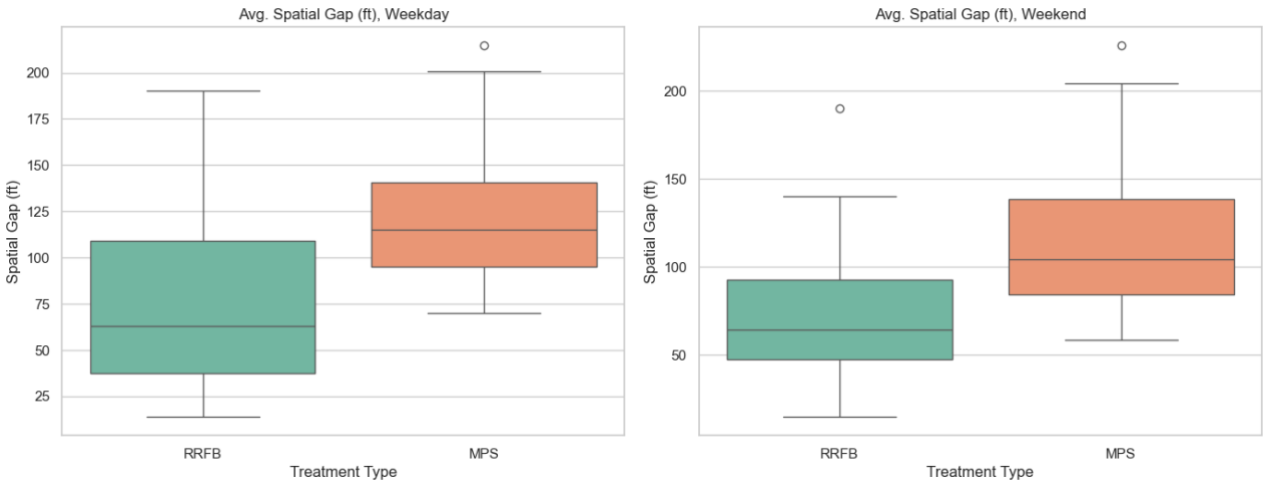

(c) Average Spatial Gap both on weekday and weekend

Figure 14 Comparison by different Surrogate Safety Measures (RRFB to MPS)

7.3 Driver yielding behavior

The driver yielding rate for MPS sites is consistently higher and more stable, with an average 0.97 and minimal variation, indicating that most drivers yield almost all the time when encountering an MPS. In contrast, the RRFB shows a much wider range of yielding rates, with an average of 0.83 (please see **Table 5** and **Figure 15**). This suggests that the driver compliance is less consistent and generally lower at the RRFB sites compared to the MPS sites. The MPS appears to be more effective in ensuring drivers yield to the pedestrians.

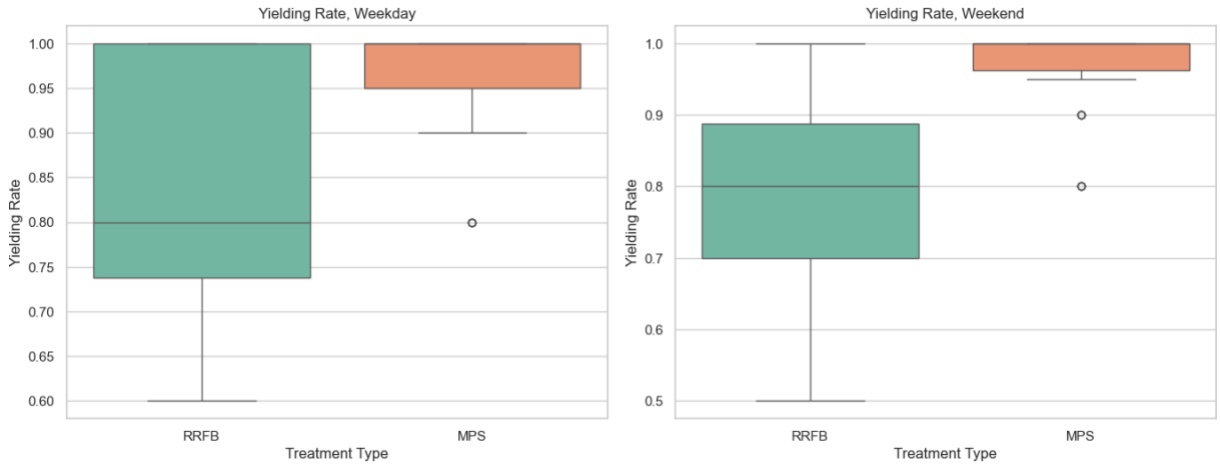

Figure 15 Driver yielding rate (RRFB to MPS)

Table 5 Summary statistics for all variables (RRFB to MPS)

Variable	Description	Observations (RRFB/MPS)	RRFB				MPS			
			Mean	Std. Dev.	Max.	Min.	Mean	Std. Dev.	Max.	Min.
Weekday										
Pedestrian count	Number of pedestrians per 15 minutes	32/32	4.4	4.8	18	3	5.04	4.16	16	2
Vehicle count	Number of vehicles per 15 minutes for both directions	32/32	108.87	30.36	176	17	105.87	28.38	185	11
Average leading vehicle speed	Average speed of leading vehicle before stopping in each lane, mph	67/78	36.93	3.76	47.58	29.68	30.17	2.65	36.13	24.63
PET	Post Encroachment Time is the time difference between when pedestrian and vehicle reach the conflict point, sec	67/78	4.84	2.82	12.35	0.31	8.85	3.23	20.27	0.17
Spatial gap	Spatial gap is the physical distance between a pedestrian and the nearest vehicle at a given time frame, feet	67/78	62.39	54.58	190.04	5.00	126.53	41.99	249.04	9.66
Temporal gap	The spatial gap is divided by the instantaneous vehicle speed to obtain the temporal gap, sec	67/78	8.72	6.32	27.15	0.32	17.16	8.55	50.60	0.38

Table 5 Summary statistics for all variables (RRFB to MPS) (cont.)

Variable	Description	Observations (RRFB/MPS)	RRFB				MPS			
			Max.	Min.	Max.	Min.	Max.	Min.	Max.	Min.
RTTC	Relative Time to Collision (RTTC) measures the time difference between the arrival of the first and second road users at a potential conflict point, assuming they maintain their current speeds, sec	67/78	5.24	3.13	16.73	0.36	12.13	6.15	32.32	0.62
Vehicle yielding rate	Yielding rate = Vehicles stopped or slowed / total leading vehicles	67/78	0.84	0.14	1.00	0.60	0.97	0.06	1.00	0.80
Weekend										
Pedestrian count	Number of pedestrians per 15 minutes	32/32	3.32	4.32	17	2	4.38	5.2	20	3
Vehicle count	Number of vehicles per 15 minutes for both directions	32/32	107.32	38.53	146	44	96.78	30.47	152	14
Average leading vehicle speed	Average speed of leading vehicle before stopping in each lane, mph	75/84	37.01	5.57	48.32	27.32	29.65	2.92	36.11	21.33
PET	Post Encroachment Time is the time difference between when pedestrian and vehicle reach the conflict point, sec	75/84	4.70	2.89	12.32	0.33	8.50	3.35	19.12	0.22

Table 5 Summary statistics for all variables (RRFB to MPS) (cont.)

Variable	Description	Observations (RRFB/MPS)	RRFB				MPS			
			Max.	Min.	Max.	Min.	Max.	Min.	Max.	Min.
Spatial gap	Spatial gap is the physical distance between a pedestrian and the nearest vehicle at a given time frame, feet	75/84	72.71	42.32	190.04	14.79	115.55	41.99	238.06	18.69
Temporal gap	The spatial gap is divided by the instantaneous vehicle speed to obtain the temporal gap, sec	75/84	6.83	6.70	23.10	0.31	15.96	7.19	39.02	0.33
RTTC	RTTC measures the time difference between the arrival of the first and second road users at a potential conflict point, assuming they maintain their current speeds, sec	75/84	5.07	2.80	14.47	0.08	8.45	3.18	19.90	0.81
Vehicle yielding rate	Yielding rate = Vehicles stopped or slowed / total leading vehicles	75/84	0.81	0.14	1.00	0.50	0.97	0.06	1.00	0.80

7.4 Pedestrian behavior

Figure 16 illustrates pedestrian crossing behaviors before and after the installation of the MPS. Initially, there was a mix of proper and improper crossings (indicating pedestrian compliance), with some pedestrians violating traffic rules by crossing without activating the signal (particularly at the RRFB sites). After the MPS installation, pedestrian counts increased, and proper crossings significantly improved. The percentage of proper crossings rose substantially, with nearly all pedestrians now

following the rules and crossing only after activating the pedestrian signal phase. This demonstrates the effectiveness of the MPS in improving pedestrian compliance.

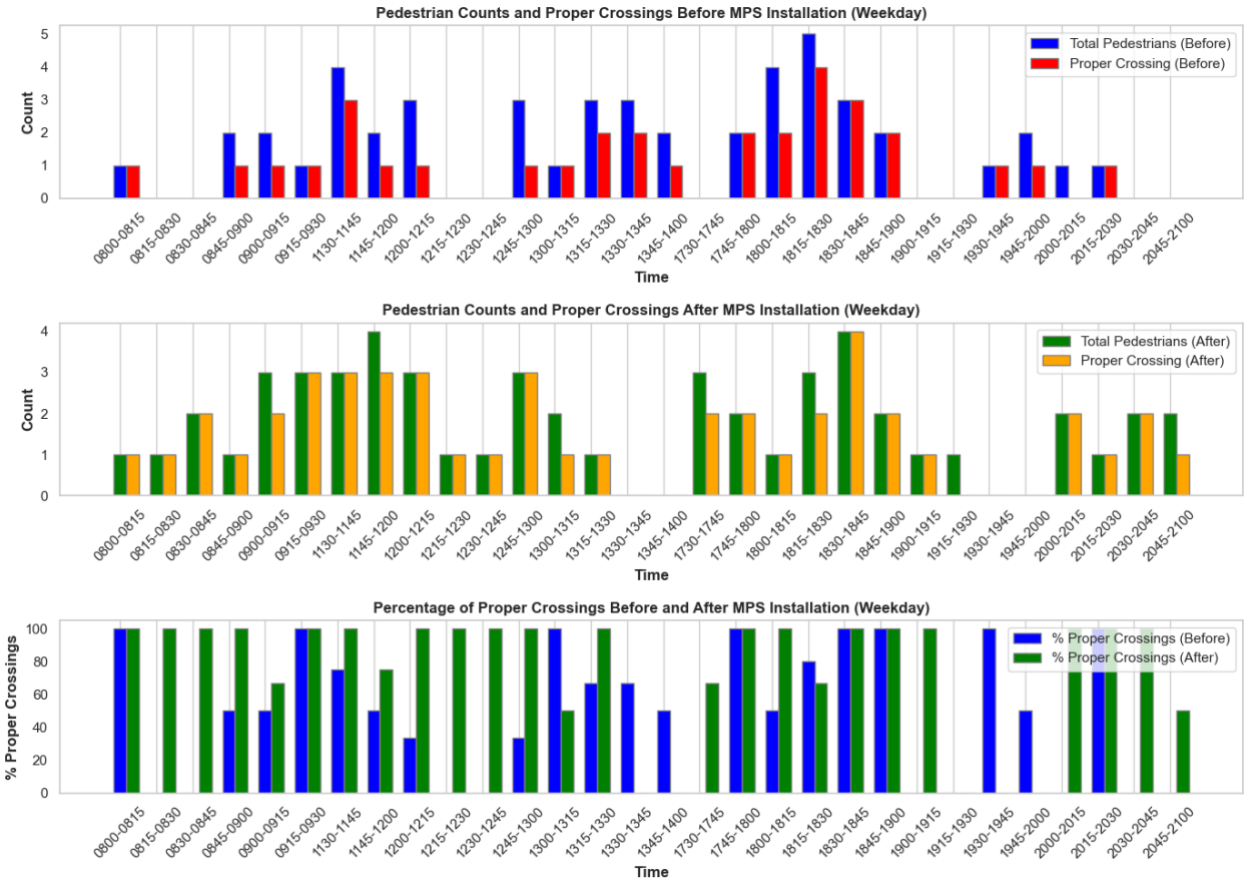

(a) Pedestrian count and proper crossing during the weekday

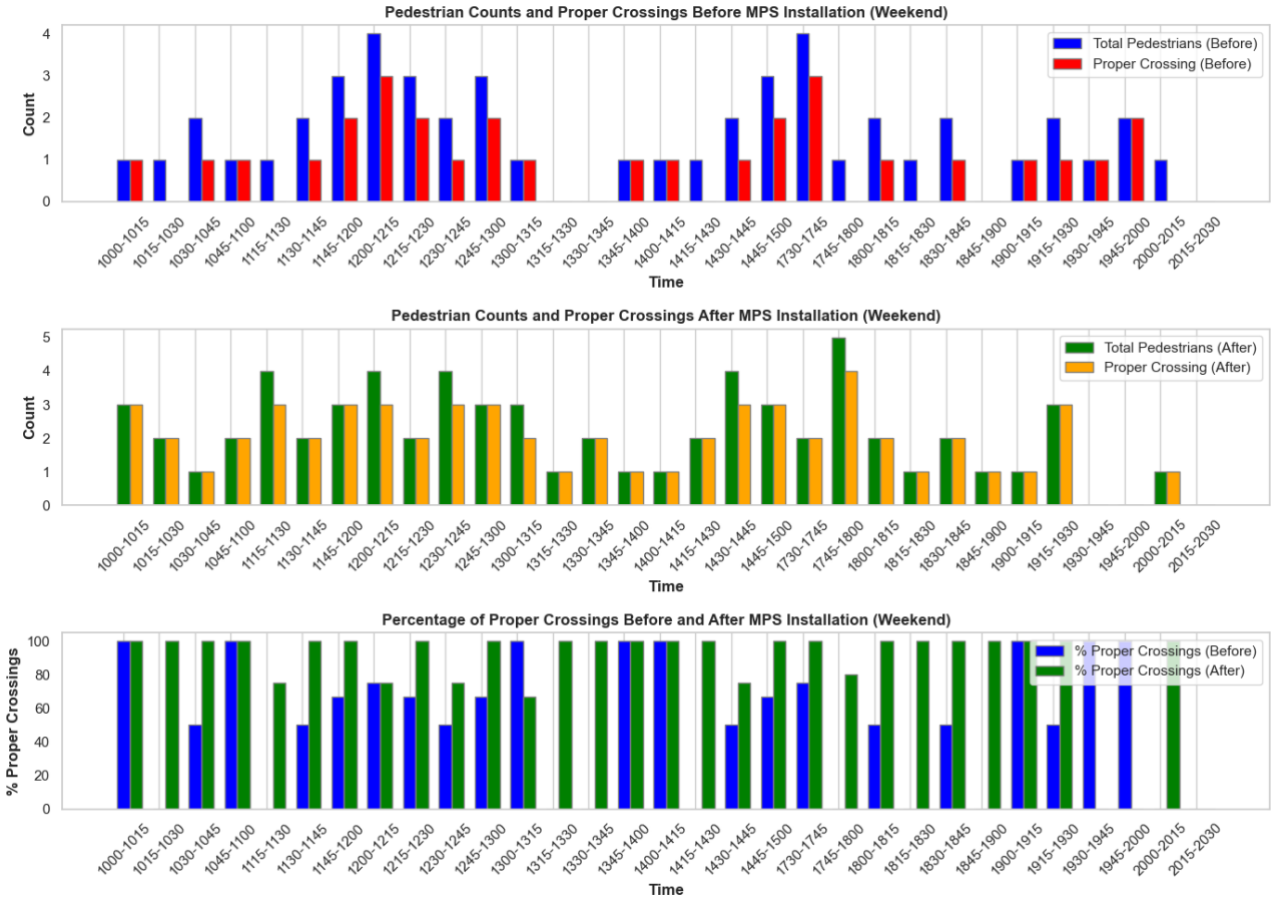

(b) Pedestrian count and proper crossing during the weekend

Figure 16 Pedestrian compliance before and after MPS installation (RRFB to MPS)

8. COMPARATIVE ANALYSIS OF UNTREATED SITES CONVERTED TO MPS

For this analysis, we used data from seven locations where there were previously no midblock system, but now MPSs have been installed (also refer to Table 3).

8.1 Leading vehicle speed

From **Figure 17**, it is observed that the leading vehicle speed, which refers to the speed of the vehicles that first interact with pedestrians, decreases after the installation of MPS. This reduction in vehicle speed after the MPS installation indicates an improvement in pedestrian safety, as drivers are likely becoming more cautious when approaching the crossing.

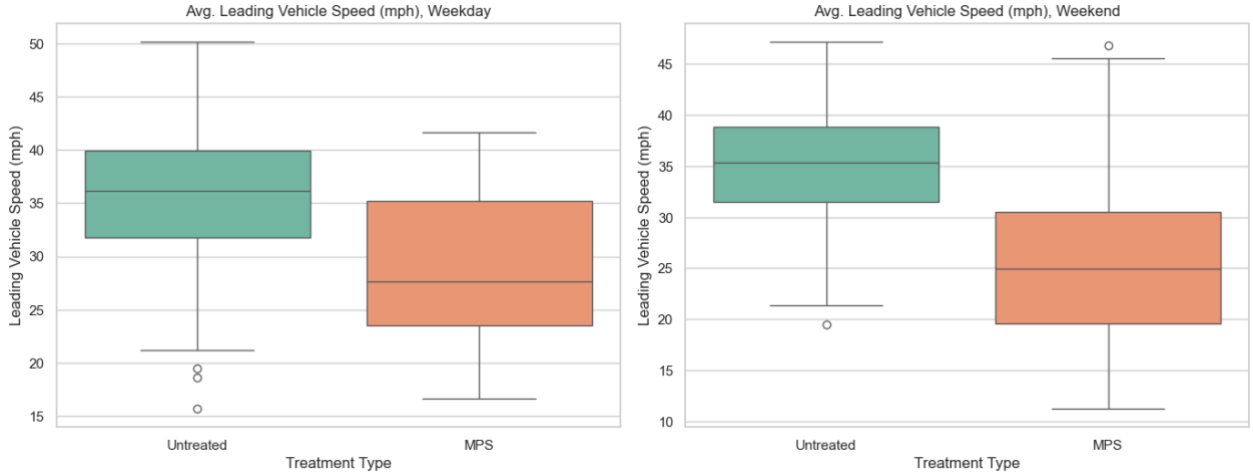

Figure 17 Average leading vehicle speed (untreated to MPS)

8.2 Surrogate Safety Measures (SSMs)

From **Figure 18** and **Table 6**, it is observed that all SSM values increase on both weekdays and weekends after the installation of MPS. This means that the MPS is improving safety. Higher SSM values show that drivers become more cautious, slow down, and give more space to the pedestrians. As a result, the risk of conflicts between vehicles and pedestrians is reduced, making the crossings safer.

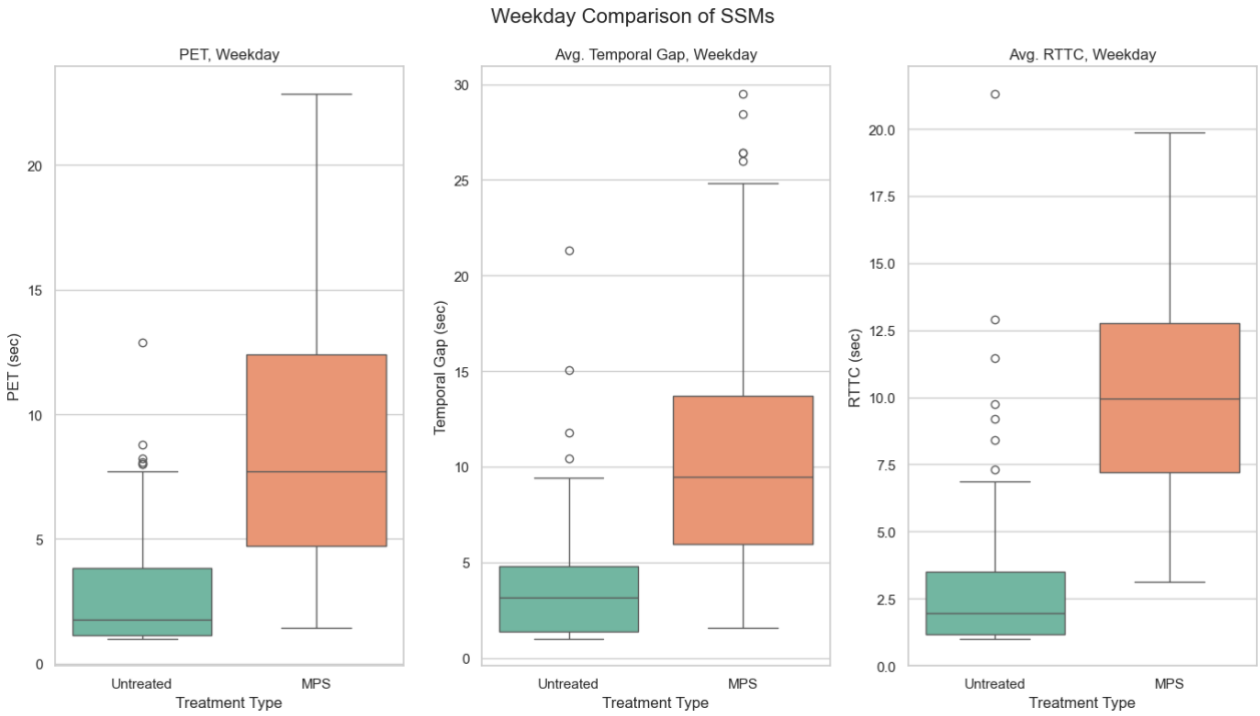

(a) Comparison of PET, Temporal Gap and RTTC on weekday

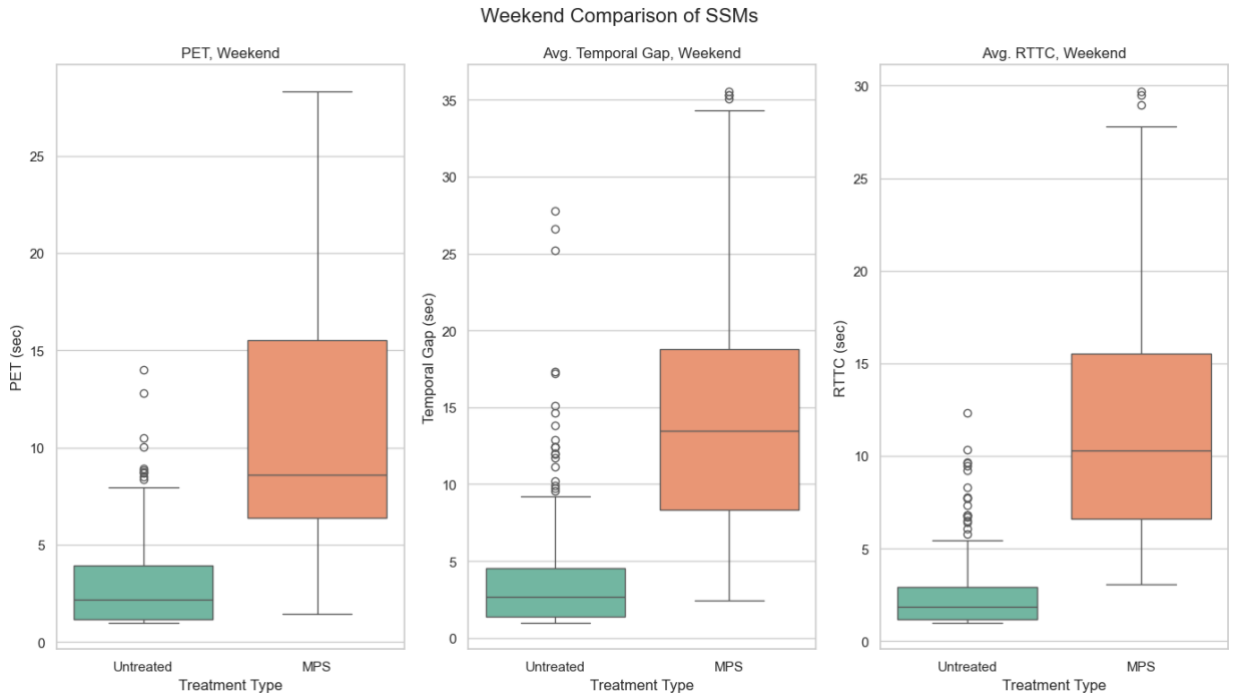

(b) Comparison of PET, Temporal Gap and RTTC on weekend

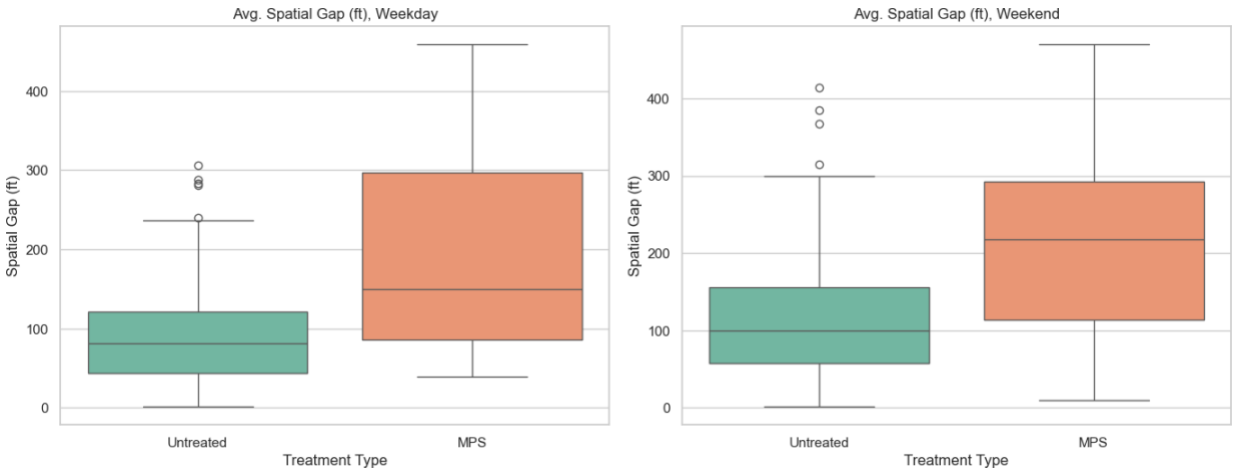

(c) Average Spatial Gap both on weekday and weekend

Figure 18 Comparison by different Surrogate Safety Measures (untreated to MPS)

8.3 Driver yielding behavior

Figure 19 shows the driver yielding rate on both weekdays and weekends, comparing conditions before and after the installation of MPS. The box plots indicate that the yielding rate significantly increases after MPS installation (96%-98%). On the other hand, before MPS installation, the yielding rates are much lower, with greater variability, especially on weekdays. This suggests that MPS installations lead to a more consistent and higher driver compliance in yielding to pedestrians.

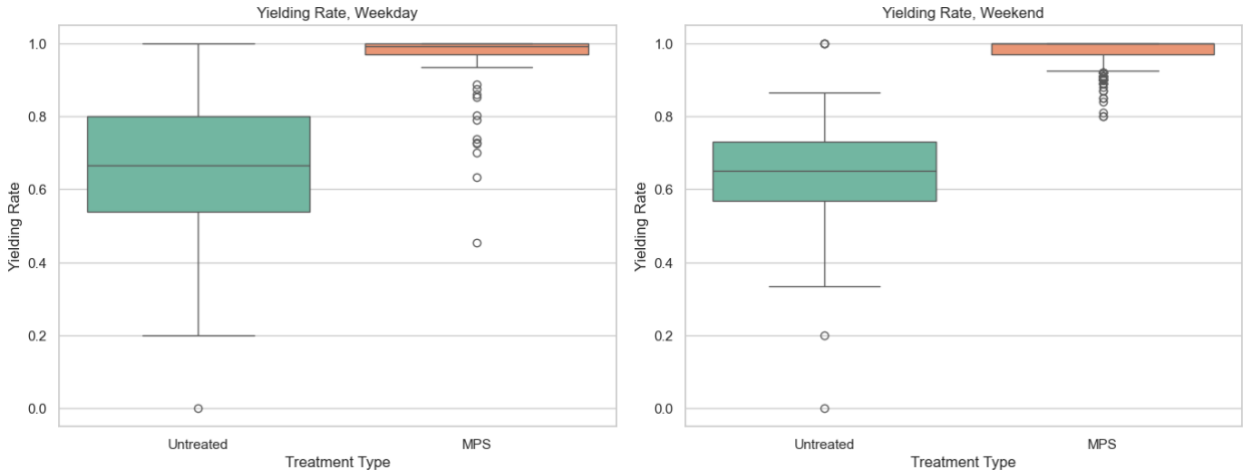

Figure 19 Driver yielding rate (untreated to MPS)

8.4 Pedestrian behavior

These locations previously did not have any signal systems, therefore the pedestrian compliance rate when there were no signals was excluded from the analysis. After installing the MPS, it was found that more than 95 percent of pedestrians followed traffic rules (please see **Figure 20**), crossing the road after activating the pedestrian signal phase. This high compliance rate indicates that the MPS installation has significantly improved pedestrian behavior, ensured safer road crossings and reducing the risk of vehicle-pedestrian conflicts. The effectiveness of the MPS in promoting proper crossing behaviors is clearly demonstrated by the substantial improvement in compliance.

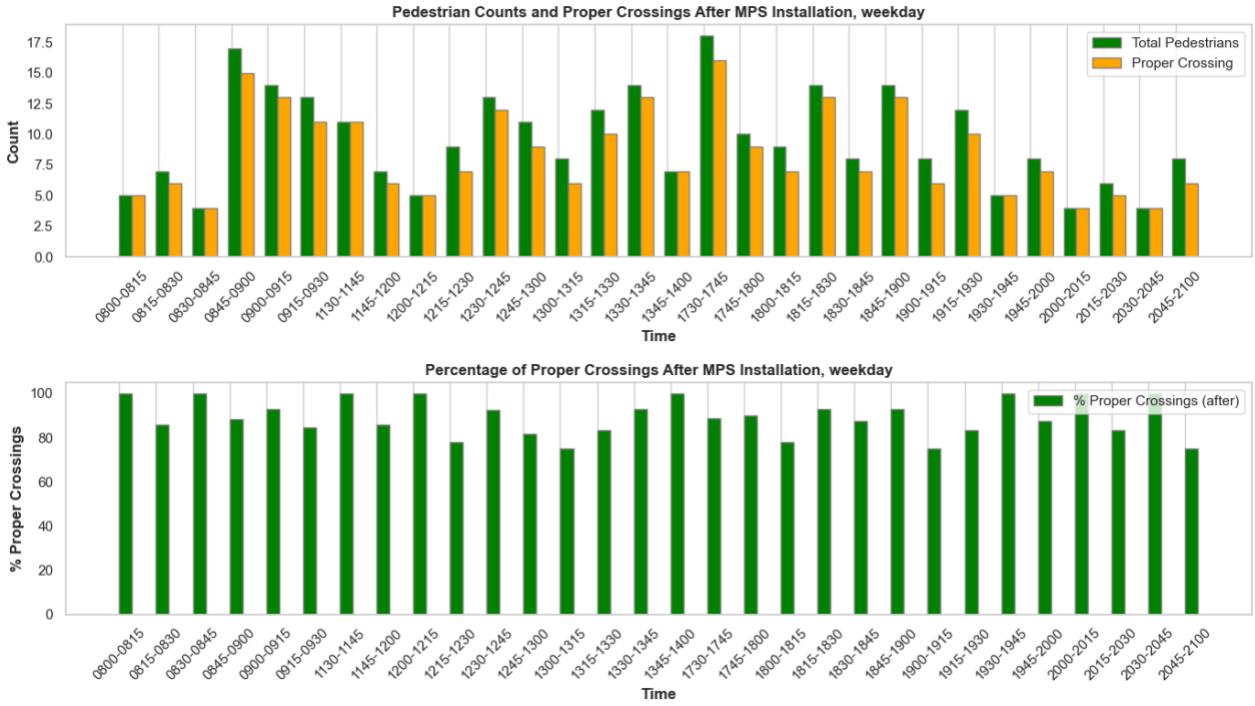

(a) Pedestrian count and proper crossing on weekday

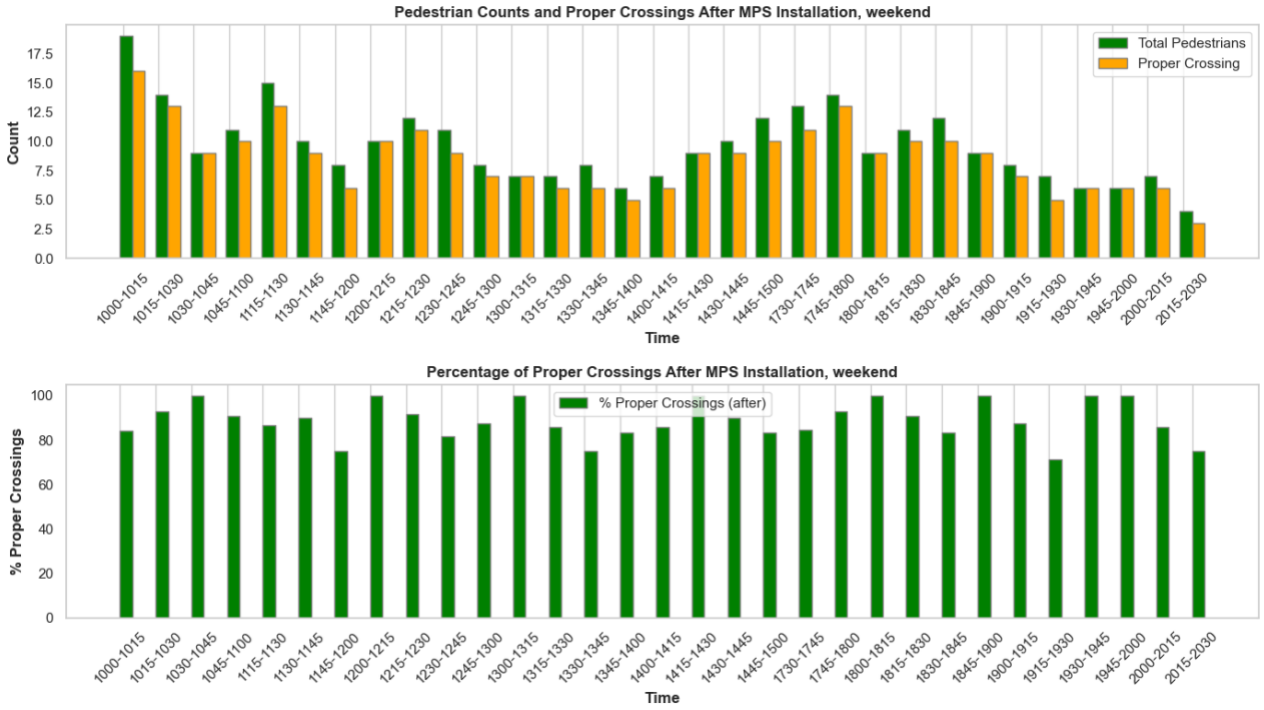

(b) Pedestrian count and proper crossing on weekend

Figure 20 Pedestrian compliance before and after MPS installation (untreated to MPS)

Table 6 Summary statistics of all variables (untreated to MPS)

Variable	Description	Observations (Untreated/MPS)	Untreated				MPS			
			Mean	Std. Dev.	Max.	Min.	Mean	Std. Dev.	Max.	Min.
Weekday										
Pedestrian count	Number of pedestrians per 15 minutes	224/224	3.49	4.36	13	0	4.5	3.91	18	4
Vehicle count	Number of vehicles per 15 minutes for both directions	224/224	95.23	31.67	130	14	101.84	26.39	199	32
Average leading vehicle speed	Average speed of leading vehicle before stopping in each lane, mph	145/226	36.52	7.16	67.18	15.69	28.90	6.59	41.62	16.67
PET	Post Encroachment Time is the time difference between when pedestrian and vehicle reach the conflict point, sec	145/226	2.77	2.17	12.87	0.12	9.50	6.0	26.21	0.43
Spatial gap	Spatial gap is the physical distance between a pedestrian and the nearest vehicle at a given time frame, feet	145/226	91.24	63.38	305.8	1.46	207.55	139.96	543.39	9.35
Temporal gap	The spatial gap is divided by the instantaneous vehicle speed to obtain the temporal gap, sec	145/226	3.65	2.90	21.32	0.01	11.54	7.74	35.76	0.59

Table 6 Summary statistics for all variables (Untreated to MPS) (cont.)

Variable	Description	Observations (Untreated /MPS)	Untreated				MPS			
			Max.	Min.	Max.	Min.	Max.	Min.	Max.	Min.
RTTC	Relative Time to Collision (RTTC) measures the time difference between the arrival of the first and second road users at a potential conflict point, assuming they maintain their current speeds, sec	145/226	2.91	2.68	21.32	0.01	10.75	4.46	24.53	0.11
Vehicle yielding rate	Yielding rate = Vehicles stopped or slowed / total leading vehicles	145/226	0.65	0.18	1.0	0	0.96	0.09	1.0	0.45
Weekend										
Pedestrian count	Number of pedestrians per 15 minutes	224/224	3.9	3.70	11	0	4.64	3.19	19	4
Vehicle count	Number of vehicles per 15 minutes for both directions	224/224	121.40	19.92	180	46	127.20	27.59	178	39
Average leading vehicle speed	Average speed of leading vehicle before stopping in each lane, mph	114/198	35.11	5.78	58.32	19.45	25.52	7.78	48.73	11.21
PET	Post Encroachment Time is the time difference between when pedestrian and vehicle reach the conflict point, sec	114/198	2.95	2.25	13.95	0.50	11.95	7.64	32.41	0.45

Table 6 Summary statistics for all variables (Untreated to MPS) (cont.)

Variable	Description	Observations (Untreated /MPS)	Untreated				MPS			
			Max.	Min.	Max.	Min.	Max.	Min.	Max.	Min.
Spatial gap	Spatial gap is the physical distance between a pedestrian and the nearest vehicle at a given time frame, feet	114/198	111.18	71.29	419.53	1.32	217.78	123.89	578.60	9.49
Temporal gap	The spatial gap is divided by the instantaneous vehicle speed to obtain the temporal gap, sec	114/198	3.79	3.78	27.77	0.01	15.49	8.73	38.39	0.44
RTTC	RTTC measures the time difference between the arrival of the first and second road users at a potential conflict point, assuming they maintain their current speeds, sec	114/198	2.43	1.85	12.3	0.09	12.38	7.26	36.63	0.17
Vehicle yielding rate	Yielding rate = Vehicles stopped or slowed / total leading vehicles	114/198	0.64	0.11	1.0	0	0.98	0.04	1	0.50

8.5 Mann-Whitney-Wilcoxon tests

The Mann-Whitney-Wilcoxon tests (also known as Mann-Whitney U test; or the Wilcoxon rank-sum test) is an analog to the two-sample t-test for independent samples, in which the actual values are replaced by rank scores. Under the Mann-Whitney-Wilcoxon tests, here, the responses are assumed to be continuous. The null hypothesis assumes that the medians from both data are the same. If the null hypothesis is rejected, i.e., p-value < 0.05, then the medians and the relevant samples are considered to be significantly different. The Mann-Whitney-Wilcoxon tests were chosen over the t-test because the

data in this study were not normally distributed, making non-parametric methods more appropriate (Anwari et al., 2023, Ahsan et al., 2024).

Table 7 Results of the Mann-Whitney-Wilcoxon tests

Variables	RRFB vs MPS		Untreated vs MPS		PHB vs MPS		Weekday vs Weekend (RRFB to MPS)		Weekday vs Weekend (Untreated to MPS)		Weekday vs Weekend (PHB to MPS)	
	Test statistic	P-value	Test statistic	P-value	Test statistic	P-value	Test statistic	P-value	Test statistic	P-value	Test statistic	P-value
Avg. leading vehicle speed	1384.0*	<0.001	4752.0*	<0.001	3018.5*	<0.001	894.7*	<0.001	1800.0	0.246	1280.0*	<0.001
PET	477.0*	<0.001	683.0*	<0.001	1465.0*	<0.001	539.0*	0.014	1184.0*	<0.001	5634.0	<0.001
Spatial gap	498.0*	<0.001	5860.0*	<0.001	2603.4*	<0.001	0.0	1.122	1815.0	0.271	8463.0*	<0.001
Temporal gap	301.0*	<0.001	1435.0*	<0.001	1380.0*	<0.001	385.0*	<0.001	1664.0	0.089	6572.0*	<0.001
RTTC	313.0*	<0.001	398.0*	<0.001	1831.0	0.392	281.0*	<0.001	1330.0*	0.002	8184.0	0.239
Vehicle yielding rate	77.5*	<0.001	63.0*	<0.001	204.3*	<0.001	33.0	0.378	81.0	0.193	86.8	0.170

* Significant at 95% confidence level.

Table 7 summarizes the results of Mann-Whitney-Wilcoxon tests comparing pedestrian and vehicles behavior across various scenarios (RRFB vs MPS, untreated vs MPS, PHB vs MPS and weekday vs weekend). For RRFB vs MPS, PHB vs MPS and untreated vs MPS comparisons, significant differences were observed across all variables. This indicates that the installation of MPS at both previously untreated locations and the site that was equipped with RRFB or PHB led to substantial improvements in pedestrian safety and driver behavior. For the weekday vs weekend comparison, only data collected after MPS installation were considered. In the RRFB to MPS, PHB to MPS and untreated to MPS scenario, significant differences were also observed. These findings indicate that pedestrian and vehicle behaviors varied between weekdays and weekends following the installation of MPS.

9. COMPARATIVE EVALUATION OF VEHICLE DELAYS

This study evaluates vehicle delays at various treatment sites, specifically focusing on transitions to MPS. The analysis considers four key site transitions to assess the effectiveness of MPS in reducing delays: Flashing Beacon to MPS, RRFB to MPS, Untreated to MPS, and PHB to MPS (refer to **Table 2**). These transitions were selected to compare delay patterns across different pedestrian treatment types and determine the relative performance of MPS in improving traffic flow.

9.1 Delay Calculation

Methodology for calculating vehicle delays (Anwari et al., 2024):

a. *Average Vehicle Speed Calculation:*
   The average vehicle speed at a particular site was calculated during periods when vehicles faced no obstructions. In this study, obstructions refer to pedestrians crossing the road. This unobstructed speed is defined as the vehicle speed without pedestrian interactions.
b. *Selection of Delay Zone:*
   A delay zone of 250 feet was defined, comprising a 200 feet upstream section and a 50 feet downstream section of the stop line. This distance was based on the maximum observed queue length across all sites, ensuring consistency for comparing delays across locations.
c. *Calculation of Travel Time and Space Mean Speed:*
   Vehicle trajectory data was used to calculate the time taken by vehicles to traverse the 250-feet delay zone. The space mean speed for each interacting vehicle was then determined based on this travel time.
d. *Delay Formula:*
   Vehicle delay was calculated using the following formula:

$$\text{Delay} = \left(\frac{\text{Delay zone length}}{\text{Space mean speed}} - \frac{\text{Delay zone length}}{\text{Free Flow Speed}}\right)$$

The delay was calculated for each vehicle individually and then averaged across all vehicles involved in an interaction with pedestrians.

e. *Validation*

The calculated delays were manually cross-checked against video footage for each pedestrian–vehicle interaction to validate the accuracy of the results.

9.2 Findings

From **Figure 21**, it is evident that delays at MPS locations are higher compared to Flashing Beacon, RRFB, and untreated sites. This is an expected outcome due to the differing functionalities of these systems. MPSs require drivers to come to a complete stop when the signal is red, leading to increased delays. In contrast, RRFBs and Flashing Beacons only alert drivers to slow down and yield to pedestrians, and a complete stop is not mandatory if no pedestrians are present, resulting in lower delays. At untreated sites, where there are no signal systems or mandatory stops, delays are naturally the lowest. Moreover, the delay distributions across all cases after MPS installation are skewed towards higher values, reflecting the longer delays experienced (refer to **Figure 21**). The variance in delays also decreases following MPS implementation, indicating more consistent and uniform stopping behavior among drivers, aligning with the compliance required by the MPS system. Compared to untreated and RRFB treatments, the difference in delays between PHB and MPS is not substantial. Nevertheless, the delay distribution after MPS installation is lower and more concentrated than PHB, suggesting improved traffic flow and reduced delays under MPS conditions.

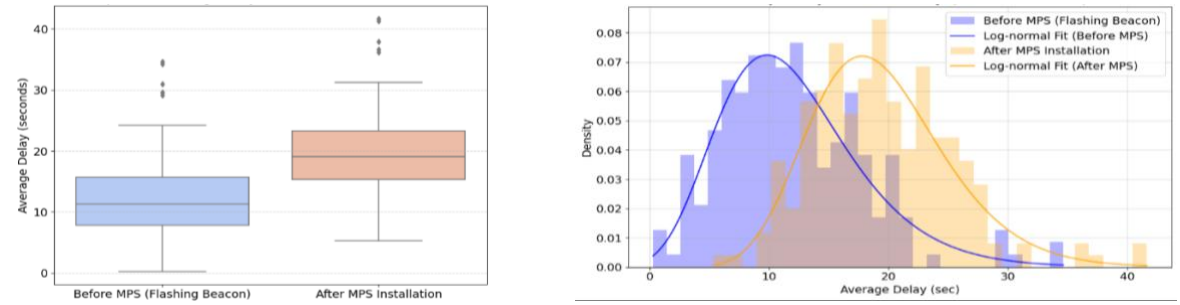

(a) Comparison of average delays and distributions before (Flashing Beacon) and after mps installation

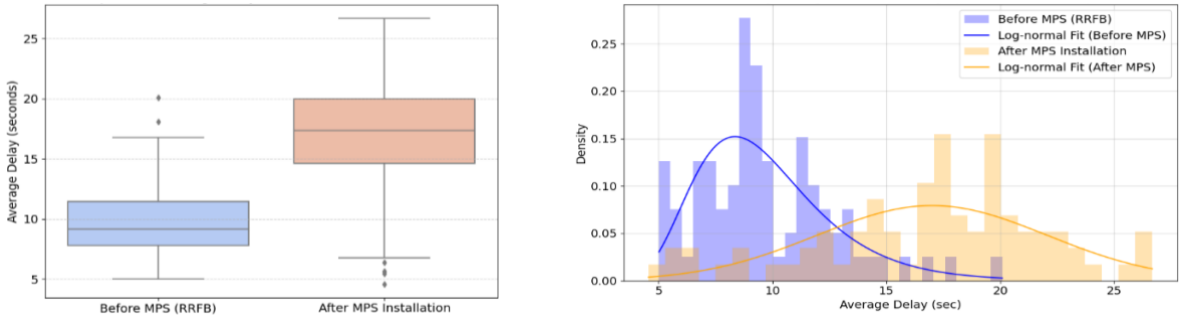

(b) Comparison of average delays and distributions before (RRFB) and after mps installation

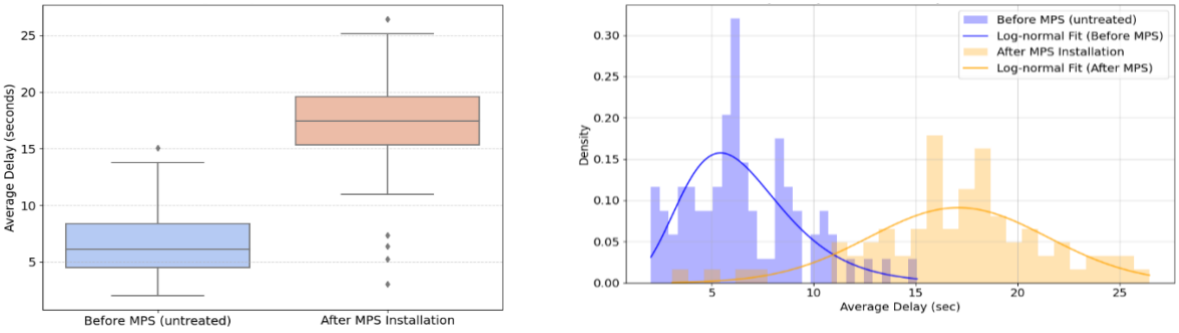

(c) Comparison of average delays and distributions before (untreated) and after mps installation

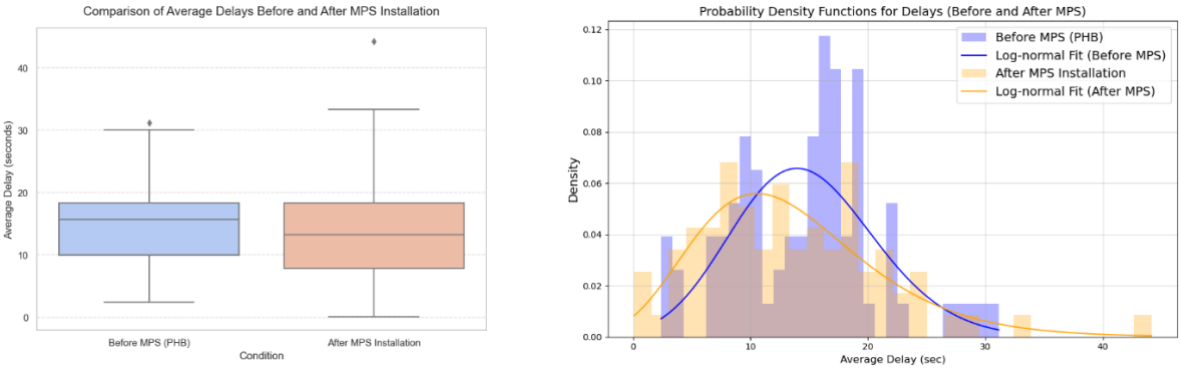

(d) Comparison of average delays and distributions before (PHB) and after mps installation

Figure 21 Comparative analysis of average delays and distributions before and after MPS installation

The Mann-Whitney-Wilcoxon test results (refer to **Table 8**) indicate that there are statistically significant differences in vehicle delays before and after the implementation of MPS across all pairs (Flashing Beacon, RRFB and untreated sites vs. MPS). However, the difference in delays between PHB and MPS was not statistically significant.

Table 8 Results of the Mann-Whitney-Wilcoxon tests on delays (sec) of before-after MPS treatment

Pair	**Test statistic**	**p-value**
Flashing Beacon vs MPS	7287*	<0.001
RRFB vs MPS	5282*	<0.001
Untreated vs MPS	4320*	<0.001
PHB vs MPS	5692	0.114
* Significant at 95% confidence level.		

10. COMPARATIVE EVALUATION OF REAR-END CONFLICTS

10.1 Site selection

This study analyzed vehicle–vehicle rear-end conflicts at various signalized locations. Specifically, two sites transitioned from PHB to MPS (Locations #7 and #9), with 1,833 and 1,929 observations respectively. Two sites transitioned from untreated to MPS (Locations #4 and #12), with 1,693 and 1,801 observations respectively, totaling 4,582 observations. One site transitioned from a RRFB to MPS (Location #11), with 1,147 and 1,378 observations from each approach, totaling 2,709 observations. Since capturing such measures requires multiple camera setups and locations that allow for convenient and secure camera placement, the research team carefully selected these sites after confirming their suitability for comprehensive video data collection.

10.2 Used metrics

Time to Collision (TTC) and Deceleration Rate to Avoid Collision (DRAC) were individually used as surrogate safety measures to assess rear-end conflicts. Only consider those vehicles that interact with pedestrians.

Time to Collision (TTC)

To estimate the risk of a potential collision between two vehicles, TTC is calculated. TTC represents the time it will take for two vehicles to collide if they continue at their current velocities and neither changes their trajectory or speed (Arun et al., 2021). The TTC is given by:

$$TTC = \frac{d}{v_{rel}}$$

Where v_{rel} is the relative speed of two conflicting vehicle, and d represents the distance between the two vehicles. Distance d is determined by the edge-to-edge distance of the two bounding boxes.

Deceleration Rate to Avoid Collision (DRAC)

DRAC represents the required deceleration rate for a vehicle to avoid a potential collision (Fu & Sayed, 2021). For vehicles traveling along the same path, DRAC can be calculated using the following equation.

$$DRAC = \frac{v_{rel}^2}{2d}$$

The analysis revealed from the above-mentioned location with that TTC values were generally higher after MPS installation compared to PHB, RRFB, and untreated sites, indicating improved safety margins. Conversely, DRAC values were lower at MPS locations, further supporting the reduction in conflict severity (refer to **Figure 22**). Since pedestrian and vehicle volumes remained relatively stable before and after the implementation, normalization was not required.

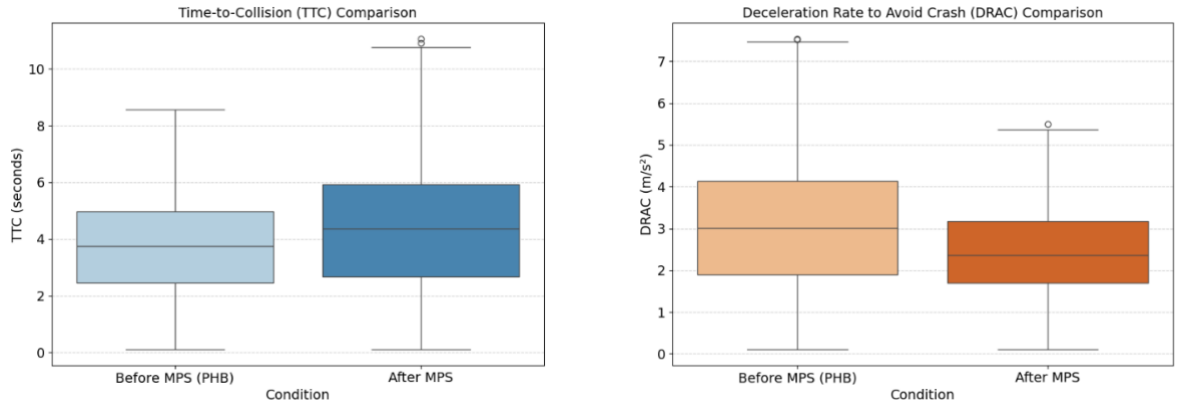

(a)

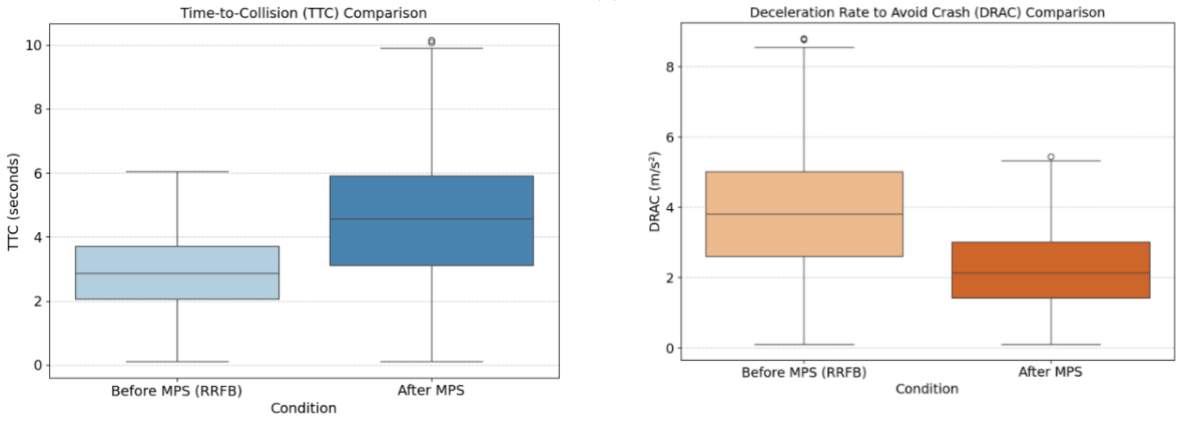

(b)

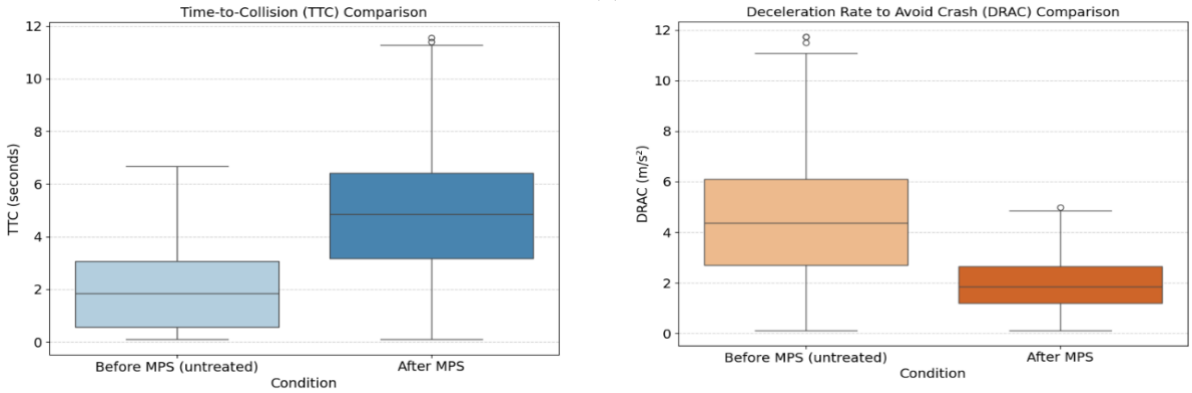

(c)

Figure 22 Comparison of TTC and DRAC at different mid-block signals (a) PHB to MPS, (b) RRFB to MPS and (c) Untreated to MPS

For classification of conflict categories, the following thresholds were applied:

- **TTC**:
  - ≤ 1 second: *Serious conflict*
  - 1 < TTC ≤ 3 seconds: *Moderate conflict*
  - >3 seconds: *No conflict*
- **DRAC**:
  - ≥ 4 m/s²: *Serious conflict*
  - 2 ≤ DRAC < 4 m/s²: *Moderate conflict*
  - < 2 m/s²: *No conflict*

Table 9 Rear-end conflict categories at different signal types.

SSMs	Signal types	Serious conflicts (%)	Moderate conflicts (%)
TTC	PHB	4.8	7.6
	MPS	3.3	4.2
DRAC	PHB	4.1	6.9
	MPS	2.9	4.8
TTC	RRFB and Flashing Beacon	9.3	15.5
	MPS	3.6	5.6
DRAC	RRFB and Flashing Beacon	10.2	14.8
	MPS	3.8	11.7
TTC	Untreated	10.9	15.8
	MPS	2.7	6.1
DRAC	Untreated	9.8	13.8
	MPS	2.5	7.7

10.2 Findings

As presented in **Table 9**, MPS implementation consistently reduced the percentage of both serious and moderate rear-end conflicts across all treatment transitions. The most notable improvements were observed at sites that transitioned from RRFB and Flashing Beacon and from untreated conditions to MPS. For example, serious TTC conflicts dropped from 9.3% to 3.6%, and moderate TTC conflicts from 15.5% to 5.6% after transitioning from RRFB and Flashing Beacon to MPS. Similarly, DRAC-based serious conflicts reduced from 10.2% to 3.8%, and moderate conflicts from 14.8% to 11.7% in the same transition. The untreated sites showed an even more significant reduction, with serious TTC conflicts dropping from 10.9% to 2.7%, and DRAC conflicts from 9.8%

to 2.5%. Although the PHB to MPS transition showed relatively smaller differences than other signals, the overall trend confirms that MPS installations contribute to a measurable reduction in rear-end conflicts.

11. LONG-TERM EVALUATION OF MPS

As requested by FDOT and beyond the original scope of the project, the long-term effects of MPS were also evaluated. The first MPS became operational in Miami (Location 14, as listed in **Table 2**), which was previously an uncontrolled crossing. The research team collected data prior to the installation and immediately after its implementation in November 2022. To assess the long-term impact of the MPS, additional data were collected at the same location in September 2024.

11.1 Leading vehicle speed

Analysis revealed that at the previously uncontrolled site, vehicles that first interacted with pedestrians (i.e., leading vehicles) often traveled above the posted speed limit of 30 mph. However, following the installation of the MPS, leading vehicle speeds decreased to below the speed limit (see **Table 10** and **Figure 23**). No statistically significant difference was observed between the immediate and long-term post-installation periods. This may be attributed to the fact that drivers and pedestrians quickly adapted to the MPS, as it operates similarly to conventional traffic signals.

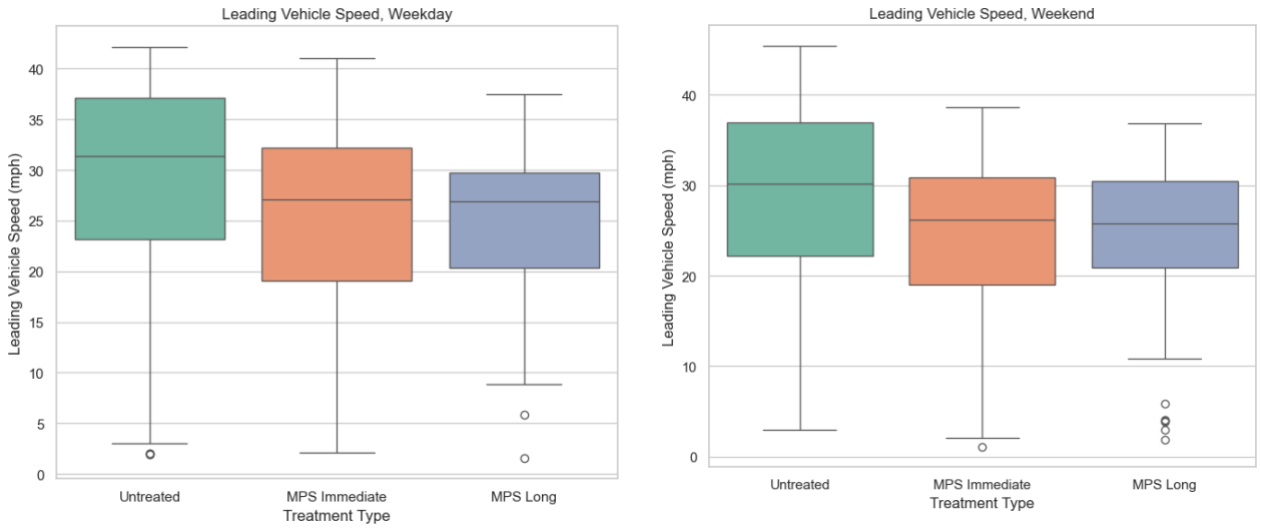

Figure 23 Average leading vehicle speed (long term effect of MPS)

11.2 Surrogate Safety Measures (SSMs)

To assess the safety impact of MPS installations, surrogate safety measures such as PET, Temporal Gap, RTTC, and Spatial Gap were analyzed (refer to **Figure 24** and **Table 10**). Results indicate that immediately after MPS installation, all SSMs improved significantly compared to the

uncontrolled condition, suggesting safer pedestrian-vehicle interactions. These improvements remained consistent in the long-term data, indicating that the MPS continued to promote safer behaviors over time. No statistically significant differences were found between the immediate and long-term post-installation periods for PET, RTTC, or Spatial Gap. This consistency suggests that the MPS's safety benefits are sustained over time.

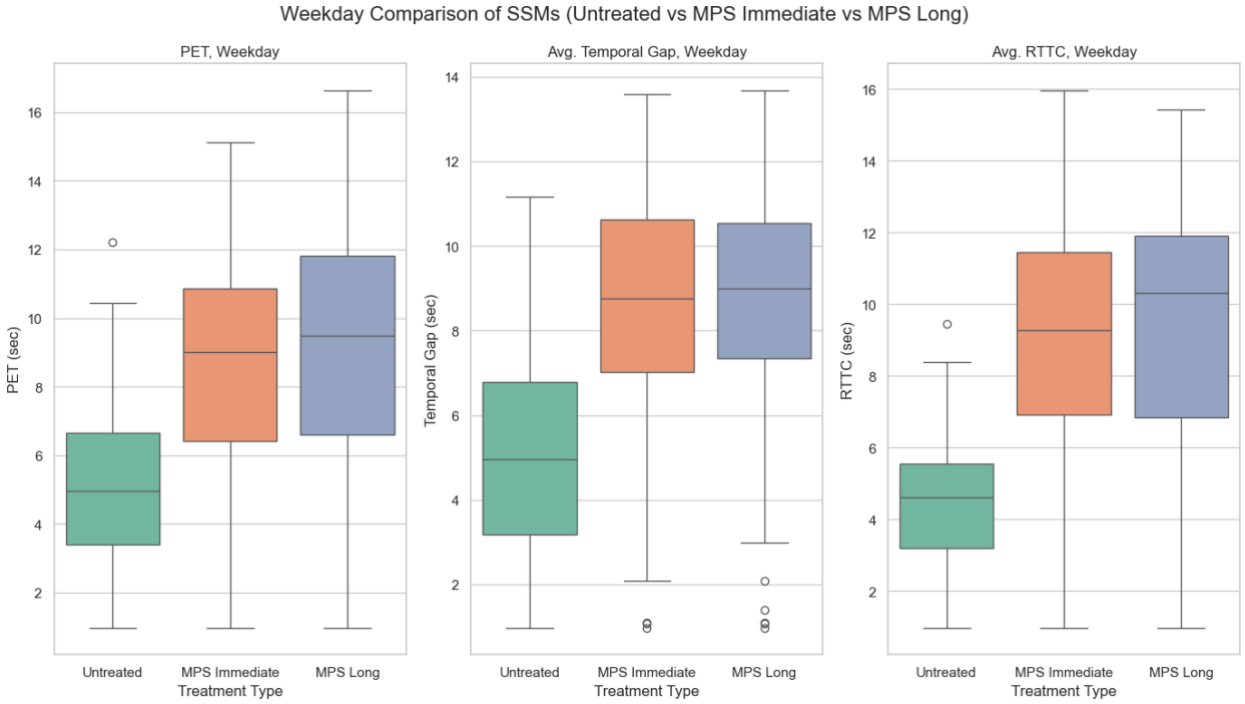

(a) Comparison of PET, Temporal Gap and RTTC on weekday

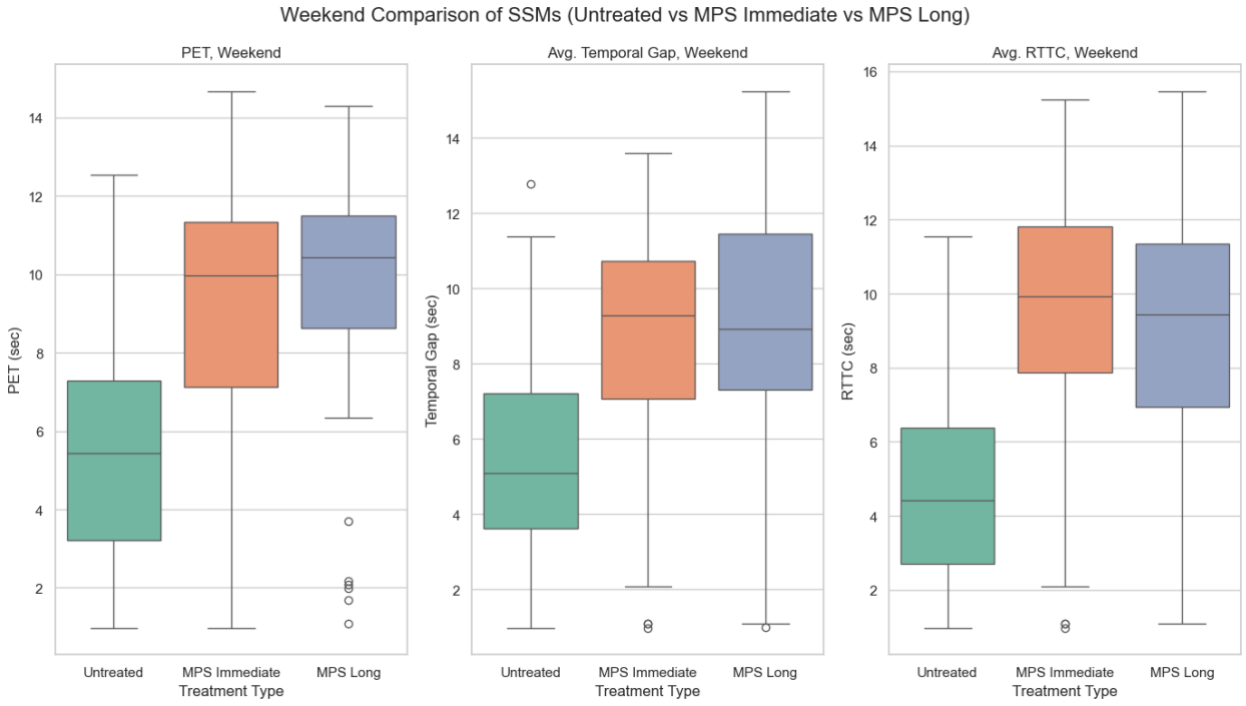

(b) Comparison of PET, Temporal Gap and RTTC on weekend

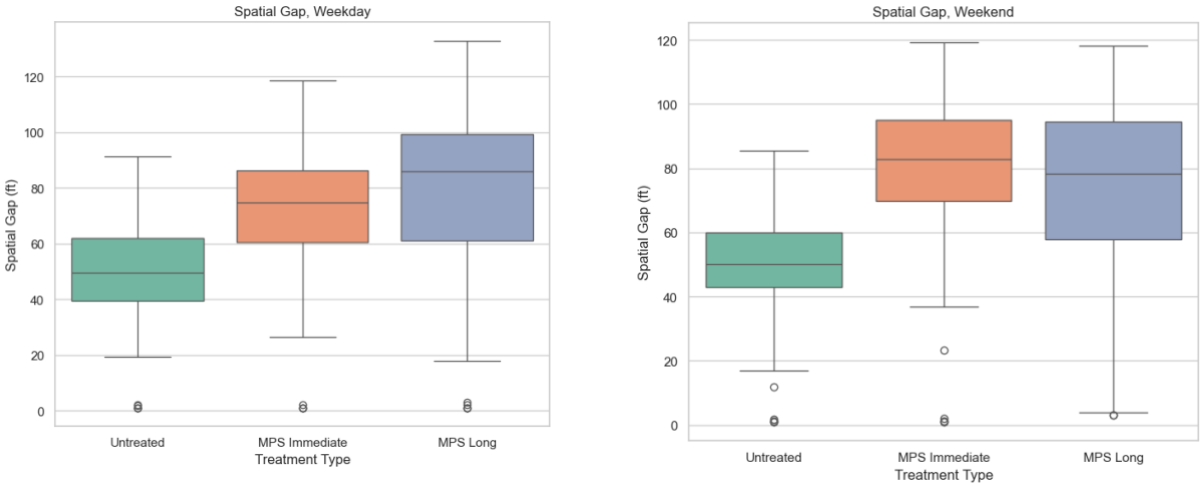

(c) Average Spatial Gap both on weekday and weekend

Figure 24 Comparison by different Surrogate Safety Measures (long term effect of MPS)

11.3 Driver and pedestrian behavior

Following the installation of the MPS, notable improvements were observed in both driver and pedestrian behavior. The driver yielding rate increased to approximately 97% (refer to **Figure 25**), indicating a significant improvement in compliance with pedestrian right-of-way. Similarly, the

pedestrian compliance rate—defined as the percentage of pedestrians who activated the signal and crossed only after activation—also reached around 97%. These high compliance rates remained consistent over the long term, suggesting sustained behavioral change. Minor instances of non-compliance may be attributed to drivers or pedestrians who are either unfamiliar with the MPS operation or intentionally choose to disregard the signal. Nevertheless, the consistently high rates indicate that the majority of road users are adapting well and adhering to the rules, demonstrating the effectiveness of the MPS in promoting safe crossing behavior.

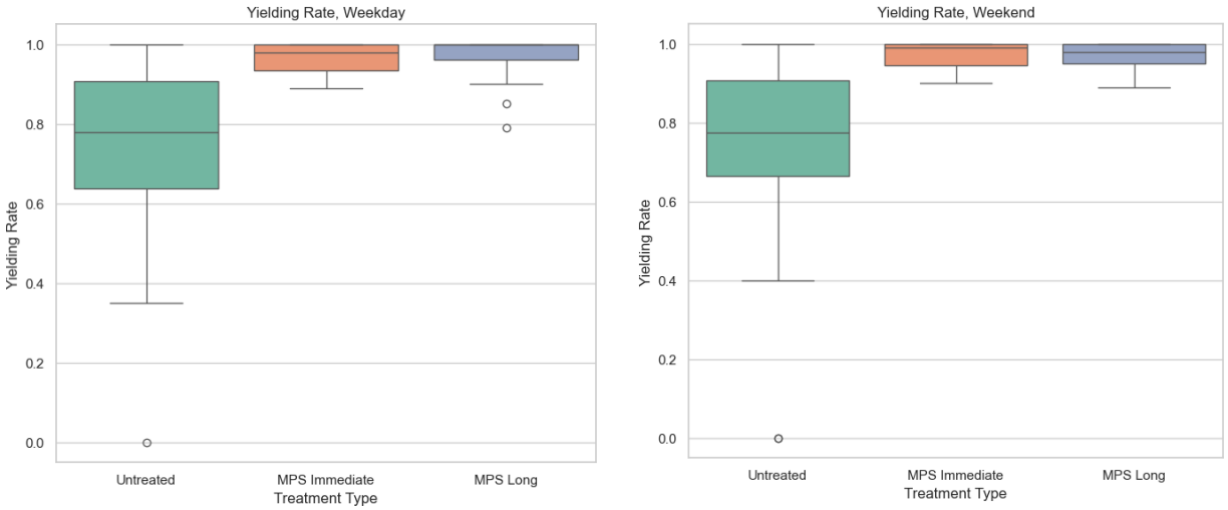

Figure 25 Driver yielding rate (long term effect of MPS)

Table 10 Long -term effect of MPS

Variable	Description	Untreated				MPS (immediate)				MPS (long term)			
		Mean	Std. Dev.	Max.	Min.	Mean	Std. Dev.	Max.	Min.	Mean	Std. Dev.	Max.	Min.
Weekday													
Pedestrian count	Number of pedestrians per 15 minutes	4.37	2.48	11	0	4.88	2.80	13	0	4.50	2.64	12	0
Vehicle count	Number of vehicles per 15 minutes for both directions	90.33	28.83	124	19	97.34	31.82	136	24	88.49	19.64	153	17
Average leading vehicle speed	Average speed of leading vehicle before stopping in each lane, mph	32.27	6.39	51.38	1.62	27.43	4.47	41.49	1.83	27.38	3.98	38.83	1.08
PET	Post Encroachment Time is the time difference between when pedestrian and vehicle reach the conflict point, sec	4.79	2.97	12.87	0.89	9.82	4.72	16.24	1.07	9.63	4.83	18.49	1.63
Spatial gap	Spatial gap is the physical distance between a pedestrian and the nearest vehicle at a given time frame, feet	48.29	21.48	89.42	1.38	78.29	18.38	117.39	2.35	84.79	20.25	129.4	1.48
Temporal gap	The spatial gap is divided by the instantaneous vehicle speed to obtain the temporal gap, sec	4.30	2.74	17.53	0.73	8.70	3.68	17.68	0.92	9.03	3.28	15.39	0.84
RTTC	Relative Time to Collision (RTTC) measures the time difference between the arrival of the first and second road users at a potential conflict point, assuming they maintain their current speeds, sec	4.86	2.08	11.79	0.48	9.80	4.02	16.10	0.39	10.17	3.18	16.78	0.37
Vehicle yielding rate	Yielding rate = Vehicles stopped or slowed / total leading vehicles	0.76	0.32	1	0	0.97	0.08	1.0	0.70	0.975	0.06	1	0
Vehicle delays	Vehicle delays per interaction, sec	6.68	4.72	29.4	1.28	17.83	5.72	31.84	1.35	18.02	4.79	30.29	2.63

Table 10 Long -term effect of MPS (cont.)

Variable	Description	Untreated				MPS (immediate)				MPS (long term)			
		Mean	Std. Dev.	Max.	Min.	Mean	Std. Dev.	Max.	Min.	Mean	Std. Dev.	Max.	Min.
Pedestrian compliance rate	Ratio of pedestrian cross the road after activating signal	-	-	-	-	0.97	0.09	1	0	0.97	0.08	1	0
Weekend													
Pedestrian count	Number of pedestrians per 15 minutes	3.80	3.21	12	0	4.12	3.25	11	0	4.25	2.97	13	0
Vehicle count	Number of vehicles per 15 minutes for both directions	101.45	22.26	154	24	99.67	20.30	145	28	103.4	25.38	148	31
Average leading vehicle speed	Average speed of leading vehicle before stopping in each lane, mph	32.36	8.82	48.49	2.45	27.83	9.57	45.29	1.97	28.10	6.38	38.82	1.25
PET	Post Encroachment Time is the time difference between when pedestrian and vehicle reach the conflict point, sec	5.29	3.33	13.62	0.71	10.07	3.95	16.49	0.55	10.86	2.99	15.46	0.28
Spatial gap	Spatial gap is the physical distance between a pedestrian and the nearest vehicle at a given time frame, feet	47.80	23.58	84.38	1.12	82.66	18.49	118.26	1.11	78.48	20.44	118.39	1.08
Temporal gap	The spatial gap is divided by the instantaneous vehicle speed to obtain the temporal gap, sec	5.38	3.64	12.84	0.09	8.90	2.55	19.47	0.37	9.08	3.51	18.83	0.33
RTTC	RTTC measures the time difference between the arrival of the first and second road users at a potential conflict point, assuming they maintain their current speeds, sec	4.70	2.93	14.83	0.11	9.85	3.59	18.83	0.36	10.12	3.82	17.38	0.25

Table 10 Long -term effect of MPS (cont.)

Variable	Description	Untreated				MPS (immediate)				MPS (long term)			
		Mean	Std. Dev.	Max.	Min.	Mean	Std. Dev.	Max.	Min.	Mean	Std. Dev.	Max.	Min.
Vehicle yielding rate	Yielding rate = Vehicles stopped or slowed / total leading vehicles	0.78	0.35	1.0	0	0.98	0.11	1	0.75	0.97	0.09	1	0.78
Vehicle delays	Vehicle delays per interaction, sec	6.92	3.62	26.30	1.84	16.93	5.92	32.40	2.49	17.51	3.82	31.30	1.86
Pedestrian compliance rate	Ratio of pedestrian cross the road after activating signal	-	-	-	-	0.97	0.08	1	0	0.98	0.08	1	0

11.4 Summary of long-term evaluation of MPS

After the installation of the MPS, significant improvements were observed across all safety and behavioral measures. The long-term results remained consistent with the immediate post-installation outcomes, indicating that the effectiveness of the MPS was sustained over time. Both sets of results confirm that the MPS is a safe and reliable treatment for enhancing pedestrian safety at midblock crossings.

12. DETAIL SAFETY EVALUATION OF MPS, PHB, RRFB AND FLASHING BEACON

In this study, since MPSs have been newly implemented, there is no available post-implementation crash data. Waiting several years for sufficient crash data to assess their effectiveness would not be practical for implementing a potentially promising safety strategy. A more effective alternative involves using conflicts- (near misses) based surrogate safety measures (SSMs), such as PET, RTTC, and DRAC. These measures offer immediate insights into potential conflicts and near-misses, enabling faster and more accurate evaluation of safety interventions. This study addresses the limitations of traditional crash-based evaluations by utilizing vehicle-pedestrian conflict data. Furthermore, it applies the Conflict Modification Factors (CoMF) as an alternative metric to the conventional Crash Modification Factors (CMF) to assess safety improvements. The study also incorporates dynamic data, including vehicle speeds, pedestrian volumes, and traffic volumes, to provide a more detailed and accurate evaluation of safety performance. This method captures important interactions that traditional crash data often misses. In addition, the study compares the effectiveness of MPSs relative to other mid-block crossing treatments, such as PHB, RRFB, and Flashing Beacon.

12.1 Descriptive study

Previous studies have identified RTTC as one of the most effective SSMs for analyzing pedestrian-vehicle conflicts, outperforming other metrics such as PET, Spatial Gap, and Temporal Gap (Ahsan et al., 2024; Ahsan, Abdel-Aty, & Abdelrahman, 2025; Anwari et al., 2023; Chen et al., 2017). RTTC is particularly advantageous as it captures the entire interaction between pedestrians and vehicles, taking into account their actual speeds and trajectories (Ahsan et al., 2024; Ahsan, Abdel-Aty, & Abdelrahman, 2025). RTTC is calculated (Eq. 1) as the absolute difference between the Time to Collision for a vehicle (TTCv) and that for a pedestrian (TTCp):

$$\text{RTTC} = abs(TTCv - TTCp) \quad (1)$$

Where,

$$\text{TTCp} = \frac{Pedestrian\ distance\ from\ conflict\ point}{pedestrian\ speed}$$

$$\text{TTCv} = \frac{Vehicle\ distance\ from\ conflict\ point}{vehicle\ speed}$$

In this study, RTTC calculations considered only leading vehicles that first interacted with pedestrians, as trailing vehicles were unlikely to directly contribute to the conflict. The analysis

identified the initial point of potential contact between the vehicle and the pedestrian, whether it was the front-left or front-right corner of the vehicle. RTTC was computed using the average values of the last 10 frames (videos are 20 frames/second) recorded before the vehicle reached the conflict point or came to a stop, ensuring that the analysis focused on the most critical moments of interaction. To maintain data relevance, any TTCp, or TTCv values exceeding 10 seconds were not considered conflicts, as they allowed sufficient time for the driver or pedestrian to respond. Following the methodology from a previous study (Ahsan et al., 2025), RTTC thresholds were defined as follows: RTTC $\leq$ 1.0 represents serious conflicts, 1.0 < RTTC $\leq$ 3.0 represents moderate conflicts, and values exceeding 3.0 seconds were not considered conflicts. The total number of serious and moderate conflicts was recorded for each 30-minute interval (refer **Table 11**).

Table 11 Recorded serious and moderate conflicts from each study site.

#	District	Route	Treatment Type	Date of 'Before' Data Collection	Date of 'After' Data Collection	Before Period Serious Conflicts	Before Period Moderate Conflicts	After Period Serious Conflicts	After Period Moderate Conflicts
MPS sites									
1	Alachua	SR 26	Uncontrolled to MPS	Dec 19, Dec 21 2021	Sept 5, Sept 7, 2024	19	29	12	21
2	Alachua	SR 26	Uncontrolled to MPS	Nov 7, Nov 9 2021	Sept 5, Sept 7, 2024	18	27	9	17
3	Duval	SR 212	Uncontrolled to MPS	Oct 13, Nov 7 2021	Jan 25, Jan 27, 2024	19	25	10	16
4	Franklin	US 98	Uncontrolled to MPS	Oct 17, Oct 19 2021	April 13, April 15, 2024	16	27	8	20
5	Brevard	SR A1A	Uncontrolled to MPS	Sept 21, Sept 25 2021	Dec 19, Dec 23, 2023	15	26	7	17
6	Brevard	SR A1A	Uncontrolled to MPS	Sept 18, Sept 29 2021	Dec 23, 2023 Jan 4, 2024	14	19	8	15
7	Miami-Dade	SW 1st Street	Uncontrolled to MPS	Nov 21, Dec 01, 2021	Nov 6, 2022, and Jan 11, 2023	25	36	16	23
8	Alachua	SR 24A/SR 331	Flashing Beacon to MPS	Oct 13, Oct 17 2021	May 23, May 25, 2024	15	22	8	14
9	Marion	US 41	RRFB to MPS	July 10, July 12, 2021	Dec 7, Dec 9, 2023	18	27	12	18
10	St. Lucie	SR A1A	PHB to MPS	Sep 15, Oct 31 2021	Jan 16, Jan 18, 2025	18	26	14	21
11	St. Lucie	SR A1A	PHB to MPS	Sep 12, Nov 11 2021	Dec 19, Dec 21, 2024	16	15	13	13
12	St. Lucie	SR A1A	PHB to MPS	Sep 12, Nov 11 2021	Dec 19, Dec 21, 2024	11	17	9	14

Table 11 Recorded serious and moderate conflicts from each study site (cont.)

#	District	Route	Treatment Type	Date of 'Before' Data Collection	Date of 'After' Data Collection	Before Period Serious Conflicts	Before Period Moderate Conflicts	After Period Serious Conflicts	After Period Moderate Conflicts
MPS sites									
13	St. Lucie	SR A1A	PHB to MPS	Oct 28, Oct 31 2021	Jan 16, Jan 18, 2025	13	18	10	15
14	St. Lucie	SR A1A	PHB to MPS	Sept 12, Sept 14, 2021	Jan 16, Jan 18, 2025	15	17	13	14
Reference Sites/ Control sites									
1	St. Johns	SR 207	PHB	Sept 2. Sept 5, 2021	May 4, May 6, 2024	21	28	25	31
2	St. Johns	SR A1A	PHB	Sept 2. Sept 5, 2021	Feb 8, Feb 10, 2024	16	31	18	37
3	Miami-Dade	W Flagler St.	PHB	Oct 6, Oct 9, 2021	Sept. 19, Sept. 21, 2024	22	29	25	35
4	Brevard	SR A1A	RRFB	Sept 18. Sept 21, 2021	May 11, May 13, 2023	16	28	19	38
5	Broward	SR A1A	Uncontrolled	Oct 9, Nov 22 2021		12	19	-	-

This study incorporates three types of speed metrics: the speed of leading vehicles interacting with pedestrians, the average speed of all vehicles during each 30-minute interval, and the posted speed limit at each site. Additionally, the study considers land-use mix data for each location which was extracted from FDOT GIS shape file (FDOT, GIS). The land-use mix reflects the diversity of activities and services available in an area, influencing both pedestrian and vehicular traffic. Locations with a higher variety of land uses tend to attract a wider range of visitors and trip purposes, such as shopping, dining, or recreation. This diversity often results in increased pedestrian activity and vehicle flow due to the area's ability to meet various needs. Further insights including the calculation of land-use mix of each location can be found in studies by (Ahsan et al., 2024; Ahsan, Abdel-Aty, & Abdelrahman, 2025; Anwari et al., 2023; Goswamy & Abdel-Aty, 2023). Other variables used in the analysis, along with their brief descriptions, are provided in **Table 12**. These variables are categorized into three main aspects: traffic and pedestrian dynamics, road characteristics, and contextual and temporal Factors.

Table 12 Summary Statistics of each variable used in the final analysis

Variable	Description	Value type	Mean	Std. Dev.	Max.	Min.
Traffic and Pedestrian Dynamics						
Average leading vehicle speed	Average speed of each leading vehicle before stopping that interact with pedestrian, mph	Continuous variable	26.6	8.60	59.81	1.72
Average vehicles' speed	Average speed of all vehicles during each 30-minute interval, mph	Continuous variable	34.2	12.94	61.04	11.91
Vehicle volume	Total vehicles passing the crosswalk during each 30-minute interval	Continuous variable	285	62.49	398	38
Pedestrian volume	Total no. of pedestrians crossed the road during each 30-minute interval	Continuous variable	5.8	4.72	29	0
Road Characteristics						
MPS treatment	MPS treatment	1: Present 0: Otherwise	0.52	0.49	1	0
Raised/vegetation median	Median those are raised or vegetation	1: Raised/veg. 0: Otherwise	0.18	0.38	1	0
Lane count	Total number of lanes	Continuous variable	2.98	0.36	4	2
Lane width	Lane width, feet	Continuous variable	10.38	1.64	14	11
Posted speed limit	Posted speed limit	Continuous variable	36.80	17.43	55	25
Contextual and Temporal Factors						
Land-use mix	Land-use mix of each site, collected from FDOT GIS shape file	Continuous variable	0.45	0.07	0.57	0
Weekday	Day other than Saturday and Sunday	1: Weekday 0: Otherwise	0.46	0.49	1	0
Morning peak	Morning peak time (8am to 10am)	1: Morning 0: Otherwise	0.22	0.41	1	0
Afternoon Peak	Afternoon peak time (4pm to 6pm)	1: Afternoon 0: Otherwise	0.19	0.39	1	0

12.2 Methodology

For calculating CMFs to evaluate the safety impact of a treatment, studies commonly use both Cross-Sectional (CS) and Before–After methods, incorporating a Comparison Group (CG) and the Empirical Bayesian (EB) approach (Hauer, 1997). The CG method involves analyzing treated sites alongside reference groups with similar characteristics that remain unchanged, allowing for a robust comparison (Abuzwidah & Abdel-Aty, 2024). In this study, the same methodological framework used for calculating CMFs was adopted; however, since the analysis was based on conflict rather than crash

data, Conflict Modification Factors (CoMFs) were used throughout. The interpretation of CoMF values is as follows:

- CoMF < 1.0: The treatment (e.g., MPS) is effective in reducing conflicts.
- CoMF = 1.0: The treatment has no effect; conflicts remain unchanged.
- CoMF > 1.0: The treatment is associated with an increase in conflicts, indicating a potential negative safety impact.

Empirical Bayes Before-After Method

The EB method is a statistical approach widely applied in before-after studies to evaluate the effectiveness of safety interventions, particularly in transportation safety research. Unlike traditional techniques, the EB method addresses challenges like random variability and regression-to-the-mean bias, which are common in observational data. This approach enables researchers to accurately estimate the impact of interventions (e.g., crash or conflict reduction) by isolating the treatment effect from external influences or natural variations in the data.

By combining data from treated and reference groups, as suggested in previous studies (Abuzwidah & Abdel-Aty, 2024; Hauer, 1997), the EB approach will offer a robust and reliable estimation of the expected impact of safety measures on conflict frequencies.

The expected conflict frequency $\widehat{E_\iota}$ is calculated as Eq. (2):

$$\widehat{E_\iota} = (\gamma_i \times y_i) + (1 - \gamma_i)\eta_i \quad (2)$$

Here, γ_i is the weight determined based on the negative binomial model's over-dispersion parameter and the predicted conflict frequency, y_i is observed conflict count during the pre-treatment period, and η_i is observed conflict count from the reference sites.

The weighting factor γ_i is calculated as Eq. (3):

$$\gamma_i = \frac{1}{1 + k \times y_i} \quad (3)$$

$Here\ k$ is over-dispersion parameter, indicating the variance in crash frequencies relative to the mean.

The standard deviation $\widehat{\sigma_\iota}$ of the predicted conflict frequency is calculated as Eq. (4):

$$\widehat{\sigma_\iota} = \sqrt{(1 - \gamma_i) \cdot \widehat{E_\iota}} \quad (4)$$

Scaling factors for adjusting post-intervention period ρ_{var} is for changes in variables like traffic volume or speed between the "Before" and "After" periods. It is given as Eq (5):

$$\rho_{\text{var}} = \frac{\text{var}_{\text{after}}^{\alpha_i}}{\text{var}_{\text{before}}^{\alpha_i}} \tag{5}$$

When there is no significant change between pre- and post-intervention conditions, the scaling factor becomes 1. α_i is regression coefficient for each variable from SPF.

The adjusted conflict frequency for the post-intervention period $\widehat{\pi_\iota}$ is:

$$\widehat{\pi_\iota} = \widehat{E_\iota} \cdot \rho_{\text{var}} \tag{6}$$

The effectiveness of a safety intervention is assessed using the Effectiveness Index $\widehat{\theta_\iota}$ defined as Eq (7):

$$\widehat{\theta_\iota} = \frac{\widehat{\lambda_\iota}/\widehat{\pi_\iota}}{1 + \left(\widehat{\sigma_\iota^2}/\widehat{\pi_\iota^2}\right)} \tag{7}$$

Here, $\widehat{\lambda_\iota}$ is actual conflict count observed during the post-intervention period. If $\widehat{\theta_\iota}$ is less than 1, the treatment is considered to be effective in reducing the expected number of conflicts.

The percentage reduction in conflict frequency $\widehat{\tau_\iota}$ is given by Eq (8):

$$\widehat{\tau_\iota} = \left(1 - \widehat{\theta_\iota}\right) \times 100\% \tag{8}$$

The aggregate effectiveness index $\hat{\theta}$ across all treated sites is calculated as Eq (9):

$$\hat{\theta} = \frac{\frac{\sum_{i=1}^{m} \widehat{\lambda_\iota}}{\sum_{i=1}^{m} \widehat{\pi_\iota}}}{1 + \left(\frac{\text{var}(\sum_{i=1}^{m} \widehat{\pi_\iota})}{(\sum_{i=1}^{m} \widehat{\pi_\iota})^2}\right)} \tag{9}$$

Where m is the total number of treated sites.

The variance of the aggregated prediction is:

$$\text{var}\left(\sum_{i=1}^{k} \widehat{\pi_\iota}\right) = \sum_{i=1}^{k} \rho_{\text{var}}^2 \cdot \text{var}\left(\widehat{E_\iota}\right) \tag{10}$$

The standard deviation $\hat{\sigma}$ for overall effectiveness is calculated as Eq (11):

$$\hat{\sigma} = \sqrt{\frac{\theta^2\left[\left(\frac{\mathrm{var}\left(\sum_{i=1}^{k}\hat{\pi}_i\right)}{\left(\sum_{i=1}^{k}\hat{\pi}_i\right)^2}\right)^2 + \left(\frac{\mathrm{var}\left(\sum_{i=1}^{k}\hat{\lambda}_i\right)}{\left(\sum_{i=1}^{k}\hat{\lambda}_i\right)^2}\right)^2\right]}{\left[1 + \left(\frac{\mathrm{var}\left(\sum_{i=1}^{k}\hat{\pi}_i\right)}{\left(\sum_{i=1}^{k}\hat{\pi}_i\right)^2}\right)\right]^2}} \quad (11)$$

This method provides a comprehensive framework for accurately estimating the effectiveness of safety measures while accounting for variability and potential biases.

Safety Performance Functions (SPFs) for EB Method

SPFs are predictive models used to estimate the expected number of crashes, conflicts, or other safety-related outcomes based on explanatory variables such as traffic volume, roadway characteristics, and environmental factors. Among the modeling approaches, Generalized Linear Models (GLMs) with a Negative Binomial (NB) distribution are widely used to account for the overdispersion typically observed in crash or conflict data. However, in many real-world datasets, observations may not be independent but instead exhibit correlation within clusters. For instance, when data is collected repeatedly over time from the same location or across spatially related sites, the outcomes may be influenced by shared underlying characteristics. Ignoring such correlations can lead to biased parameter estimates and underestimated standard errors. To address this, Generalized Estimating Equations (GEE) with a Negative Binomial family are increasingly considered as an alternative to GLMs (Abdel-Aty & Abdalla, 2004; Cui & Feng, 2008; Mohammadi et al., 2014).

In this study, conflict data were aggregated every 30 minutes over a continuous period of 10 to 12 hours per day for each location. This results in a dataset with repeated measures within each location, where conflicts observed at different time intervals are likely to be correlated due to shared traffic conditions, environmental factors, and spatial influences. The GEE framework is particularly suitable for this scenario, as it explicitly accounts for the within-location correlation through its working correlation structure (e.g., Exchangeable or AR-1) (Cui & Feng, 2008; Mohammadi et al., 2014). By modeling population-averaged effects, GEE provides robust inferences even in the presence of intra-cluster dependencies, making it an essential addition to GLMs for estimating SPFs. This dual approach allows to capture both conditional effects (using GLMs) and robust population trends (using GEEs), ensuring comprehensive and reliable safety analysis.

Negative Binomial Generalized Linear Model (NB-GLM)

GLM models the conditional mean of the response variable Y given the covariates. It assumes all observations are independent and is widely used for count data with overdispersion (Abdel-Aty & Radwan, 2000; Abuzwidah & Abdel-Aty, 2024; Hauer, 1997; Shirazi et al., 2016). Response variable Y_i (e.g., conflict counts) follows:

$$Y_i \sim \text{Negative Binomial}(\mu_i, \alpha) \quad (12)$$

Where, μ_i is expected conflicts for observation i, and α is dispersion parameter, controlling overdispersion.

The variance of Y_i is modeled as:

$$\text{Var}(Y_i) = \mu_i + \alpha\mu_i^2 \quad (13)$$

Where, $\alpha = \frac{\text{Var}_{\text{obs}}(Y_i) - \mu_i}{\mu_i^2}$; and $\text{Var}_{\text{obs}}(Y_i)$ is the observed variance of the response variable.

The following log-link function (Eq. 14) relates the mean response μ_i to the covariates.

$$\log(\mu_i) = \beta_0 + \beta_1 X_{1i} + \beta_2 X_{2i} + \cdots + \beta_p X_{pi} \quad (14)$$

Here, $X_{1i}, X_{2i}, \ldots, X_{pi}$ is predictors (e.g., traffic volume, pedestrian count), and $\beta_0, \beta_1, \ldots, \beta_.$ are model coefficients. Parameters β and α are estimated via maximum likelihood estimation (MLE).

Negative Binomial Generalized Estimating Equations (NB-GEE)

GEE models the population-averaged mean of the response variable, explicitly accounting for within-cluster correlation (Mohammadi et al., 2014). It is ideal for repeated or grouped data as this study where conflict counts are recorded every 30 minutes across multiple locations.

Response variable Y_{ij} for the j-th observation in the i-th cluster follows:

$$Y_{ij} \sim \text{Negative Binomial}\left(\mu_{ij}, \alpha\right) \quad (15)$$

Where, μ_{ij} is expected conflicts for observation j in cluster i, $and\ \alpha$ is dispersion parameter that accounts for overdispersion in the NB model.

The variance of Y_{ij} is modeled as:

$$\mathrm{Var}(Y_{ij}) = \phi V(\mu_{ij}) = \mu_{ij} + \alpha\mu_{ij}^2 \tag{16}$$

Here, ϕ is scale parameter, and $V(\mu_{ij})$ is the variance function specific to the NB distribution. The dispersion parameter α is calculated as:

$$\alpha = \frac{\sum_{i=1}^{m}\sum_{j=1}^{n_i}\frac{(Y_{ij}-\mu_{ij})^2}{\mu_{ij}^2} - (N-p)}{N-p} \tag{17}$$

Here, $N-p$ is residual degrees of freedom. Although ϕ adjusts the variance for any additional variability in the GEE framework, we calculate α specifically to model the overdispersion inherent to the NB distribution. This ensures that the variance structure reflects the relationship $\mathrm{Var}(Y_{ij}) = \phi(\mu_{ij} + \alpha\mu_{ij}^2)$, aligning the NB assumptions with the GEE framework for accurate modeling of over dispersed count data.

The log-link function relates the mean response μ_{ij} to the predictors:

$$\log(\mu_{ij}) = \beta_0 + \beta_1 X_{1ij} + \beta_2 X_{2ij} + \cdots + \beta_p X_{pij} \tag{18}$$

Here, X_{1ij} represents a predictor variable (e.g., traffic volume, pedestrian count) for observation j in cluster i.

GEE includes a working correlation matrix $R(\rho)$ to model within-cluster correlation (Cui & Feng, 2008; Mohammadi et al., 2014); Exchangeable: equal correlation ρ between all observations within a cluster. Autoregressive (AR-1): correlation decreases with increasing time lag. Independent: assumes no correlation.

Parameters β are estimated using quasi-likelihood estimation (Cui & Feng, 2008; Mohammadi et al., 2014):

$$U(\beta) = \sum_{i=1}^{m} D_i^T V_i^{-1}(Y_i - \mu_i) = 0 \tag{19}$$

Where, D_i is derivative of the mean vector μ_i with respect to β, and V_i is covariance matrix, incorporating $R(\rho)$. The inclusion of $R(\rho)$ allows GEE to account for within-cluster correlations,

making it particularly suitable for clustered or repeated measures data where traditional NB models may fall short.

Cross Sectional Method

The CS Method applies a similar framework to the SPFs but explicitly incorporates the treatment effect (e.g., MPS treatment) as an explanatory variable (Abuzwidah & Abdel-Aty, 2024; Park & Abdel-Aty, 2016). This approach enables the evaluation of how the presence of a treatment modifies the expected conflict frequency across locations.

Model Formulation:

Using the same NB framework as the original SPF (see Eq. 14), the expected number of conflicts is now modeled to include the treatment effect as Eq. (20):

$$\log(\mu_i) = \beta_0 + \beta_1 X_{1i} + \beta_2 X_{2i} + \cdots + \beta_p X_{pi} + \beta_T T_i \quad (20)$$

Here, β_T is coefficient representing the treatment effect, and T_i is binary indicator for the presence of treatment ($T_i = 1$ for treated locations, $T_i = 0$ for otherwise).

The treatment's effect is quantified through the CoMF, which is calculated as Eq (21):

$$\text{CoMF}_T = e^{\beta_T} \quad (21)$$

This allows the predicted conflict frequencies to vary based on the presence or absence of treatment. The standard error (SE) of the CoMF is calculated as (Park & Abdel-Aty, 2016):

$$SE_T = \frac{e^{\beta_T + SE_{T_x}} - e^{\beta_T - SE_{T_x}}}{2} \quad (22)$$

where β_T denotes the coefficient of treatment indicator variable T_i and SE_{T_x} denotes the standard error of β_T from the NB model.

Goodness of Fit

When comparing NB-GLM and NB-GEE, using Akaike Information Criterion (AIC) and Quasi-Likelihood Information Criterion (QIC) is not appropriate for direct comparison due to their differing frameworks. AIC, used in NB-GLM, evaluates model fit based on maximum likelihood, assuming independent observations, while QIC, used in NB-GEE, accounts for quasi-likelihood and

within-cluster correlation. Since AIC and QIC rely on different likelihood structures, their values are not directly comparable. Instead of comparing AIC and QIC, alternative metrics such as Mean Absolute Error (MAE) or Mean Squared Error (MSE) can be used to assess predictive performance on the same test dataset, providing a common ground for evaluation.

For NB-GLM, the log-likelihood measures how well the model explains the observed data, given the parameter estimates. It is expressed as:

$$\text{Log-Likelihood (NB GLM)} = \sum_{i=1}^{n} \log P\left(Y_i | \mu_i, \alpha\right) \tag{23}$$

Y_i is observed response for observation i (e.g. conflict counts), μ_i is predicted mean response for observation i and, α is dispersion parameter to account for overdispersion.

The Akaike Information Criterion (AIC) evaluates model fit while penalizing complexity, defined as:

$$\text{AIC} = 2k - 2\log L \tag{24}$$

Where, k is number of model parameters and $\log L$ is Log-likelihood of the model.

For NB-GEE model that accounts for within-cluster correlation, the Quasi-Likelihood Information Criterion (QIC) is used as an analog to AIC (Mohammadi et al., 2014). It is defined as:

$$\text{QIC} = -2\text{l}(\beta) + 2\text{trace}(W) \tag{25}$$

Where $\text{l}(\beta)$ is quasi-likelihood under the working correlation and W is model-based covariance matrix.

To evaluate predictive accuracy, MAE and MSE are defined as follows:

$$\text{MAE} = \frac{1}{n}\sum_{i=1}^{n} |Y_i - \mu_i|$$

And,

$$\text{MSE} = \frac{1}{n}\sum_{i=1}^{n} (Y_i - \mu_i)^2 \tag{26}$$

Where n is total number of observations.

Before-After Comparison Group Study

A before-and-after CG study evaluates treated sites by comparing them with an untreated group of control or comparison sites. In this study, data were collected from reference sites during both the before period, when MPSs had not yet been installed at the treatment sites, and the after period, when MPSs were operational. Therefore, these reference sites served as comparison sites. This approach does not explicitly adjust for variations in traffic volume or temporal factors. Instead, it calculates the ratio of observed crashes or conflicts during the after period to those recorded during the before period for the comparison sites CoMF is calculated from the following Eq. 27 (Gross, 2010; Monsere et al., 2017).

$$\text{CoMF} = \left(\frac{N_{\text{observed},T,A}}{N_{\text{expected},T,A}}\right) / \left(1 + \frac{\text{Var}\left(N_{\text{expected},T,A}\right)}{N^2_{\text{expected},T,A}}\right) \tag{27}$$

And variance of CoMF is:

$$\text{Variance (CoMF)} = \frac{\text{CoMF}^2\left[\left(\frac{1}{N_{\text{observed},T,A}}\right) + \left(\frac{\text{Var}\left(N_{\text{expected},T,A}\right)}{N^2_{\text{expected},T,A}}\right)\right]}{1 + \frac{\text{Var}\left(N_{\text{expected},T,A}\right)^2}{N^2_{\text{expected},T,A}}} \tag{28}$$

Where,

$$N_{\text{expected},T,A} = N_{\text{observed},T,B}\left(\frac{N_{\text{observed},C,A}}{N_{\text{observed},C,B}}\right)$$

$$\text{Var}\left(N_{\text{expected},T,A}\right) = N^2_{\text{expected},T,A}\left(\frac{1}{N_{\text{observed},T,B}} + \frac{1}{N_{\text{observed},C,B}} + \frac{1}{N_{\text{observed},C,A}}\right)$$

$N_{\text{observed},T,B}$= The total number of conflicts recorded during the before period of MPS installation.

$N_{\text{observed},T,A}$= The total number of conflicts recorded during the after MPS installation.

$N_{\text{observed},C,B}$= The total number of conflicts recorded during the before period for sites in the comparison (untreated) group.

$N_{\text{observed},C,A}$= The total number of conflicts recorded during the after period for sites in the comparison (untreated) group.

12.3 Results and Discussion

Empirical Bayes and Comparison Group Methods

To develop SPF for the EB method, data were analyzed across four reference groups: PHB sites, RRFB sites, a combination of PHB and RRFB sites, and all sites combined. Observations were aggregated in 30-minute intervals for all locations. For CoMF evaluation, when PHBs were used as the reference group, only sites that initially operated as PHBs and later transitioned to MPSs were considered. The same approach was applied to other reference groups (RRFB and combination of PHB and RRFB) to ensure consistency in evaluation. In the CG method, untreated sites were excluded from the reference group, as data was not collected from that location after MPS installation at other untreated sites. For further details, refer to **Table 13**. Location numbers align with those provided in **Table 11**.

Table 13 Reference groups and final evaluation sites for EB method

Reference Group	Ref. Group Sites	Evaluation Sites
All	All	All
PHB	1, 2, 3	10, 11, 12, 13, 14
RRFB	4	8[a], 9
PHB and RRFB	1, 2, 3, 4	8[a], 9, 10, 11, 12, 13, 14
a: Flashing Beacon and RRFB have similar functionality; therefore, they were evaluated collectively.		

For the final CoMF evaluation, the NB-GEE model was selected due to its better performance across multiple evaluation metrics compared to NB-GLM. The NB-GEE model consistently demonstrated lower MAE and MSE, indicating more accurate predictions with smaller residuals (refer to **Table 14** and **Table 15**). Additionally, it accounts for within-cluster correlation through the correlation coefficient $R(\rho)$, which is crucial for clustered traffic data. Since AIC and QIC rely on different likelihood structures, their values are not directly comparable. These findings emphasize the reliability of the NB-GEE model for CoMF development in this study. All three correlation structures: Exchangeable, Autoregressive (AR-1), and Independent were tested to evaluate their performance in the GEE model. Based on the results, the Exchangeable correlation structure provided the best fit, as indicated by MAE and MSE compared to the other two. **Figure 26** highlights a sample of the prediction results and accuracy for the PHB reference group, demonstrating the robustness of the NB-GEE model for CoMF evaluation. In the NB-GEE model (refer to **Table 14** and **Table 15**), average leading vehicle speed, average vehicles' speed, vehicle volume, pedestrian volume, lane count, posted speed limit,

land-use mix, weekday, morning peak, and afternoon peak have positive and statistically significant coefficients, indicating an increased expected conflict frequency as these variables increase. Conversely, raised/vegetation median and lane width have negative coefficients, suggesting that presence of raised/vegetation median and wider lanes are associated with a reduction in conflicts.

Table 14 SPF based on different reference groups for serious conflicts

Variable	Estimate (std. error) based on different reference groups							
	All		PHBs and RRFB		PHBs		RRFB	
	NB-GLM	NB-GEE	NB-GLM	NB-GEE	NB-GLM	NB-GEE	NB-GLM	NB-GEE
Traffic and Pedestrian Dynamics								
Constant	1.312** (0.0562)	1.012** (0.0292)	1.561** (0.0320)	1.138** (0.088)	1.287** (0.1539)	1.181** (0.120)	1.428** (0.127)	1.111** (0.158)
Average leading vehicle speed	0.561** (0.032)	0.1509* (0.088)	0.1725* (0.09)	0.632** (0.095)	0.433** (0.064)	0.393** (0.126)	0.593** (0.222)	0.918** (0.173)
Average vehicles' speed	0.787** (0.200)	0.844** (0.223)		0.319** (0.1601)		0.710* (0.399)	0.922** (0.218)	1.076** (0.109)
Ln (Vehicle volume)	1.012** (0.0292)	0.634** (0.301)	0.844** (0.2231)	1.287** (0.153)	0.751** (0.015)	0.741** (0.253)	1.46** (0.134)	1.257** (0.113)
Pedestrian volume	0.0854** (0.022)	0.644** (0.093)	0.274** (0.073)	0.261** (0.033)				0.676** (0.236)
Road Characteristics								
Lane count	0.6007** (0.298)	0.547** (0.222)	0.100* (0.0573)	0.526* (0.313)	0.4163* (0.2301)	0.6175* (0.378)		
Raised/vegetation Median		-0.094* (0.054)		-0.163** (0.0398)				
Lane width		-0.234** (0.110)				-0.847** (0.024)		
Posted speed limit		0.469** (0.185)	0.946** (0.025)	0.286** (0.0630)	0.634** (0.071)	0.163** (0.039)		
Contextual and Temporal Factors								
Land-use mix	0.243* (0.145)	0.424* (0.246)	0.9822** (0.2437)	0.658* (0.397)	0.621** (0.314)	0.296** (0.109)		
Weekday		0.115** (0.047)		0.963** (0.054)		0.286** (0.063)	0.768** (0.154)	0.425** (0.156)
Morning peak	0.559* (0.325)	0.266** (0.121)	0.247** (0.121)	0.293* (0.177)	0.119** (0.055)	0.213* (0.109)	0.502** (0.128)	0.804** (0.260)
Afternoon Peak		1.137** (0.086)		0.731** (0.054)				
Goodness of Fit								
AIC/QIC	10024/-	-/10078	9647/-	-/9826	9534/-	-/9608	6727/-	-/6859
Dispersion Parameter	0.44	0.48	0.31	0.37	0.29	0.35	0.31	0.35
Correlation Coefficient, $R(\rho)$		0.46		0.39		0.42		0.42
MAE	0.7026	0.5259	0.6943	0.5586	0.6536	0.4735	0.5346	0.3950
MSE	1.7164	0.9863	1.7240	1.3864	1.7178	1.2866	1.5691	0.8636

** Significant at 95% confidence level.
* Significant at 90% confidence level.

Table 15 SPF based on different reference group for all conflicts (serious and moderate)

Variable	Estimate (std. error) based on different reference groups							
	All		PHBs and RRFB		PHBs		RRFB	
	NB-GLM	NB-GEE	NB-GLM	NB-GEE	NB-GLM	NB-GEE	NB-GLM	NB-GEE
Traffic and Pedestrian Dynamics								
Constant	2.138** (0.109)	2.010** (0.215)	1.010** (0.208)	1.625** (0.130)	1.757** (0.106)	1.064** (0.095)	1.010** (0.208)	1.368** (0.171)
Average leading vehicle speed	0.210** (0.029)	0.186** (0.032)	0.916** (0.241)	0.154** (0.039)	0.265** (0.105)	0.298** (0.113)	0.916** (0.241)	0.894** (0.198)
Average vehicles' speed		0.423** (0.110)	0.334** (0.114)	0.224* (0.13)		0.305** (0.104)	0.334** (0.114)	0.521** (0.123)
Ln (Vehicle volume)	0.774** (0.218)	0.692** (0.231)	0.500* (0.281)	0.352** (0.176)	0.883** (0.298)	0.466** (0.113)	0.500* (0.281)	0.529** (0.162)
Pedestrian volume		0.106* (0.062)		0.399** (0.135)		0.357** (0.123)		0.301** (0.101)
Road Characteristics								
Lane count		0.499** (0.118)		0.501** (0.202)	0.399** (0.134)	0.982** (0.226)		
Raised/vegetation Median		-0.521** (0.149)		-0.051** (0.010)		-0.490** (0.108)		
Lane width		-0.817** (0.119)	-0.916** (0.130)	-0.778** (0.212)		-0.806** (0.227)		
Posted speed limit	0.825** (0.271)	0.770** (0.252)	0.949** (0.212)	0.789** (0.238)	0.658** (0.272)	0.664** (0.154)		
Contextual and Temporal Factors								
Land-use mix		0.629** (0.167)		0.1.301** (0.106)		0.309** (0.110)		
Weekday	0.536** (0.210)	0.613** (0.103)	0.990** (0.121)	1.00** (0.141)	0.445** (0.151)	0.630** (0.166)	0.974** (0.251)	0.734** (0.111)
Morning peak		0.095** (0.012)		0.107** (0.020)	0.466** (0.094)	0.601** (0.072)	1.084** (0.132)	1.153** (0.289)
Afternoon Peak				0.691** (0.101)				
Goodness of Fit								
AIC/QIC	9307/-	-/9439	9325/-	-/9427	8946/-	-/9026	6426/-	-/6503
Dispersion Parameter	0.47	0.46	0.30	0.33	0.32	0.36	0.33	0.36
Correlation Coefficient, $R(\rho)$		0.36		0.32		0.38		0.40
MAE	1.1945	0.7233	0.9867	0.3365	0.9521	0.5055	0.9645	0.4260
MSE	2.1055	1.2951	2.0740	1.0521	2.0546	1.1318	1.9809	0.7399

** Significant at 95% confidence level.

* Significant at 90% confidence level.

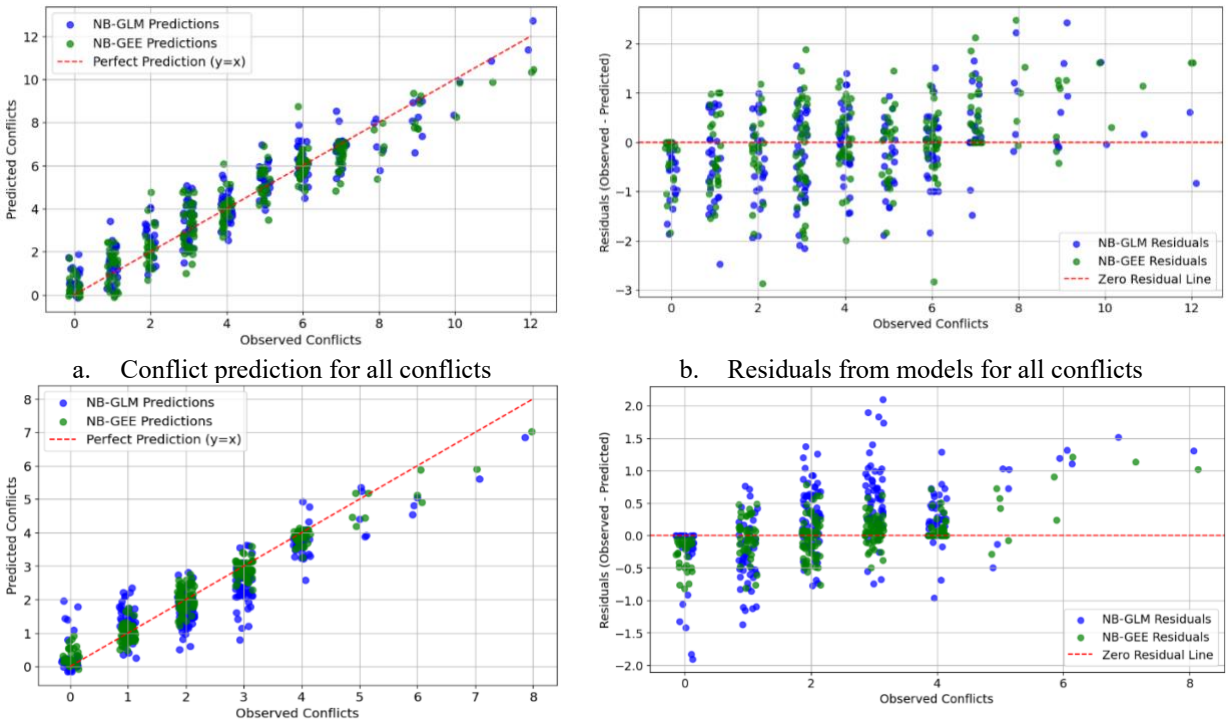

a. Conflict prediction for all conflicts

b. Residuals from models for all conflicts

c. Conflict prediction for serious conflicts

d. Residuals from models for serious conflicts

Figure 26 Conflict prediction and their residuals from NB-GEE and NB-GLM models for reference group: PHBs

Table 16 summarizes the CoMFs for MPSs across different reference groups, evaluated using EB and CG methods. For all sites combined, MPSs reduced serious conflicts by 45%, and reductions for all conflicts were 48% using the EB method. For the combined PHB and RRFB reference group, serious conflicts decreased by 33% using the EB method and 38% with the CG method, while reductions for all conflicts were 38% and 37%. Using PHBs as the reference group, MPSs reduced serious conflicts by 27% and 33% for the EB and CG methods, respectively, and all conflicts by 33% and 31%. For RRFBs as the reference group, serious conflicts were reduced by 47% and 55%, while reductions for all conflicts were 54% and 53%.

Table 16 CoMFs of MPSs based on EB and CG method

Conflict Type	**CoMF (std. error) of MPSs based on different reference groups**						
	Empirical Bayes				Comparison Group		
	All	PHBs, RRFB	PHBs	RRFB	PHBs and RRFB	PHBs	RRFB
Serious	0.55 (0.03)	0.67 (0.07)	0.73 (0.04)	0.53 (0.06)	0.62 (0.13)	0.67 (0.16)	0.45 (0.17)
All	0.52 (0.04)	0.62 (0.03)	0.67 (0.03)	0.46 (0.02)	0.63 (0.09)	0.69 (0.11)	0.47 (0.12)

Cross Sectional Method

The CS method evaluated the impact of MPSs across different reference categories. The first category included all locations that transitioned to MPSs, irrespective of whether they were previously PHB, RRFB, untreated, or remained unchanged. The second category focused on PHB RRFB and Flashing Beacon locations, including those that transitioned to MPSs or remained same during both periods. The third category specifically analyzed PHB locations, considering those that either transitioned to MPSs or remained as PHBs throughout the study period. Lastly, the fourth category examined RRFB and Flashing Beacon locations, including those that transitioned to MPSs or remained as RRFBs during the analysis period. The NB-GEE model was also selected for this analysis, as it effectively accounts for within-cluster correlations and consistently demonstrates lower MAE and MSE values (refer to **Table 17** and **Table 18**). Here also all variables except raised/vegetation median and lane width have positive and statistically significant coefficients, indicating an increased expected conflict frequency as these variables increase. Conversely, raised/vegetation median and lane width have negative coefficients, suggesting that presence of raised/vegetation median and higher lane width are associated with a reduction in conflicts.

Table 17 SPFs based on different reference groups for serious conflicts

Variable	Estimate (std. error) based on different reference groups							
	All locations		PHBs, RRFB, Flashing Beacon		PHBs		RRFB, Flashing Beacon	
	NB-GLM	NB-GEE	NB-GLM	NB-GEE	NB-GLM	NB-GEE	NB-GLM	NB-GEE
Traffic and Pedestrian Dynamics								
Constant	1.258** (0.106)	1.211** (0.229)	1.445* (0.209)	1.386** (0.128)	1.462** (0.160)	1.343** (0.192)	1.191** (0.182)	1.423** (0.212)
Average leading vehicle speed	0.395* (0.235)	0.493** (0.151)	0.289* (0.161)	0.290** (0.128)	0.388* (0.228)	0.402** (0.099)	0.195* (0.105)	0.229** (0.108)
Average vehicles' speed	0.762** (0.165)	0.749** (0.215)	0.977* (0.206)	0.679** (0.229)	0.949** (0.168)	1.351** (0.277)	0.551** (0.238)	0.565** (0.149)
Ln (Vehicle volume)	1.018** (0.155)	0.893** (0.122)	0.560** (0.262)	0.591** (0.196)	0.580** (0.124)	0.527** (0.215)	0.724** (0.273)	0.811** (0.154)
Pedestrian volume		0.899** (0.240)						
Road Characteristics								
MPS treatment	-0.550** (0.017)	-0. 597** (0.010)	-0.409** (0.090)	-0.386** (0.066)	-0.284** (0.012)	-0.301** (0.018)	-0.639** (0.080)	-0.616** (0.074)
Lane count	0.906** (0.141)	1.420* (0.244)		0.611** (0.099)				0.607** (0.177)
Raised/vegetation Median		-0.904** (0.264)		-0.544** (0.101)		-0.881** (0.111)		
Lane width	-0.860** (0.125)	-0.686** (0.200)				-0.970** (0.193)		
Posted speed limit	0.995** (0.108)	1.158** (0.144)		1.238** (0.149)		-0.740** (0.101)		0.197** (0.051)
Contextual and Temporal Factors								
Land-use mix	0.921** (0.124)	1.269** (0.186)		0.633** (0.256)		0.431** (0.108)	0.568** (0.164)	0.703** (0.229)
Weekday		1.218** (0.242)	0.957** (0.200)	0.666** (0.181		1.500** (0.153)	0.561** (0.227)	0.612** (0.198)
Morning peak	0.683** (0.241)	0.434** (0.106)	0.630** (0.280)	0.643** (0.290)	0.775** (0.161)	0.895** (0.225)	0.596** (0.137)	0.409** (0.108)
Afternoon Peak	0.115** (0.023)	0.098* (0.054)						
AIC/QIC	8834/-	-/8941	9267/-	-/9351	9119/-	-/9180	6213/-	-/6289
Dispersion Parameter	0.49	0.44	0.28	0.27	0.29	0.31	0.32	0.34
Correlation Coefficient, $R(\rho)$		0.35		0.35		0.37		0.41
MAE	0.5406	0.3246	0.6155	0.4001	0.5628	0.3410	0.5246	0.2080
MSE	1.5523	0.8295	1.6208	0.9132	1.5711	0.7521	1.5296	0.5110

** Significant at 95% confidence level.
* Significant at 90% confidence level.

Table 18 SPFs based on different reference groups for all conflicts

Variable	Estimate (std. error) based on different reference groups							
	All locations		PHBs, RRFB, Flashing Beacon		PHBs		RRFB, Flashing Beacon	
	NB-GLM	NB-GEE	NB-GLM	NB-GEE	NB-GLM	NB-GEE	NB-GLM	NB-GEE
Traffic and Pedestrian Dynamics								
Constant	1.368** (0.200)	1.099** (0.281)	1.184** (0.242)	1.382** (0.284)	1.297** (0.229)	1.436** (0.102)	1.404** (0.237)	1.342** (0.140)
Average leading vehicle speed	0.504** (0.227)	0.604** (0.233)	0.962** (0.218)	0.800** (0.225)	1.138** (0.131)	0.988** (0.105)	0.425* (0.257)	0.622** (0.175)
Average vehicles' speed	0.931** (0.247)	0.974** (0.220)	0.732** (0.117)	1.095** (0.209)	0.668** (0.201)	0.397** (0.072)	1.069** (0.107)	0.883** (0.092)
Ln (Vehicle volume)	1.047** (-0.145)	1.128** (0.131)	0.762** (0.118)	0.604** (0.099)	0.319** (0.108)	0.428** (0.100)	0.402* (0.211)	0.519** (0.120)
Pedestrian volume	0.056* (0.031)	0.040* (0.021)						0.0875* (0.046)
Road Characteristics								
MPS treatment	-0.615** (0.032)	-0.693** (0.091)	-0.815** (0.039)	-0.720** (0.028)	-0.427** (0.065)	-0.447** (0.081)	-0.823** (0.110)	-0.755** (0.091)
Lane count	0.399** (0.107)	0.500** (0.118)		0.209** (0.050)		0.397** (0.095)		
Raised/vegetation Median		-0.496** (0.095)		-0.821** (0.141)		-0.510** (0.108)		-0.464** (0.224)
Lane width	-0.230** (0.101)	-0.355** (0.109)						
Posted speed limit	0.336** (0.091)	0.314** (0.013)		0.297** (0.117)		0.566** (0.240)	0.109** (0.022)	0.111* (0.065)
Contextual and Temporal Factors								
Land-use mix	0.404** (0.100)	0.577** (0.104)			0.332** (0.106)	0.439** (0.093)		
Weekday	0.503** (0.221)	0.628** (0.210)	0.421** (0.123)	0.467** (0.208)	0.862** (0.110)	0.619** (0.091)	0.384* (0.209)	0.918** (0.110)
Morning peak	0.499** (0.170)	0.506** (0.113)	0.636** (0.184)	0.731** (0.266)	0.062** (0.006)	0.049** (0.002)	0.749** (0.111)	0.521** (0.100)
Afternoon Peak							0.093** (0.044)	0.019* (0.011)
AIC/QIC	9046/-	-/9109	9431/-	-/9503	9315/-	-/9397	6419/-	-/6501
Dispersion Parameter	0.40	0.42	0.31	0.32	0.28	0.32	0.31	0.35
Correlation Coefficient, $R(\rho)$		0.34		0.37		0.36		0.40
MAE	0.7565	0.4267	0.8551	0.2278	0.8012	0.3761	0.5562	0.1034
MSE	1.7630	0.7295	1.8603	0.4360	1.8087	0.8790	1.5605	0.3086

** Significant at 95% confidence level.

* Significant at 90% confidence level.

Table 19 highlights the CoMFs for MPSs derived from the CS method across various site categories. Compared to all locations, MPSs achieved a 45% reduction in serious conflicts and a 50% reduction in all conflicts. Relative to PHBs, RRFB, and Flashing Beacon sites, MPSs resulted in a 32% reduction in serious conflicts and a 51% reduction in all conflicts. When compared specifically to PHBs, MPSs demonstrated a 26% reduction in serious conflicts and a 36% reduction in all conflicts. Lastly, compared to RRFB and Flashing Beacon sites, MPSs achieved a 46% reduction in serious conflicts and a 53% reduction in all conflicts.

Table 19 CoMFs of MPSs based on CS method

Conflict types	CoMF (std. error) of MPSs based on different reference groups			
	All locations	PHBs, RRFB and Flashing Beacon	PHBs	RRFB and Flashing Beacon
Serious	0.55 (0.01)	0.68 (0.06)	0.74 (0.02)	0.54 (0.07)
All	0.50 (0.09)	0.49 (0.03)	0.64 (0.08)	0.47 (0.09)

Prior studies have consistently demonstrated that PHB are generally safer than RRFB or Flashing Beacon. The primary reason for this is the mandatory stop requirement for vehicles during the red phase of PHB, ensuring driver compliance and pedestrian safety. In contrast, RRFB and Flashing Beacon serve only as visual warnings and do not require vehicles to stop unless a pedestrian is actively crossing, leading to inconsistent driver behavior. This study compared the safety performance of MPSs against different reference groups, including PHBs, RRFB, combinations of PHBs, RRFB and Flashing Beacon. Across all categories, MPSs demonstrated consistent reductions in serious and moderate conflicts. Notably, when compared to PHBs which share similar functionalities but differ in signal phase management; MPSs provided additional safety benefits by reducing both serious and total conflicts. Unlike PHBs, which remain dark when inactive, MPS systems operate seamlessly with regular traffic signals, maintaining a green phase until pedestrian activation. Importantly, even at locations where PHBs were replaced with MPS systems, no changes were made to the signal architecture (except for signal heads) or road geometry. The transition to MPS involved only reprogramming the signal phases, highlighting the adaptability and cost-effectiveness of this intervention. The results showed that, compared to PHBs, MPSs reduced serious and total conflicts by 27% and 33% using the EB method, 33% and 31% using CG method, and 26% and 36% using CS method, respectively.

13. DETAIL DELAY EVALUATION OF MPS, PHB, RRFB AND FLASHING BEACON

This section will evaluate the impact of MPSs on vehicle delays and compare them with other midblock signal systems.

13.1 Data Description

The methodology for calculating vehicle delays has been included in the previous section (section 8). To develop the Delay Function (DF) for vehicle delay, key factors such as traffic flow, pedestrian activity, road characteristics, and temporal patterns were incorporated (refer to **Table 20**). Specific traffic and pedestrian dynamics, such as leading vehicle speed, average speed, and speed variability were considered. Additionally, land-use mix, derived from FDOT GIS shapefile (GIS, 2024), represents the diversity of surrounding land uses, such as residential, commercial, and recreational areas. Locations with higher land-use diversity tend to influence pedestrian activity throughout the day. For further details on land-use mix calculations, refer to (Ahsan et al., 2024; Ahsan, Abdel-Aty, & Abdelrahman, 2025; Goswamy & Abdel-Aty, 2023).

Table 20 Summary Statistics of each variable used in the final analysis

Variable	Description	Value type	Mean	Std. Dev.	Max.	Min.
Traffic and Pedestrian Dynamics						
Average leading vehicle speed	Average speed of each leading vehicle before stopping that interact with pedestrian, mph	Continuous variable	25.8	6.7	59.81	1.72
Average vehicles' speed	Average speed of all vehicles during each 15-minute interval, mph	Continuous variable	35.3	9.63	61.04	11.91
Vehicles' standard deviation of speed	Std. dev. of vehicles' during each 15-minute interval, mph	Continuous variable	6.8	2.98	16.67	0.95
Vehicle volume	Total vehicles passing the crosswalk during each 15-minute interval	Continuous variable	113	36.50	206	8
Pedestrian volume	Total no. of pedestrians crossed the road during each 15-minute interval	Continuous variable	1.67	0.74	18	0
Road Characteristics						
MPS treatment	MPS treatment	1: Present 0: Otherwise	0.54	0.41	1	0
Raised/vegetation median	Median those are raised or vegetation	1: Raised/veg. 0: Otherwise	0.16	0.37	1	0
Lane count	Total number of lanes	Continuous variable	2.47	0.42	4	2
Lane width	Lane width, feet	Continuous variable	9.43	1.66	14	11
Posted speed limit	Posted speed limit	Continuous variable	35.75	16.96	55	25
Contextual and Temporal Factors						
Land-use mix	Land-use mix of each site, collected from FDOT GIS shape file	Continuous variable	0.44	0.07	0.57	0
Weekday	Day other than Saturday and Sunday	1: Weekday 0: Otherwise	0.46	0.49	1	0
Morning peak	Morning peak time (8am to 10am)	1: Morning 0: Otherwise	0.21	0.41	1	0
Afternoon Peak	Afternoon peak time (4pm to 6pm)	1: Afternoon 0: Otherwise	0.14	0.35	1	0

13.2 Methodology

This study employed both Cross-Sectional (CS) and Before-After analytical approaches, incorporating a Comparison Group (CG) and the Empirical Bayesian (EB) method. This approach adopted from the safety literature in identifying the Crash Modification Factors (Hauer, 1997), to evaluate the impact of MPSs on vehicle delays and to estimate Delay Modification Factors (DMFs). Data were collected from reference sites during both the before period, when MPSs had not yet been

installed at the treatment sites, and the after period, when MPSs were operational. In the Comparison Group method, these reference sites served as comparison sites. The interpretation of DMF values is as follows:

- DMF < 1.0: The treatment (e.g., MPS) is effective in reducing vehicle delays.
- DMF = 1.0: The treatment has no effect; delays remain unchanged.
- DMF > 1.0: The treatment is associated with an increase in delays.

Empirical Bayes Before-After Method

EB method is a well-established technique in transportation safety studies, particularly for evaluating changes in crash frequencies following safety interventions. It addresses limitations common in observational studies such as regression to the mean, random fluctuations, and confounding variables by combining data from treated and untreated sites to produce more reliable estimates of intervention effects. In this study, the EB method was adapted for use with a continuous outcome variable (i.e. vehicle delay) instead of its conventional use with count data like crashes. The adaptation involves utilizing the Gamma distribution to model delays, as delays are continuous and often exhibit overdispersion. By incorporating delay data from both treated and reference sites, the EB approach allows for the robust estimation of treatment effects (e.g., delay reduction or increase). This adaptation demonstrates the flexibility of the EB method in addressing transportation challenges beyond crash analysis. The DMF based on EB method was calculated using the same procedure and methodology as the Conflict Modification Factor (CoMF) described in detail in Section 11.

Delay Functions (DFs) for EB Method

The delay data used in this study is continuous and positive with right-skewed distribution, making the Gamma Generalized Linear Model (Gamma-GLM) with a log link an appropriate choice for modeling However, in real-world applications, data collected over time or across multiple sites often exhibit clustering or correlation. For example, delay measurements taken repeatedly at the same locations are likely to be influenced by shared characteristics such as signal timing plans, traffic flow patterns, or surrounding land use. When such intra-cluster correlations are ignored, traditional GLMs may produce biased coefficient estimates and unreliable standard errors, ultimately affecting the accuracy of the model. To overcome these limitations, Gamma Generalized Estimating Equations (Gamma-GEE) can be used as an extension to Gamma-GLMs. Gamma-GEEs to explicitly account for correlations within clusters, providing more robust parameter estimates when data are grouped or

temporally/spatially related (Lee et al., 2010). This makes Gamma-GEE particularly suitable for modeling delay data across multiple locations or over time, ensuring that the DFs used in the EB method produce reliable and valid estimates.

Gamma Generalized Linear Model (Gamma-GLM)

The Gamma-GLM models the conditional mean of the response variable Y_i (e.g., delays) given covariates. The response variable Y_i follows the **Gamma distribution**:

$$Y_i \sim \text{Gamma}\ (\mu_i, \phi) \tag{29}$$

Where, μ_i is mean delay for observation i, modeled using a log-link function; and ϕ is dispersion parameter (inverse of the shape parameter) that controls the variance of Y_i

The variance of Y_i is given as:

$$\text{Var}(Y_i) = \phi\mu_i^2 \tag{30}$$

This variance structure indicates that the variance increases with the square of the mean, making the Gamma-GLM suitable for over dispersed continuous data.

To ensure that the mean delay μ_i is always positive, the log-link function is used to relate the mean response μ_i to the covariates:

The following log-link function (Eq. 31) relates the mean response μ_i to the covariates.

$$\log(\mu_i) = \beta_0 + \beta_1 X_{1i} + \beta_2 X_{2i} + \cdots + \beta_p X_{pi} \tag{31}$$

Here, $X_{1i}, X_{2i}, \ldots, X_{pi}\ is$ predictors (e.g., traffic volume, pedestrian count), and $\beta_0, \beta_1, \ldots, \beta_.$ are model coefficients. Parameters β and α are estimated via maximum likelihood estimation (MLE).

The fitted model predicts the expected mean delay μ_i for each observation i:

$$\mu_i = \exp(\beta_0 + \beta_1 X_{1i} + \beta_2 X_{2i} + \cdots + \beta_p X_{pi}) \tag{32}$$

The dispersion parameter ϕ is calculated from the residual deviance of the model (Mohamed et al., 2022):

$$\phi = \frac{Residual\ Deviance\ (D)}{Residual\ Degrees\ of\ Freedom}$$

Where,

$$D = 2\sum_{i=1}^{n}\left[\frac{Y_i - \mu_i}{\mu_i} - \log\left(\frac{Y_i}{\mu_i}\right)\right]$$

Gamma Generalized Estimating Equations (Gamma-GEE)

GEE models the population-averaged mean of the response variable while explicitly accounting for within-cluster correlation. It is particularly suitable for repeated or grouped data, such as delay measurements recorded over time across multiple locations.

In this framework, response variable Y_{ij}, representing the delay for the *j*-th observation in the *i*-th cluster follows a gamma distribution:

$$Y_{ij} \sim \text{Gamma}(\mu_{ij}, \phi) \tag{33}$$

Where, μ_{ij} is mean delay for the observation j in cluster i, $and\ \phi$ is dispersion parameter (inverse of shape parameter), accounting for overdispersion.

The variance of Y_{ij} is modeled as:

$$\text{Var}(Y_{ij}) = \phi V(\mu_{ij}) = \phi.\mu_{ij}^2 \tag{34}$$

Where,

$$\phi = \frac{\sum_{i=1}^{m}\sum_{j=1}^{n_i}\left(\frac{Y_{ij} - \mu_{ij}}{\mu_{ij}}\right)^2}{\text{Total Degrees of Freedom}}$$

In Eq. 15, ϕ is scale parameter, also referred to as the dispersion parameter in the GEE framework, which accounts for overdispersion in the data. $V(\mu_{ij})$ is the variance function specific to the Gamma distribution.

The log-link function relates the mean response μ_{ij} to the predictors:

$$\log(\mu_{ij}) = \beta_0 + \beta_1 X_{1ij} + \beta_2 X_{2ij} + \cdots + \beta_p X_{pij} \tag{35}$$

Here, X_{1ij} represents a predictor variable (e.g., traffic volume, pedestrian count) for observation *j* in cluster *i*.

GEE includes a working correlation matrix $R(\rho)$ to model within-cluster correlation (Cui & Feng, 2008; Mohammadi et al., 2014); *Exchangeable*: equal correlation ρ between all observations within a

cluster. *Autoregressive (AR-1):* correlation decreases with increasing time lag. *Independent*: assumes no correlation.

Parameters β are estimated using quasi-likelihood estimation (Cui & Feng, 2008; Mohammadi et al., 2014):

$$U(\beta) = \sum_{i=1}^{m} D_i^T V_i^{-1}(Y_i - \mu_i) = 0 \tag{36}$$

Where, D_i is derivative of the mean vector μ_i with respect to β, m is number of clusters and V_i is covariance matrix, incorporating $R(\rho)$. The inclusion of $R(\rho)$ allows GEE to account for within-cluster correlations, making it particularly suitable for clustered or repeated measures data.

Cross Sectional (CS) Method

For the CS method using the Gamma-GLM or Gamma-GEE framework, the methodology can be adapted to handle continuous response variables (e.g., delays) while incorporating the treatment effect as an explanatory variable. Here's how the model is formulated:

$$\log(\mu_i) = \beta_0 + \beta_1 X_{1i} + \beta_2 X_{2i} + \cdots + \beta_p X_{pi} + \beta_T T_i \tag{37}$$

Here, β_T is coefficient representing the treatment effect, and T_i is binary indicator for the presence of treatment ($T_i = 1$ for treated locations, $T_i = 0$ for untreated locations).

To quantify the impact of the treatment (e.g., MPS installation), DMF is calculated by exponentiating the treatment coefficient as Eq (19):

$$DMF_T = e^{\beta_T} \tag{38}$$

To estimate the uncertainty around the DMF, the standard error of the exponentiated coefficient is approximated using the delta method. The following approximation can be used to calculate the standard error (SE_x) of the DMF (Park & Abdel-Aty, 2016):

$$SE_T = \frac{e^{\beta_T + SE_{T_x}} - e^{\beta_T - SE_{T_x}}}{2} \tag{39}$$

where, β_T denotes the coefficient of treatment indicator variable T_i and SE_{T_x} denotes the standard error of β_T from the fitted model (Gamma-GLM or Gamma-GEE). The goodness of fit was calculated using the same procedure and methodology as the Conflict Modification Factor (CoMF) described in detail in Section 9.

Before-After Comparison Group (CG) Method

The before–after CG method is used to evaluate the impact of treatment (MPSs) by comparing observed changes at treated sites with corresponding changes at untreated reference (comparison) sites. In this study, delay data were collected at both treated and comparison sites during the before period (prior to MPS installation) and the after period (once MPSs became operational). DMF is calculated from the following Eq. 40 (Gross, 2010; Monsere et al., 2017).

$$DMF = \left(\frac{N_{\text{observed},T,A}}{N_{\text{expected},T,A}}\right) / \left(1 + \frac{\text{Var}\left(N_{\text{expected},T,A}\right)}{N^2_{\text{expected},T,A}}\right) \tag{40}$$

And variance of DMF is:

$$\text{Variance (DMF)} = \frac{\text{DMF}^2\left[\left(\frac{1}{N_{\text{observed},T,A}}\right) + \left(\frac{\text{Var}\left(N_{\text{expected},T,A}\right)}{N^2_{\text{expected},T,A}}\right)\right]}{1 + \frac{\text{Var}\left(N_{\text{expected},T,A}\right)^2}{N^2_{\text{expected},T,A}}} \tag{41}$$

Where,

$$N_{\text{expected},T,A} = N_{\text{observed},T,B}\left(\frac{N_{\text{observed},C,A}}{N_{\text{observed},C,B}}\right)$$

$$\text{Var}\left(N_{\text{expected},T,A}\right) = N^2_{\text{expected},T,A}\left(\frac{1}{N_{\text{observed},T,B}} + \frac{1}{N_{\text{observed},C,B}} + \frac{1}{N_{\text{observed},C,A}}\right)$$

$N_{\text{observed},T,B}$= Mean delay at treated sites during the before period.

$N_{\text{observed},T,A}$= Expected mean delay at treated sites in the after period in the absence of treatment.

$N_{\text{observed},C,B}$= Mean delay at comparison sites during the before period

$N_{\text{observed},C,A}$= Mean delay at comparison sites during the after period

13.3 Results and Discussion

Empirical Bayes and Comparison Group Methods

To implement the EB approach, the DFs were developed using data from four different reference groups: (1) PHB-only sites, (2) RRFB-only sites, (3) a combination of PHB and RRFB sites, and (4) all reference sites combined. Vehicle delay was measured at each pedestrian-vehicle interaction. For each evaluation scenario, the selection of treatment sites was aligned with the corresponding reference group. For instance, when using PHB sites as the reference, only those treatment locations that were previously equipped with PHBs and later upgraded to MPSs were included in the evaluation. This ensured that the baseline conditions were comparable, maintaining consistency in the EB analysis framework. A similar matching strategy was applied for RRFB-based and combined-reference models. In the CG method, untreated sites were excluded from the reference group, as data was not collected from that location after MPS installation at other untreated sites. **Table 11** summarizes the alignment between reference groups and corresponding evaluation sites used in the EB analysis.

For the final DMF evaluation, the Gamma-GEE model was selected over Gamma-GLM due to its superior performance across multiple evaluation metrics. As shown in **Table 21**, the Gamma-GEE model consistently achieved lower MAE and MSE, indicating more accurate and reliable predictions of vehicle delay. Its ability to account for within-cluster correlation through the working correlation structure $R(\rho)$ makes it particularly suitable for analyzing clustered traffic data. Since AIC (used in Gamma-GLM) and QIC (used in Gamma-GEE) are based on different likelihood frameworks, they are not directly comparable, reinforcing the use of MAE and MSE for performance assessment. Among the tested correlation structures—Exchangeable, Autoregressive (AR-1), and Independent—the Exchangeable structure provided the best fit. **Figure 27** illustrates the prediction accuracy for the PHB reference group, highlighting the model's robustness. In the Gamma-GEE model (refer **Table 21**), vehicle delay decreases with an increase in average leading vehicle speed, average vehicle speed, lane width, and posted speed limit, indicating that higher speeds and wider lanes help reduce delays. Conversely, delay increases with greater standard deviation of vehicle speed, vehicle volume, pedestrian volume, lane count, and the presence of a raised or vegetated median, suggesting that higher speed variability, increased vehicle-pedestrian interactions, and roadway design elements contribute to

longer delays. Additionally, land-use mix, weekdays, and peak periods (morning and afternoon) are associated with higher vehicle delays, highlighting the influence of land-use diversity and temporal factors on traffic flow at crossings.

Table 21 DFs based on different reference groups for EB method

Variable	Estimate (std. error) based on different reference groups							
	All		PHBs and RRFB		PHBs		RRFB	
	Gamma-GLM	Gamma-GEE	Gamma-GLM	Gamma-GEE	Gamma-GLM	Gamma-GEE	Gamma-GLM	Gamma-GEE
Traffic and Pedestrian Dynamics								
Constant	5.673** (0.425)	4.987** (0.396)	6.862** (0.204)	5.592** (0.266)	5.037** (0.318)	4.183** (0.226)	6.113** (0.505)	5.396** (0.395)
Average leading vehicle speed	-0.379** (0.105)	-0.593** (0.146)	-0.821** (0.214)	-0.701** (0.294)	-0.824** (0.200)	-0.773** (0.101)	-0.602** (0.118)	-0.629** (0.102)
Average vehicles' speed	-0.609* (0.234)	-0.465** (0.120)	-0.383** (0.116)	-0.395* (0.181)	-0.339** (0.155)	-0.413* (0.103)	-0.401** (0.108)	-0.509** (0.201)
Std. dev. of vehicle speed	0.693** (0.249)	0.502** (0.204)	0.593** (0.173)	0.492** (0.184)	0.502** (0.109)	0.492** (0.200)	0.408** (0.128)	0.530** (0.199)
Ln (Vehicle volume)	0.201** (0.093)	0.279** (0.088)	0.199** (0.070)	0.250** (0.059)	0.222** (0.082)	0.190** (0.065)	0.208* (0.118)	0.173* (0.099)
Pedestrian volume		0.099** (0.010)		0.069** (0.021)		0.096** (0.013)		0.076** (0.018)
Road Characteristics								
Lane count	0.169** (0.015)	0.224* (0.124)	0.150** (0.014)	0.178* (0.105)	0.111* (0.061)	0.196* (0.109)		
Raised/vegetation Median	0.269** (0.114)	0.333** (0.107)	0.294** (0.102)	0.241** (0.115)		0.283** (0.100)		
Lane width		-0.290** (0.114)		-0.551** (0.102)	-0.329** (0.118)	-0.309* (0.184)		
Posted speed limit		-0.577** (0.211)		-0.493** (0.241)		-0.511** (0.196)		
Contextual and Temporal Factors								
Land-use mix	0.385** (0.121)	0.399** (0.139)	0.290* (0.153)	0.254* (0.137)	0.290* (0.171)	0.250* (0.131)		
Weekday	0.332** (0.124)	0.273** (0.097)	0.282** (0.111)	0.335* (0.192)	0.190** (0.073)	0.253* (0.151)	0.230* (0.128)	0.221** (0.102)
Morning peak	0.073** (0.025)	0.055** (0.015)	0.042** (0.011)	0.049* (0.019)	0.060** (0.010)	0.013** (0.005)	0.020** (0.006)	0.050** (0.013)
Afternoon Peak							0.091* (0.051)	0.102* (0.054)
Goodness of Fit								
AIC/QIC	8693/-	-/9172	8592/-	-/8857	7163/-	-/7340	6284/-	-/6486
Dispersion Parameter	2.40	1.99	1.35	1.27	1.39	1.42	1.51	1.55
Correlation Coefficient, $R(\rho)$		0.31		0.37		0.36		0.41
MAE	1.339	0.858	2.984	1.438	1.5894	0.8684	3.073	2.389
MSE	1.419	0.884	3.106	1.639	2.0826	0.9683	3.190	2.503

** Significant at 95% confidence level.
* Significant at 90% confidence level.

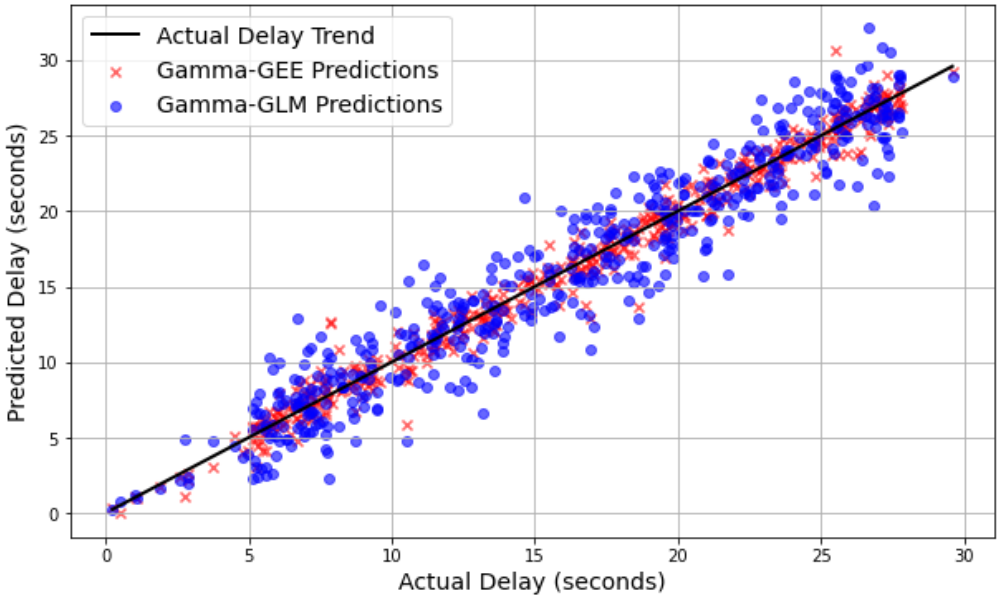
Actual Delay Trend
Gamma-GEE Predictions
Gamma-GLM Predictions
Predicted Delay (seconds)
Actual Delay (seconds)
0
5
10
15
20
25
30

(a)

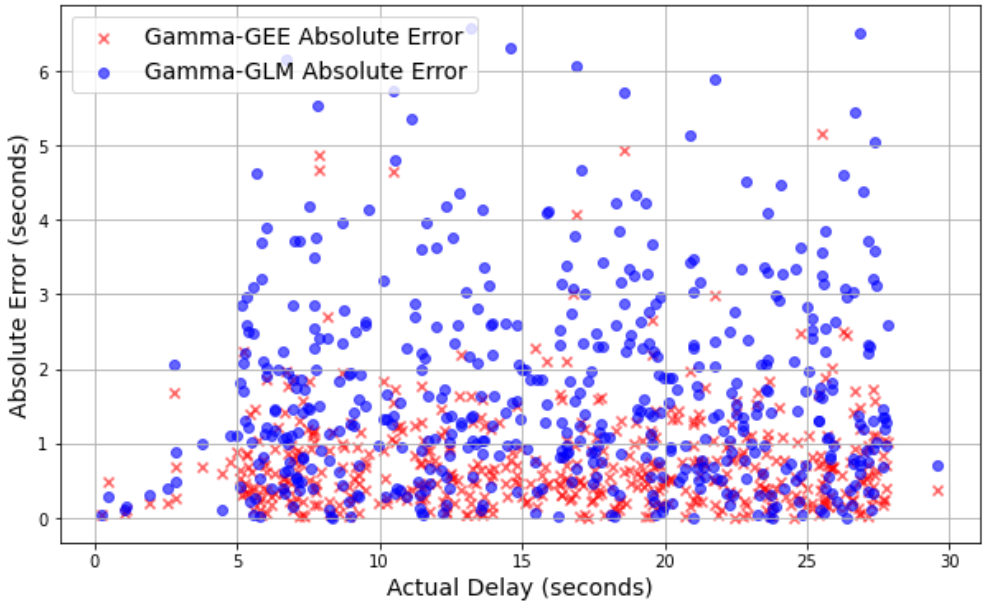
Gamma-GEE Absolute Error
Gamma-GLM Absolute Error
Absolute Error (seconds)
Actual Delay (seconds)
0
1
2
3
4
5
6
0
5
10
15
20
25
30

(b)

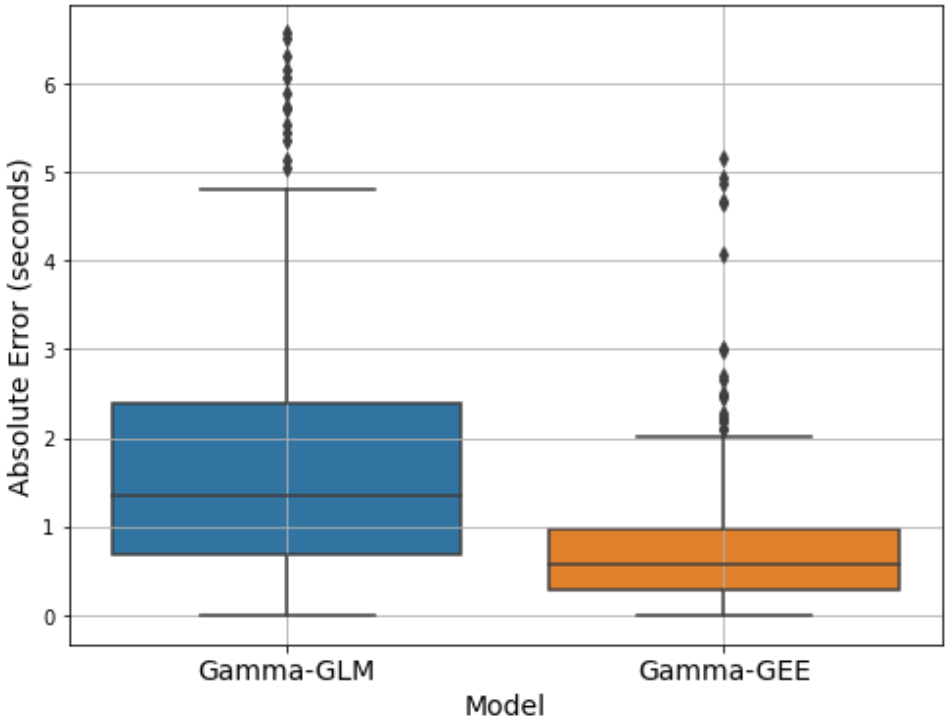

(c)

Figure 27 (a) Comparison of actual and predicted delay, (b) Absolute error, (c) Box plot to compare errors of Gamma-GLM and Gamma-GEE model (Reference Group: PHB)

Table 22 presents the DMFs for MPSs across different reference groups, evaluated using the EB and CG methods. For all sites combined, MPSs reduce vehicle delay by 2% according to the EB method, whereas the CG method shows a 1% increase, indicating minimal overall impact. For the combined PHB and RRFB reference group, MPSs result in a 2% increase in delay using the EB method and a 3% increase using the CG method. When using PHBs as the reference group, MPSs reduce vehicle delay by 5% in the EB method and by 7% in the CG method, highlighting improved efficiency at locations previously equipped with PHBs. Conversely, when using RRFBs as the reference group, MPSs lead to an 8% increase in delay under the EB method and an 11% increase in the CG method.

Table 22 DMFs of MPSs based on EB method and CG method.

Reference Group	**DMF (std. error) of MPSs**	
	Empirical Bayes	Comparison Group
All	0.98 (0.06)	1.01 (0.11)
PHBs, RRFB	1.02 (0.04)	1.03 (0.10)
PHBs	0.95 (0.03)	0.93 (0.08)
RRFB	1.08 (0.04)	1.11 (0.09)

Cross Sectional Method

The CS method evaluates vehicle delays of MPSs across different reference categories. The first category included all locations that transitioned to MPSs, irrespective of whether they were previously PHB, RRFB, untreated, or remained unchanged. The second category focused on PHB, RRFB and Flashing Beacon locations, including those that transitioned to MPSs or remained same during both periods. The third category specifically analyzed PHB locations, considering those that either transitioned to MPSs or remained as PHBs throughout the study period. Lastly, the fourth category examined RRFB and Flashing Beacon locations, including those that transitioned to MPSs or remained as RRFBs during the analysis period. Here also Gamma-GEE model was selected, as it effectively accounts for within-cluster correlations and consistently demonstrates lower MAE and MSE values (refer to **Table 23**). The model results align with those from the EB method, where vehicle delay decreases with an increase in average leading vehicle speed, average vehicle speed, and posted speed limit, while it increases with higher speed variability, vehicle and pedestrian volumes, lane count, and the presence of a raised or vegetated median. Similarly, land-use mix, weekdays, and peak periods (morning and afternoon) contribute to increased vehicle delays.

Table 23 DFs based on different reference groups for CS method

Variable	Estimate (std. error) based on different reference groups							
	All locations		PHBs, RRFB, Flashing Beacon		PHBs		RRFB, Flashing Beacon	
	Gamma-GLM	Gamma-GEE	Gamma-GLM	Gamma-GEE	Gamma-GLM	Gamma-GEE	Gamma-GLM	Gamma-GEE
Traffic and Pedestrian Dynamics								
Constant	2.968** (0.329)	2.068** (0.296)	2.973** (0.383)	2.593** (0.198)	3.072** (0.335)	2.904** (0.213)	1.977** (0.199)	1.739** (0.190)
Average leading vehicle speed	-0.294** (0.100)	-0.301** (0.094)	-0.228** (0.087)	-0.199** (0.062)	-0.249** (0.113)	-0.265** (0.098)	-0.107** (0.020)	-0.134** (0.032)
Average vehicles' speed	-0.391** (0.119)	-0.290** (0.104)	-0.296** (0.110)	-0.258** (0.097)	-0.169* (0.088)	-0.148** (0.035)	-0.122** (0.034)	-0.099** (0.020)
Std. dev. of vehicle speed	0.106** (0.045)	0.119** (0.031)	0.098** (0.019)	0.101** (0.012)	0.078* (0.045)	0.066* (0.035)	0.091** (0.011)	0.080** (0.009)
Ln (Vehicle volume)	0.731** (0.242)	0.693** (0.194)	0.539** (0.138)	0.518** (0.127)	0.503** (0.198)	0.499** (0.101)	0.684** (0.230)	0.580** (0.181)
Pedestrian volume	0.048* (0.025)	0.099** (0.015)		0.085** (0.017)		0.059** (0.010)	0.065** (0.019)	0.058** (0.012)
Road Characteristics								
MPS treatment	0.029** (0.001)	0. 028** (0.001)	0.0099** (0.002)	0.0198** (0.002)	-0.0408** (0.003)	-0. 062** (0.004)	0.113** (0.011)	0.131** (0.025)
Lane count	0.095** (0.014)	0.088* (0.025)	0.074** (0.011)	0.096** (0.017)	0.090* (0.029)	0.081** (0.015)		0.060** (0.012)
Raised/vegetation Median	0.052** (0.010)	0.039** (0.008)	0.028* (0.016)	0.032** (0.010)	0.026* (0.010)	0.025** (0.008)		
Posted speed limit		-0.330** (0.115)	-0.472** (0.219)	-0.439** (0.183)		-0.397** (0.114)		-0.269* (0.140)
Contextual and Temporal Factors								
Land-use mix	0.088** (0.021)	0.082** (0.015)		0.068** (0.022)		0.094* (0.016)		0.075** (0.030)
Weekday	0.227** (0.105)	0.334** (0.111)	0.225** (0.105)	0.350** (0.121)	0.302** (0.101)	0.255** (0.102)	0.299** (0.102)	0.323** (0.100)
Morning peak	0.040** (0.019)	0.051** (0.015)	0.045** (0.010)	0.039* (0.011)	0.025** (0.012)	0.028** (0.009)	0.042** (0.011)	0.036** (0.008)
Afternoon Peak				0.185** (0.067)		0.093** (0.015)		
Goodness of Fit								
AIC/QIC	8073/-	-/8115	7439/-	-/7505	6529/-	-/6596	4852/-	-/4901
Dispersion Parameter	2.38	2.50	1.42	1.32	1.35	1.39	1.46	1.49
Correlation Coefficient, $R(\rho)$		0.35		0.40		0.33		0.41
MAE	1.974	1.118	1.763	1.073	1.593	0.953	2.755	1.090
MSE	1.997	1.212	1.778	0.996	1.600	0.972	2.764	1.102

** Significant at 95% confidence level.
* Significant at 90% confidence level.

Table 24 presents the DMFs of MPSs from CS method across different reference groups. For all sites combined, vehicle delay increased by 2%. When considering PHB, RRFB, and Flashing

Beacon locations, MPSs resulted in a 3% increase in delay. However, when PHBs were used as the reference group, MPSs reduced vehicle delay by 6%, highlighting a potential improvement compared to PHBs. In contrast, when using RRFB and Flashing Beacon locations as the reference group, MPSs led to a 14% increase in vehicle delay.

Table 24 DMFs of MPSs based on CS method.

Reference Group	DMF (std. error)
All	1.02 (0.05)
PHBs, RRFB, Flashing Beacon	1.03 (0.06)
PHBs	0.94 (0.04)
RRFB, Flashing Beacon	1.14 (0.08)

Findings from all three methods (EB, CG, and CS) indicate that when considering all reference sites together and comparing MPSs to PHBs, RRFBs, and Flashing Beacons, MPSs do not lead to significant delay improvements. Furthermore, when compared specifically to RRFBs and Flashing Beacons, MPSs increase vehicle delays by 8-14%. The results suggest that delays at MPS locations are significantly higher than at RRFB and Flashing Beacon sites, which is expected given the fundamental differences in their operational mechanisms. MPSs require vehicles to come to a complete stop when the signal is red, inherently leading to higher delays. In contrast, RRFBs and Flashing Beacons only alert drivers to slow down and yield to pedestrians, allowing vehicles to proceed without stopping if no pedestrians are present, thereby minimizing delays. However, when compared to PHBs, which share similar functionalities but differ in signal phase management, MPSs result in lower vehicle delays. The study found that compared to PHBs, MPS systems reduced vehicle delays by 5-7%.

14. CONCLUSIONS

MPSs represent a relatively new traffic control device recommended by the National Committee on Uniform Traffic Control Devices (NCUTCD) Signal Technical Committee (STC). FDOT began implementing MPS systems in November 2022, currently operational at 14 locations across Florida. Extensive before-and-after CCTV video data were collected from these 14 MPS locations and 5 reference sites across Florida. Of the 14 treatment sites, 7 were previously untreated (without any signal system), 5 had PHBs, 1 had RRFB, and 1 had a Flashing Beacon prior to the installation of MPSs. The reference groups included 3 locations with PHBs, 1 location with an RRFB, and 1 unsignalized location. The collected videos were processed in three main steps: object detection, object tracking, and converting pixel coordinates into GPS coordinates. The video processing utilized advanced computer vision techniques, specifically the Real-Time DEtection TRansformer (RT-DETR) model for detection and the ByteTrack algorithm for tracking. The GPS points extracted from the trajectories were then used to calculate variables such as speed, direction, and other parameters required for the study.

14.1 Pedestrian safety improvements

Initially, pedestrian safety improvements were assessed using box plots of Post Encroachment Time (PET), Relative Time to Collision (RTTC), spatial gap, and temporal gap, along with the Mann–Whitney–Wilcoxon test. The results indicated that MPSs were associated with significantly improved safety outcomes than PHB, RRFB, Flashing Beacons, and uncontrolled locations. Building upon these initial findings, a more comprehensive evaluation was later conducted using advanced statistical modeling techniques.

Since MPSs have been newly implemented, there is no available post-implementation crash data. Waiting several years for sufficient crash data to assess their effectiveness would not be practical for implementing a potentially promising safety strategy. A more effective alternative involves using conflicts- (near misses) based surrogate safety measures (SSMs). This study utilized vehicle-pedestrian conflict data from using RTTC value. RTTC thresholds were defined as follows:

- RTTC $\leq$ 1.0 represents serious conflicts,
- 1.0 < RTTC $\leq$ 3.0 represents moderate conflicts, and
- RTTC > 3.0 was not considered a conflict.

The number of serious and moderate conflicts was recorded for each 30-minute interval to comprehensively assess pedestrian-vehicle interactions. The effectiveness of MPSs was evaluated by calculating Conflict Modification Factors (CoMFs) and comparing their safety performance with other midblock crossing systems. The study employed both Cross-Sectional (CS) and Before-After evaluation methods, incorporating a Comparison Group (CG) and the Empirical Bayesian (EB) approach to calculate CoMFs.

Prior studies have consistently demonstrated that PHB are generally safer than RRFB or Flashing Beacon. The primary reason for this is the mandatory stop requirement for vehicles during the red phase of PHB, ensuring driver compliance and pedestrian safety. In contrast, RRFB and Flashing Beacon serve only as visual warnings and do not require vehicles to stop unless a pedestrian is actively crossing, leading to inconsistent driver behavior. This study compared the safety performance of MPSs against different reference groups, including PHBs, RRFB, combinations of PHBs, RRFB and Flashing Beacon. Across all categories, MPSs demonstrated consistent reductions in serious and moderate conflicts. Notably, when compared to PHBs which share similar functionalities but differ in signal phase management; MPSs provided additional safety benefits by reducing both serious and total conflicts. Unlike PHBs, which remain dark when inactive, MPS systems operate seamlessly with regular traffic signals, maintaining a green phase until pedestrian activation. Notably, at locations where PHBs were replaced with MPSs, there were no changes to the signal infrastructure or road geometry, except for modifications to the signal heads and signal phase reprogramming. The results showed that, compared to PHBs, MPSs reduced serious and total conflicts by 27% and 33% using the EB method, 33% and 31% using CG method, and 26% and 36% using CS method, respectively.

14.2 Vehicle delay analysis

The effectiveness of MPSs was assessed by computing Delay Modification Factors (DMFs) using CS and Before-After evaluation methods, incorporating CG approach and EB method. Findings from all three methods indicate that MPSs do not reduce vehicle delays compared to RRFBs and Flashing Beacons; MPSs lead to 8% to 14% more delay. This outcome is expected, as RRFBs and Flashing Beacons only alert drivers to slow down and yield to pedestrians, allowing vehicles to proceed without stopping if no pedestrians are present. In contrast, MPSs require vehicles to come to a complete stop when the signal is red, inherently leading to longer delays. These results align with prior research (Anwari et al., 2024), which found that PHBs also introduce more delay than RRFBs. However, when

comparing MPSs to PHBs, the study found that MPSs reduced vehicle delays by 5% to 7% compared to PHB.

14.3 Rear-end conflict reduction

Rear-end vehicle conflicts were analyzed using surrogate safety measures: TTC and DRAC. The findings clearly indicate that MPS installations lead to significant safety improvements at midblock crossings. Across all treatment transitions, MPSs consistently reduced both serious and moderate rear-end conflicts, with the most substantial improvements observed at sites that transitioned from RRFBs, Flashing Beacons, and untreated conditions. For instance, serious TTC conflicts were reduced by over 60% at RRFB sites, and by nearly 75% at previously untreated sites, while DRAC-based serious conflicts showed similar levels of reduction. Although sites that changed from PHBs to MPSs showed smaller reductions, the overall trend confirms that MPSs help vehicles maintain safer distances and require less aggressive braking to avoid collisions.

14.4 Long-term evaluation of MPS

For the long-term evaluation, data were collected from one location at three key stages: before MPS installation, immediately after installation, and approximately 1.5 years post-installation. Following the implementation of the MPS, significant improvements were observed across all safety and behavioral metrics. The long-term results were consistent with the immediate post-installation findings, demonstrating that the benefits of the MPS were sustained over time.

14.5 Overall conclusion

This study demonstrates that MPSs offer a balanced solution for improving safety and efficiency at midblock pedestrian crossings. Compared to other signalized crossings; especially PHBs, MPSs were found to reduce pedestrian-vehicle conflicts significantly, lower vehicle delays and minimize rear-end conflict risks. The vehicle yielding rate at MPS locations was observed to be 97%, meaning almost all drivers stopped for pedestrians. Pedestrian compliance was also above 95%, as most pedestrians followed traffic rules and crossed only after activating the signal. Given their adaptability, ease of implementation, and improved safety performance, MPS systems can be considered as a preferred alternative when upgrading existing crossings or installing new pedestrian signal systems.

LIST OF REFERENCES

Abdel-Aty, M. A., & Radwan, A. E. (2000). Modeling traffic accident occurrence and involvement. *Accident Analysis & Prevention*, *32*(5), 633–642. https://doi.org/10.1016/S0001-4575(99)00094-9

Abdel-Aty, M., & Abdalla, M. F. (2004). Modeling drivers' diversion from normal routes under ATIS using generalized estimating equations and binomial probit link function. *Transportation*, *31*(3), 327–348. https://doi.org/10.1023/B:PORT.0000025396.32909.DC/METRICS

Abuzwidah, M., & Abdel-Aty, M. (2024). Assessing the impact of express lanes on traffic safety of freeways. *Accident Analysis & Prevention*, *207*, 107718. https://doi.org/10.1016/J.AAP.2024.107718

Ahsan, M. J., Abdel-Aty, M., & Abdelrahman, A. S. (2025). Evaluating the safety impact of mid-block pedestrian signals (MPS). *Accident Analysis & Prevention*, *210*, 107847. https://doi.org/10.1016/J.AAP.2024.107847

Ahsan, M. J., Abdel-Aty, M., Anik, B. M. T. H., & Islam, Z. (2025). An ensemble time-embedded transformer model for traffic conflict prediction at RRFB pedestrian crossings. *Transportation Engineering*, *20*, 100318. https://doi.org/10.1016/J.TRENG.2025.100318

Ahsan, M. J., Abdel-Aty, M., & Anwari, N. (2024). Vehicle-Pedestrian near miss analysis at signalized mid-block crossings. *Journal of Safety Research*, *91*, 68–84. https://doi.org/10.1016/J.JSR.2024.08.006

Ahsan, M. J., Abdel-Aty, M., Anwari, N., & Barbour, N. (2025). Evaluating drivers' braking behavior at mid-block pedestrian crosswalks using video data and a mixed logit model with heterogeneity in the means. *Transportation Research Interdisciplinary Perspectives*, *31*, 101380. https://doi.org/10.1016/J.TRIP.2025.101380

Anwari, N., Abdel-Aty, M., & Ahsan, M. J. (2024). Comparative Evaluation of Vehicle Delays at Midblock Rectangular Rapid Flashing Beacon and Pedestrian Hybrid Beacon Pedestrians' Crossings. *Journal of Transportation Engineering, Part A: Systems*, *151*(2), 04024105. https://doi.org/10.1061/JTEPBS.TEENG-8400

Anwari, N., Abdel-Aty, M., Goswamy, A., & Zheng, O. (2023). Investigating surrogate safety measures at midblock pedestrian crossings using multivariate models with roadside camera data. *Accident Analysis & Prevention*, *192*, 107233. https://doi.org/10.1016/J.AAP.2023.107233

Arun, A., Haque, M. M., Bhaskar, A., Washington, S., & Sayed, T. (2021). A bivariate extreme value model for estimating crash frequency by severity using traffic conflicts. *Analytic Methods in Accident Research*, *32*, 100180. https://doi.org/10.1016/J.AMAR.2021.100180

Bochkovskiy, A., Wang, C.-Y., & Liao, H.-Y. M. (2020). *YOLOv4: Optimal Speed and Accuracy of Object Detection*. https://arxiv.org/abs/2004.10934v1

Chen, P., Zeng, W., Yu, G., & Wang, Y. (2017). Surrogate Safety Analysis of Pedestrian-Vehicle Conflict at Intersections Using Unmanned Aerial Vehicle Videos. *Journal of Advanced Transportation*, *2017*(1), 5202150. https://doi.org/10.1155/2017/5202150

Cui, J., & Feng, L. (2008). Correlation Structure and Model Selection for Negative Binomial Distribution in GEE. *Communications in Statistics - Simulation and Computation*, *38*(1), 190–197. https://doi.org/10.1080/03610910802446985

Fitzpatrick, K., Cynecki, M. J., Pratt, M. P., Park, E. S., Beckley, M. E., & Institute, T. T. (2019). *Evaluation of Pedestrian Hybrid Beacons on Arizona Highways*. https://doi.org/10.21949/1503647

Fitzpatrick, K., Geedipally, S., Kutela, B., & Koonce, P. (2024). Midblock Pedestrian Signal Safety Effectiveness. *Transportation Research Record*, *2678*(4), 243–256.

https://doi.org/10.1177/03611981231184196/ASSET/IMAGES/10.1177_03611981231184196-IMG3.PNG

Fitzpatrick, K., Park, E. S., & Development, U. S. F. H. A. O. of S. R. and. (2010). *Safety Effectiveness of the HAWK Pedestrian Crossing Treatment*. https://doi.org/10.21949/1503647

Florida Department of Highway Safety and Motor Vehicles Crash Dashboard. (2025). https://www.flhsmv.gov/traffic-crash-reports/crash-dashboard/

Florida Pedestrian and Bicycle Strategic Safety Plan. (2021).

Fu, C., & Sayed, T. (2021). Random parameters Bayesian hierarchical modeling of traffic conflict extremes for crash estimation. *Accident Analysis & Prevention*, *157*, 106159. https://doi.org/10.1016/J.AAP.2021.106159

Geographic Information System (GIS). (2024). https://www.fdot.gov/statistics/gis/default.shtm

Goswamy, A., & Abdel-Aty, M. (2023). Safety Effectiveness of Rectangular Rapid Flashing Beacons Pedestrian Enhancement. *Journal of Transportation Engineering, Part A: Systems*, *149*(8), 04023070. https://doi.org/10.1061/JTEPBS.TEENG-7507/ASSET/835FF108-29A4-40BA-B62B-08643B668A71/ASSETS/IMAGES/LARGE/FIGURE1.JPG

Goswamy, A., Abdel-Aty, M., & Islam, Z. (2023). Factors affecting injury severity at pedestrian crossing locations with Rectangular RAPID Flashing Beacons (RRFB) using XGBoost and random parameters discrete outcome models. *Accident Analysis & Prevention*, *181*, 106937. https://doi.org/10.1016/J.AAP.2022.106937

Gross, F. P. B. N. L. C. (2010). *A Guide to Developing Quality Crash Modification Factors*. https://doi.org/10.21949/1503647

Hasanpour, M., Persaud, B., & Milligan, C. (2025). Integrating Traffic Conflict Frequency and Severity Indicators to Estimate Pedestrian Safety Performance Functions for Signalized Intersections. *Https://Doi.Org/10.1177/03611981241302331*. https://doi.org/10.1177/03611981241302331

Hauer, E. (1997). Observational Before/After Studies in Road Safety. Estimating the Effect of Highway and Traffic Engineering Measures on Road Safety. *Pergamon*, 289. https://books.emeraldinsight.com/page/detail/observational-beforeafter-studies-in-road-safety-by-ezra-hauer/?k=9780080430539

Kuhn, H. W. (1955). The Hungarian method for the assignment problem. *Naval Research Logistics Quarterly*, *2*(1–2), 83–97. https://doi.org/10.1002/NAV.3800020109

Lee, A. H., Xiang, L., & Hirayama, F. (2010). Modeling physical activity outcomes: A two-part generalized-estimating- equations approach. *Epidemiology*, *21*(5), 626–630. https://doi.org/10.1097/EDE.0B013E3181E9428B

Li, C., Li, L., Geng, Y., Jiang, H., Cheng, M., Zhang, B., Ke, Z., Xu, X., & Chu, X. (2023). *YOLOv6 v3.0: A Full-Scale Reloading*. https://arxiv.org/abs/2301.05586v1

Liang, C., Zhang, Z., Zhou, X., Li, B., Zhu, S., & Hu, W. (2022). Rethinking the Competition Between Detection and ReID in Multiobject Tracking. *IEEE Transactions on Image Processing*, *31*, 3182–3196. https://doi.org/10.1109/TIP.2022.3165376

Lin, T. Y., Maire, M., Belongie, S., Hays, J., Perona, P., Ramanan, D., Dollár, P., & Zitnick, C. L. (2014). Microsoft COCO: Common Objects in Context. *Computer Vision – ECCV 2014. ECCV 2014.*, *8693 LNCS*(PART 5), 740–755. https://doi.org/10.1007/978-3-319-10602-1_48

Mohamed, S. M., Abozaid, E. S., & AbdelLatif, S. H. (2022). Profile Monitoring of Residuals Control Charts

Under Gamma Regression Model. *Eastern-European Journal of Enterprise Technologies*, *6*(4–120), 23–31. https://doi.org/10.15587/1729-4061.2022.264904

Mohammadi, M. A., Samaranayake, V. A., & Bham, G. H. (2014). Crash frequency modeling using negative binomial models: An application of generalized estimating equation to longitudinal data. *Analytic Methods in Accident Research*, *2*, 52–69. https://doi.org/10.1016/J.AMAR.2014.07.001

Monsere, C., Figliozzi, M., Kothuri, S., Razmpa, A., Hazel, D., & Section, O. D. of T. R. (2017). *Safety effectiveness of pedestrian crossing enhancements : final report.* https://doi.org/10.21949/1503647

NHTSA's National Center for Statistics and Analysis. (2020). *Traffic Safety Facts, 2020 Data*. https://crashstats.nhtsa.dot.gov/Api/Public/ViewPublication/813310

Park, J., & Abdel-Aty, M. (2016). Evaluation of safety effectiveness of multiple cross sectional features on urban arterials. *Accident Analysis & Prevention*, *92*, 245–255. https://doi.org/10.1016/J.AAP.2016.04.017

Shahdah, U., Saccomanno, F., & Persaud, B. (2014). Integrated traffic conflict model for estimating crash modification factors. *Accident Analysis & Prevention*, *71*, 228–235. https://doi.org/10.1016/J.AAP.2014.05.019

Shirazi, M., Lord, D., Dhavala, S. S., & Geedipally, S. R. (2016). A semiparametric negative binomial generalized linear model for modeling over-dispersed count data with a heavy tail: Characteristics and applications to crash data. *Accident Analysis & Prevention*, *91*, 10–18. https://doi.org/10.1016/J.AAP.2016.02.020

Ugan, J., Abdel-Aty, M., & Cai, Q. (2022). Estimating effectiveness of speed reduction measures for pedestrian crossing treatments using an empirically supported speed choice modeling framework. *Transportation Research Part F: Traffic Psychology and Behaviour*, *89*, 276–288. https://doi.org/10.1016/J.TRF.2022.07.002

Zegeer, C., Lyon, C., Srinivasan, R., Persaud, B., Lan, B., Smith, S., Carter, D., Thirsk, N. J., Zegeer, J., Ferguson, E., Van Houten, R., & Sundstrom, C. (2017). Development of Crash Modification Factors for Uncontrolled Pedestrian Crossing Treatments. *Https://Doi.Org/10.3141/2636-01*, *2636*, 1–8. https://doi.org/10.3141/2636-01

Zhang, S., Abdel-Aty, M., Wu, Y., & Zheng, O. (2022). Pedestrian Crossing Intention Prediction at Red-Light Using Pose Estimation. *IEEE Transactions on Intelligent Transportation Systems*, *23*(3), 2331–2339. https://doi.org/10.1109/TITS.2021.3074829

Zhang, Y., Sun, P., Jiang, Y., Yu, D., Weng, F., Yuan, Z., Luo, P., Liu, W., & Wang, X. (2022). ByteTrack: Multi-object Tracking by Associating Every Detection Box. *Computer Vision – ECCV 2022*, *13682 LNCS*, 1–21. https://doi.org/10.1007/978-3-031-20047-2_1/TABLES/7

Zhao, Y., Lv, W., Xu, S., Wei, J., Wang, G., Dang, Q., Liu, Y., & Chen, J. (2024). *DETRs Beat YOLOs on Real-time Object Detection* (pp. 16965–16974). https://zhao-yian.github.io/RTDETR.